DISSERTATION FOR DOCTORAL (PhD) DEGREE

University of Sopron (Soproni Egyetem)
Faculty of Wood Engineering and Creative Industry,
József Cziráki Doctoral School of Wood Sciences and Technologies

Sustainable Polymeric Composites Reinforced by Fiber-Fabric Materials for Advanced Application

in

Material Science and Technology

PhD Program: Fibre and Nanotechnology Sciences

Author: K. M. Faridul Hasan

Research Supervisors: Dr. Tibor Alpár

Dr. Péter György Horváth

Sopron, Hungary

2022

Sustainable Polymeric Composites Reinforced by Fiber-Fabric Materials for Advanced Application

A Dissertation

submitted in partial fulfilment of the

requirements for the award of the degree of

DOCTOR OF PHILOSOPHY

By

K. M. Faridul Hasan

under the supervision of

Dr. Tibor Alpár and
Dr. Péter György Horváth

Faculty of Wood Engineering and Creative Industry,

József Cziráki Doctoral School of Wood Sciences and Technologies

University of Sopron (Soproni Egyetem)

Sopron, Hungary

2022

Sustainable Polymeric Composites Reinforced by Fiber-Fabric Materials for Advanced Application

Dissertation for doctoral (PhD) degree
University of Sopron József Cziráki Doctoral School
of Wood Sciences and Technologies

"Fiber and Nanotechnology Sciences" programme

Written by:
K. M. Faridul Hasan
….....

Made in the framework of

…..... programme

of the József Cziráki Doctoral School, University of Sopron

Tibor Alpár and Péter György Horváth
Supervisor: Dr. ….....
I recommend for acceptance (yes / no)

(signature)

96

The candidate reached …..... % at the complex exam,

Sopron, 21. 06. 2021 .....
Chairman of the Examination Board

As assessor I recommend the dissertation for acceptance (yes/no)

First assessor (Dr. .....) yes/no
(signature)

Second assessor (Dr. .....) yes/no
(signature)

(Possible third assessor (Dr. .....) yes/no
(signature)

The candidate reached .....% in the public debate of the dissertation

Sopron,

.....
Chairman of the Assessor Committee

Qualification of the doctoral (PhD) degree ….....

.....
Chairman of the University Doctoral
and Habilitation Council (UDHC)

DECLARATION

I, the undersigned **K. M. Faridul Hasan** by signing this declaration certifying that my PhD thesis entitled "**Sustainable Polymeric Composites Reinforced by Fiber-Fabric Materials for Advanced Application**" was my own work; during the dissertation, I complied with the regulations of Act LXXVI of 1999 on Copyright and the rules of the doctoral dissertation prescribed by the Cziráki József Doctoral School, especially regarding references and citations.[1]

Furthermore, I declare that during the preparation of the dissertation, I did not mislead my supervisor(s) or the programme leader with regard to the independent research work.

By signing this declaration, I acknowledge that, if it can be proved that the dissertation is not self-made or the author of a copyright infringement is related to the dissertation, the University of Sopron is entitled to refuse the acceptance of the dissertation.

Refusing to accept a dissertation does not affect any other legal (civil law, misdemeanour law, criminal law) consequences of copyright infringement.

……..

K. M. Faridul Hasan

This is to certify that the statement mentioned above made by the candidate is correct according to the best of my knowledge.

……..

Dr. Tibor Alpár

……..

Dr. Péter György Horváth

[1] **Act LXXVI of 1999** Article 34 (1) Anyone is entitled to quote details of the work, to the extent justified by the nature and purpose of the recipient work, by designating the source and the author specified therein.

Article 36 (1) Details of publicly lectures and other similar works, as well as political speeches, may be freely used for the purpose of information to the extent justified by the purpose. For such use, the source, along with the name of the author, shall be indicated, unless this is impossible.

Acknowledgements

A dissertation is an important accomplishment and achievements of life. It might not be possible to complete the necessary research works reported in this thesis without the continuous support, help, and cooperations of my supervisors (Dr. Tibor Alpár and Dr. Péter György Horváth) during my entire PhD study. I have received tremendous supports for technological knowledge sharing, materials sourcing, guidance, and advice from both of them.

Furthermore, the reported works in this could not be conducted without the cordial cooperations from the professors, teachers, and instructors from different laboratories of University of Sopron. I would like to know my cordial thanks to Dr. Miklós Bak, Prof. Dr. Zsolt Kovács, Dr. Zoltán Pásztory, Adrienn Horváth, Dr. Katalin Halász, Zsófia Kóczán, Dr. Zoltán Börcsök, Gábor Kun, Bernadett Bolodár-Varga, and Zsuzsanna Mária Mucsi for their continuous help and supports. Moreover, I am also grateful and conveying special thanks to the administrative bodies of University of Sopron for their kind supports during different official functioning of my PhD study in Sopron, Hungary.

Moreover, I would like to express my sincere gratitude to the "Tempus Public Foundation" for providing me financial assistance through awarding "Stipendium Hungaricum Scholarship" in 2019. I am also highly grateful acknowledging the supports from project, "EFOP-3.6.1-16-2016-00018: improving the role of research, development, and innovation in the higher education through institutional developments assisting intelligence specialization in Sopron and Szombathely".

Finally, I also acknowledge my gratitude to Pham Nguyen Ai Linh for the great support, enthusiasm, and motivation during my difficult situations, which helped me enormously to keep patience during my PhD. Overall, I am also grateful to the almighty creators of the Universe for providing me a beautiful life with adequate strengths, capabilities, and knowledge.

Table of Contents

List of Figures

List of Tables

List of Abbreviations

AgNP	Silver nanoparticle
ANOVA	Analysis of Variance
BC	Biocomposite
CDM	Continuum damage- mechanics
DTG	Derivative thermogravimetric
DSC	Differential scanning calorimetry
EDX	Energy-disruptive X-ray
FEA	Finite element analysis
IBS	Internal bonding strength
KFRC	Knitted fabric reinforced composites
LSPR	Localized surface plasmon resonance
MDI	Methylene diphenyl diisocyanate
MOR	Modulus of rupture
MOE	Modulus of elasticity
MUF	Melamine–urea–formaldehyde
NBC	Nanobiocomposite
NM	Nanomaterial
NP	Nanoparticle
NRC	Nonwoven reinforced composite
OPC	ordinary Portland cement
PBS	Poly(butylene) succinate
PE	Polyethylene
PHBV	Poly(3–hudroxybutyrateco–3–hydroxyvalerate)
PLA	Polylactic Acid
PP	Polypropylene
PS	Polystyrene

PVC	Poly (vinyl chloride)
R^2	Coefficient of variations
R&D	Research and development
TGA	Thermogravimetric analysis
SEM	Scanning electron microscopy
UV	Ultraviolet
WFC	Woven fabric reinforced composites
XRF	X-ray fluorescence

Abstract

The development of sustainable and innovative products through solving the constantly rising demands of end-users is one of the significant parts of research and development. Herein, four different types of novel green composites fabricated from naturally derived lignocellulosic materials are reported. The development of a green composite is reported with the reinforcement of naturally originated rice (*Oryza sativa*) straw, energy (*Miscanthus spp.*) reeds, Scots pine (*Pinus spp.*), coir (*Cocos nucifera*), flax (*Linum usitatissimum*), hemp (*Cannabis sativa*) and artificial glass fiber and woven fabrics through incorporating with OPC (ordinary Portland cement), phenol-formaldehyde (PF), methylene diphenyl diisocyanate (MDI), and epoxy resin. The works are reported in four different categories: (a) work package 1: Rice straw and energy reed fiber reinforced phenol-formaldehyde resin biocomposites, (b) work package 2: Semi-dry technology-mediated coir fiber and Scots pine particle-reinforced sustainable cementitious composite panels, (c) work package 3: Thermomechanical behavior of Methylene Diphenyl Diisocyanate-bonded flax/glass woven fabric reinforced laminated composites, and (d) work package 4: Nanosilver coating on hemp/cotton blended woven fabrics mediated from mammoth pine bark with improved coloration and mechanical properties.

In the case of work package 1, energy reed and rice straw materials were composited with PF polymeric resin to produce biocomposites. The dimensions of energy reed and rice straw elements used for this research were 0.5 to 1.66 mm and 0.1 to 3.55 mm, respectively. Hot-pressing technology was used for manufacturing the biocomposites. The proportions for mixing of rice straw/energy reed materials in composite systems were 90/0, 54/36, 36/54, and 0/90, whereas the remaining 10% belonged to PF resin. The nominal densities of the biocomposite panels were 680 kg/m^3; however, the actual densities were 713.65, 725.00, 742.79, and 764.49 kg/m^3. The main objective of this study is to develop hybrid biocomposites from different proportions of energy reeds and rice straw materials using PF resin and to find the convenient ratio and materials for biocomposites production. The obtained results demonstrate that mechanical properties and stability against the moisture increase with the increase of energy reeds loading in the composite systems. The biocomposite developed from 100% energy reed reinforced composites provided the highest mechanical properties compared to 100% rice straw. The thermal and morphological properties of the manufactured biocomposite materials were investigated and found significant thermal stability and lignocellulosic material to cement compatibility, respectively. The thermal and mechanical properties of the composite materials increase with the increase in energy reed fiber content in the composite system. Furthermore, the coefficient of variation (R^2) also demonstrates positive attributions of energy reed content. Moreover, the overall performances of the developed biocomposite panels show them as potential and novel candidates to the composite community in the coming times.

In the case of work package 2, an innovative, semi-dry technology was implemented on lignocellulosic material (coir fiber and scots pine particle) reinforced composite panels. Composite panels of 12 mm thickness and 1200 kg/m^3 nominal densities were prepared from lignocellulosic materials and OPC. Measurements determined the dimensions of the lignocellulosic materials to be the following: coir fibers were within 0.1 to 1.25 mm in length while Scots pine particles ranged from 0.355 to 1.6 mm in length. The lignocellulosic materials were loaded in different proportions (100% Scots pine, 60% Scots pine/40% coir, 50% Scots pine/50% coir, 40% Scots pine/60% coir, and 100% coir) to produce five types of composite panels. The proportions of water glass (Na_2SiO_3) additive and OPC remained constant. A cheaper and more convenient novel fabrication approach (semi-dry technology) was utilized to produce the composite panels via pressing (3.2 to 7.1 MPa). Finally, the thermal, physical,

morphological, and mechanical properties of all the composite panels were tested. The most promising finding of this research is the improved thermal and mechanical properties of the composites along with significant dimensional stability against moisture with the increase in loading of coir fibers. The SEM (scanning electron microscopy) and SEM-mediated EDX (energy-dispersive X-ray spectroscopy) also provided the morphological and elemental analysis of the fibers, types of cement, and associated composites. The FTIR (Fourier transform infrared spectroscopy) study also confirmed the successful reinforcement of the lignocellulosic materials and OPC. Moreover, the perceived thermal conductivity of the composite materials also indicates promising routes toward the development of insulation materials using renewable lignocellulosic materials.

In the case of work package 3, the glass woven fabrics were treated with silane and flax fabrics by using NaOH before the production of the composite to increase the affinity of fibers toward resin. Composite panels were prepared with four different ratios of glass and flax woven fabric reinforcement (100/0, 83.33/16.67, 50/50, and 0/100) to investigate their performance when reinforced with MDI resin in terms of mechanical, thermal, and physical properties. The composites were characterized by tensile and flexural analysis to investigate the mechanical performances. The thermogravimetric characteristics of the composites were examined for checking the thermal stability of the produced materials. The surface morphology was investigated for observing the surfaces of the composites before and after applying tensile loads. The SEM deployed EDX linear scanning was used for ensuring the signals of different chemical constituents into the matrix. FTIR test was conducted for finding out the fingerprint of chemical elements bonding of the produced composites. Besides, the water absorption and moisture content tests were also conducted to examine the moisture absorption by the pure glass, flax, and hybrid composites. Further, statistical analysis of variances was performed to test the significance of the differences in the mechanical properties of the individual types of composites developed. For investigating the relationship between the proportion of woven glass fabric in the reinforcement and the mechanical properties, regression analysis was used. The ANOVA test was also applied for checking the significance of the mechanical properties of the composites.

In the case of work package 4, The reinforcement of natural and synthetic fiber oriented woven fabrics with thermosetting polymers are getting popular nowadays. The hybridization of natural hemp with glass could facilitate the developed composite panels to be a potential candidate for automotive parts. Both hemp and glass woven fabrics were treated with greenly synthesized silver nanoparticles (AgNPs) obtained from *Tilia cordata* leaf extracts and then used as reinforcement in thermosetting epoxy resin. Three composite panels were created from five consecutive layers of glass and hemp woven fabrics (sequence is glass, hemp, glass, hemp, glass); in two of them the fabrics were loaded with 1 mM and 5 mM silver precursor loading respectively, the third one was prepared without any nanosilver loading. The presence of green AgNP was tested and confirmed by using X-ray fluorescence (XRF) and inductively coupled plasma optical emission spectroscopy (ICP OES). The nanosilver content values measured by XRF tests were 0, 655±23, and 1829±30 PPM for the composite types, control, 1 mM, and 5 mM silver precursor loaded samples, respectively. The developed hybrid composites were characterized for thermal, mechanical, physical, and morphological performance. The highest tensile strength of 40.87 MPa was found for 1 mM silver precursor treated, whereas control sample exhibited the lowest value of 16.16 MPa (without treatments). Statistical analysis of the test results also confirmed the positive influence of nanosilver loading on hybrid composites. However, the developed biocomposite panels could facilitate the industrial production units with most advanced, feasible, and multi-functional laminated products.

Structure of Dissertations

The research presented in this thesis are structured in 5 different chapters. The detailed reports of all work packages are provided under this structure of the thesis. The part of this dissertation is already published by different journals. The abstract and introduction part is written-based on the work that I have been published both as principal and coauthor by CRC Press, Springer Nature, and MDPI [7, 14, 84, 150-152], whereas the part of work package work 1 was published by Springer Nature [153], work package 2 by Elsevier [154], work package 3 by ACS [155], and work package 4 by Taylor & Francis [156]. All the chapters are mentioned below with the associated titles:

Chapter 1: Literature Reiview

A general introduction on different natural fibers, fabrics, polymers, nanoparticles, and associated biocomposites manufacturing technologies provided in this chapter. Furthermore, different research conducted by the previous scientists also provided here. However, still need to go for a long way to explore new routes and materials for composites manufacturing which are also highlighted here. The possible solutions in terms of environmentally friendly and sustainable products replacing the traditional composites also stated in this chapter.

Chapter 2: Work processes

The entire thesis is divided into four work packages to report different types of composites consecutively. A brief overview of every work packages are carried out here.

Chapter 3: General Introduction and hypothesis

In this chapter, the statement of problem corresponding to each work packages are stated elaborately along with the possible solutions and significance, in which ground the works were carried out. Moreover, a brief discussion on respective polymers and reinforcements were also provided further.

Chapter 4: Methods and Materials

The raw material and associated processing technologies to design and fabricate the composites were discussed in this chapter for all the work packages separately. Moreover, the characterization protocols and procedures of produced composites are also discussed here in this chapter.

Chapter 5: Results and Discussions

This chapter entails the discussion related to all the results and outcomes perceived in each work packages. Generally, mechanical, morphological, thermal conductivity, XRF, physical, FTIR, thermogravimetric, and colorimetric data were reported in relevant cases. In some cases, like work package 3 and 4, statistical analysis of the developed composites mechanical properties was also provided.

Chapter 6: Concluding Remarks

Finally, a compiled conclusion is drawn for all the work packages demonstrating their significance, summary, and outcomes in brief.

Chapter I: General Literature

1.1. Research Background, Potentiality, and Gaps

Cellulosic/artificial fiber reinforced composites are produced through reinforcing the respective fibers with suitable polymers/additives in the composite system. When there is at least one of the constituents in the composite systems are derived naturally can be called biocomposites. Additionally, the incorporation of nanoparticles in the composite is termed as nanocomposites. Composite materials have become a more fascinated product in this century for numerous potentialities. Natural fibers reinforced with polymeric materials like thermoplastic, thermosetting, and cementitious matrix are becoming popular significantly, especially for their light weight, strength, and sustainability features. The fiber-based composite materials provide exceptional stiffness, tensile and flexural properties, longevity, corrosion, and fire-resistant properties. Nanomaterials will also be a crucial part nowadays of developing composites with intensified performance characteristics (reducing weight, increasing mechanical properties with different improved functionalities). These remarkable characteristics have made composite materials convenient to apply for aerospace, construction, automotive, marine, biomedical, packaging, electronics, defense, furniture industries, and so on [1, 2]. Anyhow, the performances of the composite materials depend on the manufacturing processes, types of fibers used, and the polymer matrix/resin used. After all, considering the environmental sustainability and feasibility, there is a huge potentiality to develop composite panels or sheets with innovative and attractive features.

So, it is tried to develop natural fiber-based composites from coir, energy reed, bamboo, rice straw, hemp, flax, glass, carbon, lignocellulosic materials (Figure 1.1 and Figure 1.2), and so on reinforced with both thermoplastic and thermosetting polymers. In some cases, I also tried to develop some hybrid composites by reinforcing natural fiber and synthetic materials simultaneously for achieving higher thermomechanical performances. I developed some cementitious materials from natural fibers reinforced with OPC (ordinary Portland cements) [3, 4]. The mechanical properties obtained from natural reinforcements also facilitate positive reinforcement effects on the composite products. Furthermore, I also developed some nanocolorants and nanocomposites from different plants like *Tilia cordata* [5], ash plant (*Fraxinus excelsior*) [6], European yew (*Taxus baccata*) , European larch (*Larix decidua*), mushroom (*Fomes fomentarius*), and so on. The flowers, leaves, barks, fruits, and heartwood materials of plants are used for this purposes. The natural fibers also reduce extra burdens from environment through minimizing carbon footprints. Herein, considering all the positive attributions of natural fibers on composite materials the topic, “development of natural fiber reinforced sustainable composites” is selected for this research and thesis report.

As natural fibers have superior potentiality for developing biocomposite materials, they are used to produce sustainable biocomposite materials. Natural fibers are not yet studied extensively to ensure the practical applicability of the products. But as natural fibers like flax, sisal, ramie, hemp also possess superior mechanical strengths, hence could provide significant mechanical properties when reinforced with suitable polymeric materials [7]. However, after producing the composite materials, we also found superior thermomechanical and physical (water absorbency, thickness swelling, and moisture content) performances in the developed materials.

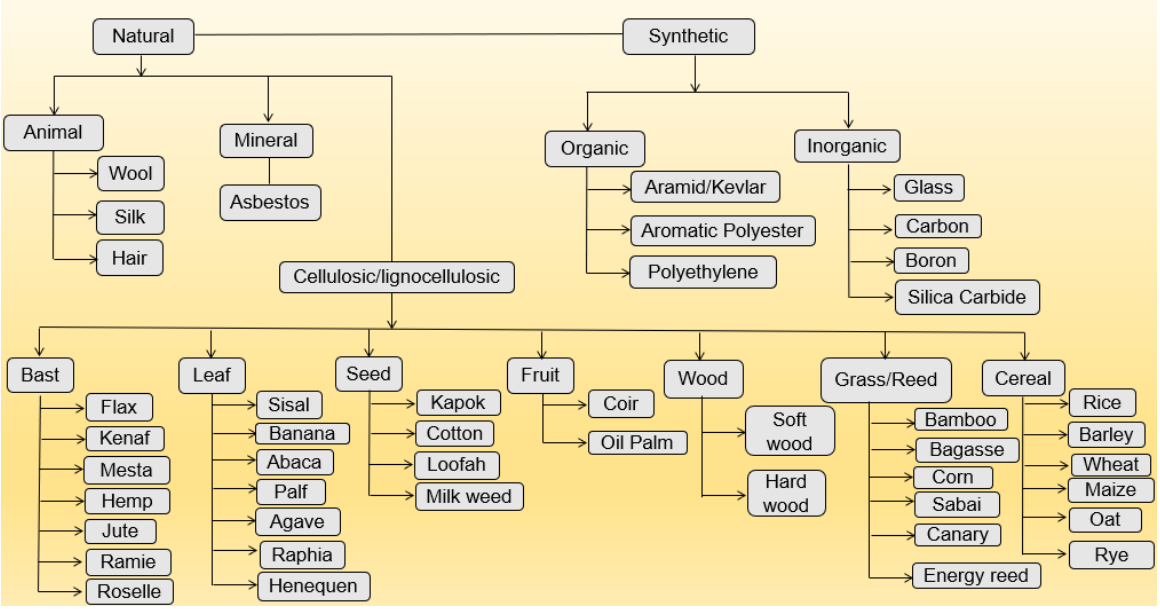

Figure 1.1: Classification of different natural fibers. Adapted with permission from Elsevier [8]. Copyright, Elsevier, 2015.

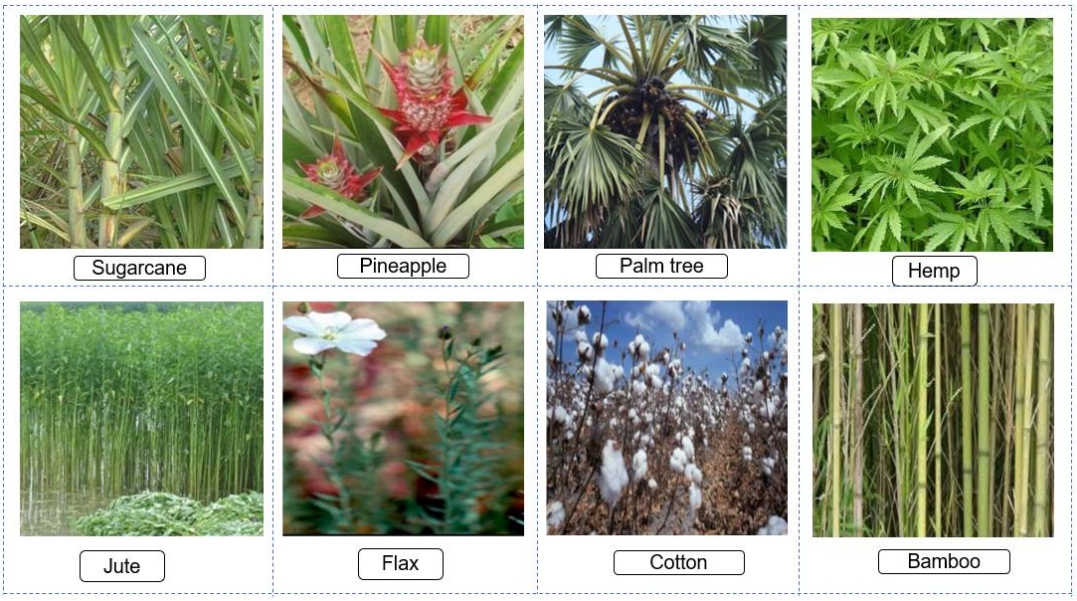

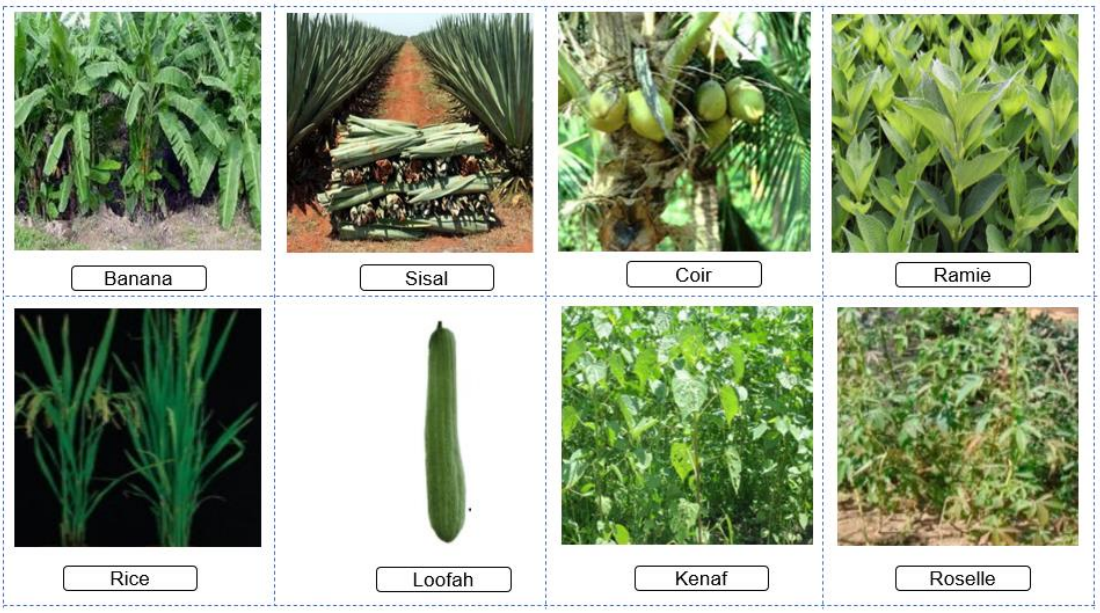

Figure 1.2 : Physical views of different natural fibers. Adapted with permission from Springer nature [7]. Copyright, Springer nature, 2021.

1.2. Natural fibers as prominent reinforcement material

Natural fibers are extensively available in nature and are found all over the world. They are renewable and biodegradable. Natural fiber-based composites are becoming popular day by day and replacing synthetic fiber-oriented composites due to their outstanding biodegradability, renewability, decomposability, stiffness, higher length-to-weight ratio, and low cost ($0.25–$4.25/kg) [7]. Natural fibers are categorized into four main classes: seed fibers (cotton, coir, and kapok), leaf fibers (sisal, agave, pineapple, and abaca), bast fibers (kenaf, ramie, hemp, jute, and flax), and stalk fibers (wood, straw, and bamboo) [9]. The extensively used natural reinforcements are cotton stalk, bamboo, rice straw, kenaf, hemp, abaca, and flax fibers. The chemical composition of these natural fibers significantly influences the performance of their composites, so their chemical properties are provided in Table 1.1.

Table 1.1: Chemical compositions of different natural fibers [10-13].

Fibers	Cellulose (%)	Hemi-cellulose (%)	Lignin (%)	Pectin (%)	Waxes (%)	Moisture Content/ Extractive (%)	Ash (%)
Cotton	89	4	0.75	6	0.6	--	--
Jute	45 to 71.5	13.6 to 21	12 to 26	0.2	--	12	0.5 to 2.0
Hemp	57 to 77	14 to 22.4	3.7 to 13	0.9	--	9	0.8
Flax	71	18.6 to 20.6	2.2	2.3	1.7	8 to 12	5 to 10
Coir	32 to 43	0.15 to 0.25	40 to 45	3 to 4	--	8	
Sisal	47 to 77	10 to 24	7 to 11	10	--	11	0.6 to 1.0
Kenaf	53.5	21	17	2	--	--	2 to 5

Sugarcane Bagasse	32 to 34	19 to 24	25 to 32	--	--	6 to 12	2 to 6
Bamboo	73.83	12.49	10.15	0.37	--	3.16-8.9	--
Ramie	68.6 to 91	5 to 16.7	0.6 to 0.7	1.9	--	9	--

Cellulose is the main chemical component of all plant-based natural fibers. It is the most noteworthy organic component produced by plants that are ample in the environment. Cellulose is composed of a long chain of glucose repeat units that are connected to form microfibrils. Chemically, it is composed of C, H, and O, having the structural formula $(C_6\ H_{10}\ O_5)_n$. Mainly, it is used to produce paper, plastic composites, and fiberboard. Besides cellulose, there is also seen the existence of hemicellulose, lignin, pectin, and a bit impurities. The chemical structures of various polymers present in natural fibers are depicted in Figure 1.3 and physical views of fibers in Figure 1.4. Moreover, wood flowers derived from hard and soft wood material are another significant source of lignocellulosic material and are shown in Figure 1.5.

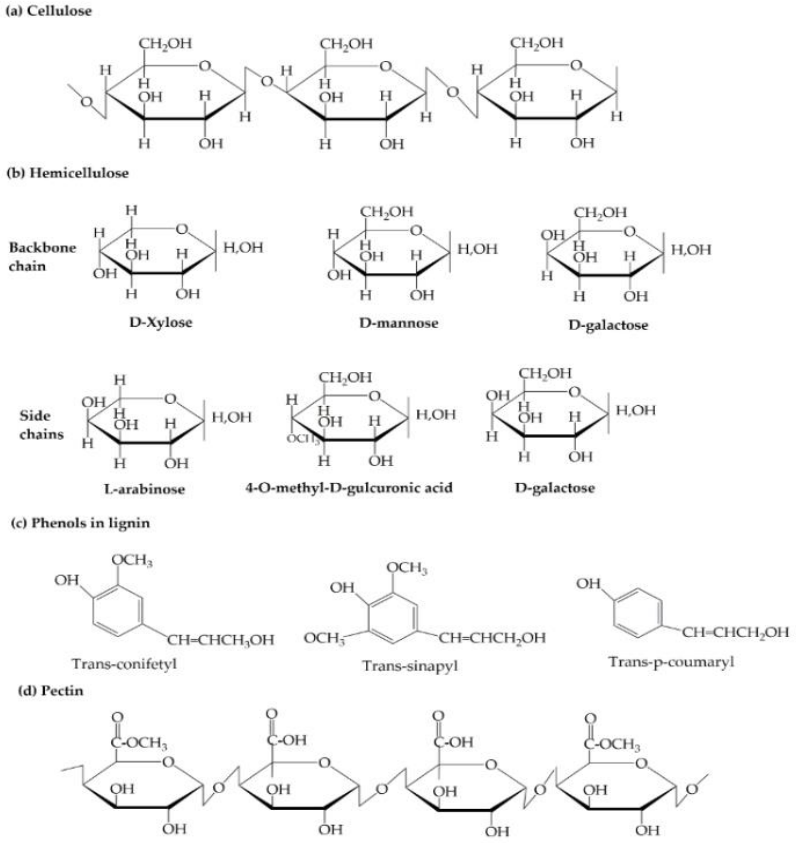

Figure 1.3: Different chemical structures of natural fibers: (a) Cellulose; (b) Hemicellulose; (c) Phenols in lignin; and (d) Pectin. Reproduced with permission from Elsevier [8]. Copyright Elsevier, 2015.

Figure 1.4: Images of few natural fibers [14]. Reprinted with permissions under Creative common license agreement. Copyright, MDPI, 2020.

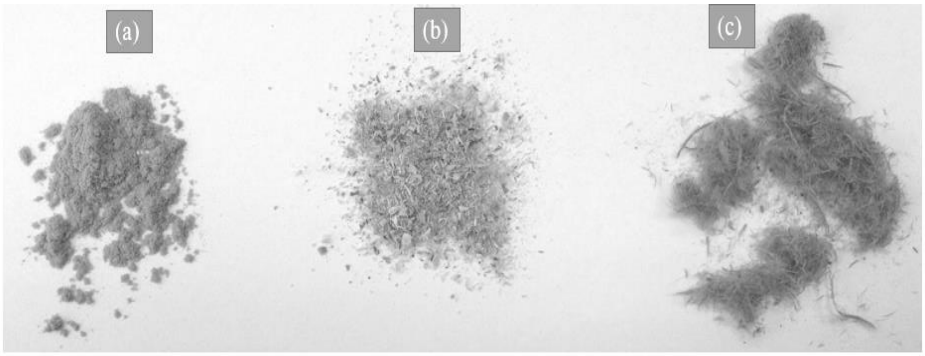

Figure 1.5: Image of (a) wood flour, (b) microparticles, and (c) fibers (actually fiber bundles). Adapted with permissions from [15]. Copyright, Wiley & Sons, 2017.

Hemp is one of the most rapidly growing natural plants and is extensively used for building materials and textile fibers [16, 17]. Likeas other natural fibers, hemp also contain significant amount of cellulose and hemicellulose (Table 1.1). Hemp fibers are abundantly available in nature, and renewable. Composites made from hemp have been used in automotive panels for a long time as eco-friendly, economical, and sustainable products [17]. Nanoparticles can enhance the mechanical properties of composites through their incorporation with cellulosic fibers (such as hemp), inorganic additives, and tributyl citrate plasticizer [18].

Coir fiber is produced by the outer part of fruits in coconut. Coir is used to produce diverse environment-friendly and biodegradable products for commercial, industrial, and household applications. It has widespread usage in mats, geotextiles, sacking, garden articles, and automotive. In terms of minimizing cost, coir could be an ideal choice for replacing glass fiber to produce thermoplastic matrix composites, due to its outstanding mechanical properties. The higher coir content (60%) increases the tensile (by 35%) and flexural strengths (by 26%) in coir/polypropylene composites [19]. However, the high fiber content (coir) negatively influences the internal bonding strength and water resistance [19]. Coir fiber has a very good capability regarding resistance against moisture, salty water, and heat.

Flax fibers are generally collected from the stem, which is a few times stronger than that of cotton [20]. Flax is a good substitute for synthetic fibers to produce composites. Flax fibers have superior mechanical properties in comparison to glass fibers. Moreover, the density of flax

is also nearly half compared to glass fibers. Therefore, when composites are formed with flax fibers, they exhibit a lighter weight and higher strength than synthetic materials [21]. Flax fibers could be reinforced with thermoplastics, thermosets, and biodegradable materials which display amiable mechanical performances.

Cotton is a widely used cellulosic fiber throughout the world. When PLA (polylactic acid) is reinforced with cotton to form composites, it exhibits good mechanical characteristics, with significant improvements in the tensile strength and Young's modulus (as shown in Table 1.2), without any reduction in strain at break [22]. Cotton burs could be a potential replacement/alternative in blending composites, rather than other agricultural plant fibers that enhance the thickness swelling, and water absorption, for post-thermal treatments [23]. Cotton has the potential to be used as a suitable reinforcement materials for producing low-cost composites. Good thermal stability of the composites was reported by different researches through improving the adhesion between cotton fiber and the polymer [24].

Ramie is a green functional bast fiber with a silky appearance, higher absorbency, air permeability, and lower wrinkle characteristics. The gummy materials obtained from ramie fibers need to be removed through a degumming process before effective industrial processing can take place [25]. It is one of the strongest biodegradable, natural fibers that exhibits high strength (Table 1.2), and antibacterial properties, and flame retardancy. PLA is brittle at room temperature, which limits the application of PLA-based polymers, but the natural fiber reinforcement (such as ramie)/nanofiller could reduce this behavior and improve the thermal and mechanical properties. The surface pretreatment of fiber like ramie is also becoming popular for significantly enhancing the mechanical properties of composites. In this regard, ramie fiber was treated with silane– that exhibited good tensile (59.3±1.2 MPa), impact (18 KJ/m^2), and flexural (135 MPa) strengths on PLA/ramie composites where 30% fibers were loaded [26].

Table 1.2: Typical properties of some selected natural fibers [1, 27-32].

Fibers	Elongation at break (%)	Density (g/cm^3)	Young's Modulus (GPa)	Tensile Strength (MPa)	Decomposition temperature (°C)
Cotton	3 to 10	1.5 to 1.6	5.5 to 12.6	287 to 597	232
Jute	1.5 to 1.8	1.3 to 1.46	10 to 30	393 to 800	215
Hemp	1.6	1.48	70	550 to 900	215
Flax	1.2 to 3.2	1.4 to 1.5	27.6 to 80	345 to 1500	220
Coir	15 to 30	1.2	4 to 6	175 to 220	285 to 465
Sisal	2 to 14	1.33 to 1.5	9 to 38	400 to 700	205 to 220
Kenaf	1.6 to 4.3	0.6 to 1.5	11 to 60	223 to 1191	229
Sugarcane Bagasse	6.3 to 7.9	1.1 to 1.6	5.1 to 6.2	170 to 350	232
Bamboo	1.9 to 3.2	1.2 to 1.5	27 to 40	500 to 575	214
Ramie	2.3 to 3.8	1.5	44 to 128	220 to 938	240

Sisal has good stiffness, durability, and resistance to salty water, which is why it has been applied for a long time in twines, ropes, papers, filters, mattresses, and carpets. Some exceptional advantages of using sisal fibers are related to its (1) lower density, (2) nonabrasive nature, (3) lower cost, (4) lower energy consumption, (5) higher possibility of filling level, (6)

biodegradability, (7) higher specific properties, and (8) generation of an agricultural-based economy in rural areas [33].

Agave is another potential natural fiber that is receiving attention from researchers and manufacturers due to its reproducibility, lighter weight, and economical aspects. Even though raw agave fibers could play a significant role in improving the reinforcing properties, some pretreatment processes of fibers have also been reported to enhance better effects. The elastic modulus of composites made from agave fibers increases with a higher loading percentage of fiber content; a similar trend was also observed for the yield strength in terms of agave/high-density polyethylene (HDPE) and agave/Polypropylene (PP) composites [34].

1.3. Fabric as potential reinforcement material for laminated composites

Fabric-based laminated composites are also used considerably for multifaceted applications in the automotive, transportation, defense, and structural and construction sectors. The fabrics used for composite materials production possess some outstanding features, including being lighter weight, higher strength, and lower cost, which helps explaining the rising interest in these fabrics among researchers. However, the fabrics used for laminates are of different types, such as knit, woven, and non-woven. Compared to knitted and non-woven fabrics, woven fabrics (some images are shown in Figure 1.6 as example) are widely used reinforcement materials. Fabrics selection for reinforcement into composites depend on different properties such as fiber types, origin, compositions, and polymeric matrices. Finite element analysis is also further facilitating the efficient prediction of final composite properties nowasdays. As fabrics are widely available throughout the world, hence the production of laminated composites from different fabrics are also feasible and cost-effective.

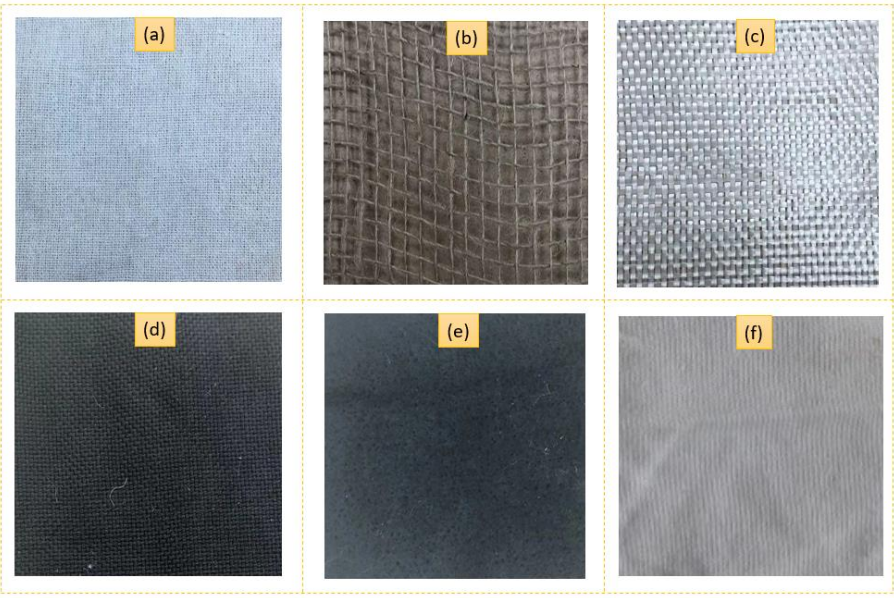

Figure 1.6: Different fabrics (physical photograph) used for composites production: (a) flax woven fabric, (b) jute woven fabric, (c) glass woven fabric, (d) carbon woven fabric, (e) carbon nonwoven fabric, and (f) cotton knit fabric. Reprinted under creative common license agreement 4.0 (http://creativecommons.org/licenses/by/4.0/) [35].

Textile fabrics (Figure 1.7) possess notable potentiality for composites used in automobiles, construction, furniture, and buildings. Both natural and synthetic fiber-based fabrics are used in composite production. However, composites made from natural fiber-based

fabrics are becoming increasingly popular due to their environmental sustainability. Conversely, synthetic fabric-based composites are also used extensively for their low cost and ease of production. Most aerospace, marine, and automotive companies currently use synthetic fiber-based composites. Fiber properties, fabric structure, the number of fabric layers, and areal density play significant roles in the composite's performance. Furthermore, together with enhanced mechanical properties, different polymeric material/nanoparticle loading also plays a notable role in providing composite materials with various functionalities like antibacterial properties and UV resistance. Generally, different thermoplastic, thermosetting, and cementitious materials are used for developing laminated fabric-based composite panels. The use of different polymeric matrix in laminated composite depends on the ultimate necessities as some polymers are suitable for better mechanical properties generation, while others are better for water absorbency and thermal conductivity.

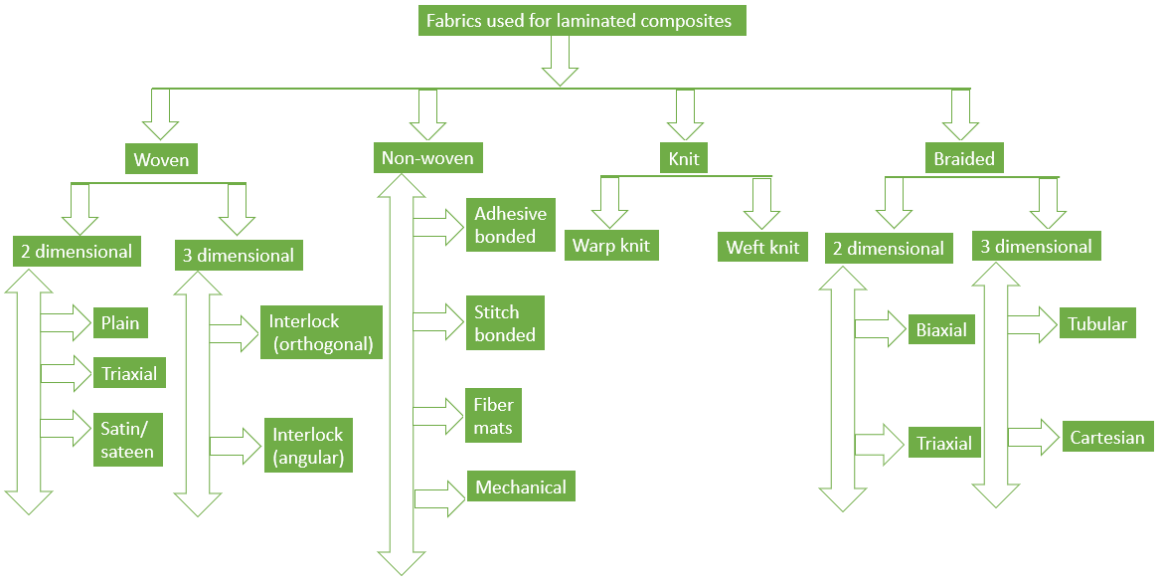

Figure 1.7: Structural classification of fabrics used for laminated composites production [35]. Adapted with permission from Springer Nature. Copyright, Springer Nature, 2021.

Not only are textile-reinforced composite materials cheaper and more widely available, but they are also increasingly being produced via automated rather than manual methods. In this regard, textile fabrics, which are pre-formed in terms of weaving, knitting, braiding, stitching, non-woven, and so, are being increasingly considered. However, the structure of selected fabrics for reinforcement plays a significant role in achieving the expected performance characteristics from composites. Yarns with higher twists provide higher strengths than those with lower twists due to efficient distributions of stress [36]. Zhou et al. [37] conducted an experiment where they studied different structures of carbon-based woven fabrics in terms of plain and twill structure and found that differences in fabric structure at uniaxial directions exert limited influences on the strength and modulus of the composites. The same study further claimed that particular fabric structure also exerts influences on the stress concentrations and crack propagations [37]. In another study, Aghaei et al. [38] mentioned that fabric geometry (woven) plays a vital role in influencing the mechanical performances of the composites. Researchers are also becoming increasingly interested in knitted fabric as another prominent potential reinforcement material for composite development. Chen et al. [39] developed sandwich composite panels with significant tensile strengths (124.28±18.64 MPa for carbon fabric/epoxy/glass knit fabric and 332.36±53.18 MPa for carbon fabric/epoxy/carbon knit fabric) and compressive performances by using weft knitted structured fabrics. Ramakrishna [40] conducted a research on wale (lengthwise yarn) and course (crosswise yarns) directions of

knitted fabric which were reinforced with epoxy resin and the developed composites were tested in terms of tensile strengths and elastic modulus, where the elastic modulus was predicted as per laminated plate theory and cross-over modeling.

Fabrics possess excellent drapability around any device or tool; this can be further facilitated with a suitable tool with specific structure, where the fabrics could be shaped with compatible resin [41]. Various processing methods, such as compression forming, roll forming, diaphragm forming, molding, and machining, are applied for the formation of fabric reinforced composites. Previously, researchers were involved with unidirectional fabric composites developments [42]. However, following this, researchers began to investigate discontinuous unidirectional fabric composites [43]. Woven fabrics were considered as a potential composite material, but the usage of knitted fabrics also became popular in later periods. However, composite material produced fom fabric reinforcement indicates numerous potentialities for high-performance composite materials. Researchers are currently examining numerical simulation softwares to predict material properties, which could facilitate adequate corrective actions prior to production. Some of the test specimens developed by our research group is shown in Figure 1.8.

Figure 1.8: Composite samples from different woven fabrics developed in our lab: (a) flax woven fabric reinforced PP composites, (b) jute woven fabric reinforced MDI composites, (c) flax woven fabric reinforced MDI nano composites (AgNP loaded), (d) flax woven fabric reinforced PLA composites, (e) hemp/glass woven fabric reinforced epoxy composites, (a) glass/flax woven fabric reinforced MUF composites.

1.4. Polymers

A matrix holds all of the reinforcing fibers and agents together in a composite to transfer/share any external stress within the constituents for providing protection against any degradative processes, either in a mechanical (tensile/flexural damage, delamination, high temperature, creep, and water absorption) or chemical form. The matrix is also termed as an embedding material, and plays a critical role in composites carrying tensile loads in the structure [44]. There are four important matrix types: (1) metallic, (2) polymeric, (3) carbon, and (4) ceramic. The most used matrices in manufacturing companies are polymeric resins, which are mainly thermosetting polymers and thermoplastics. Thermoset matrices are crosslinked during the curing process. The crosslink is produced upon heating or by adding the curing agents.

Consequently, thermoset plastics become stronger and stiffer, which has made them an attractive polymer matrix in traditional fiber-reinforced composites, such as carbon or glass fiber-based composites. Unsaturated polyester resin, epoxy resin, novolac, polyurethane, urea formaldehyde, melamine resin, and vinyl esters are popular thermoset polymers (Figure 1.9). RTM, hand lay-up, spraying, filament winding, extrusion molding, reactive injection molding, spin casting, and compression molding methods are used to process thermoset polymers [45]. All polymers exist distinct physical and mechanical properties (Table 1.3).

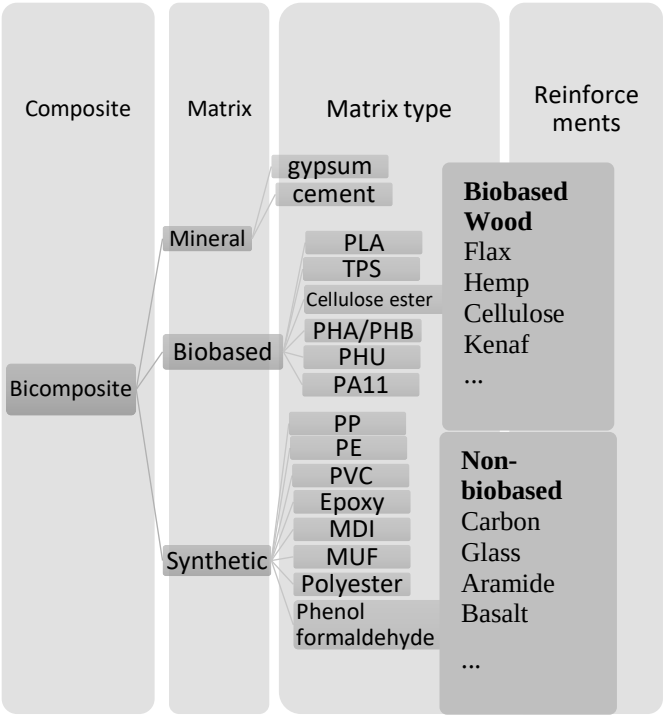

PVC– polyvinyl chloride; PHA–polyhydroxyalkanoates; PHB–poly (3-hydroxybutyrate); PHU–polyhydroxyurethanes; PA– polyamide.

Figure 1.9: Different matrices, reinforcements, and type of matrix used for biocomposites formation [46].

Table 1.3: Characteristics of different polymers used for composites production [1, 47, 48].

Polymeric resin	Type of resin	Density (g/cm^3)	Elastic modulus (GPa)	Tensile strength (MPa)	Elongation at break (%)
PLA	Thermoplastic	1.25	0.35-3.5	21-60	2.5-6
HDPE	Thermoplastic	0.94-0.96	0.4-1.5	14.5-38	2-130
LDPE	Thermoplastic	0.910-0.925	0.055-0.38	40-78	90-800
Nylon 6	Thermoplastic	1.12-1.14	2.9	43-79	20-150
PS	Thermoplastic	1.06-10.4	4-5	25-69	1-1.25
PP	Thermoplastic	0.899-0.920	0.95-1.77	26-41.4	15-700
Starch	Thermoplastic	-	0.125-0.85	5-6	31-44

Epoxy	Thermoset	-	3-6	55-130	2-10
Polyester	Thermoset	-	2.07-4.41	41.4-89.6	2-2.6

Conversely, thermoplastic polymers require a suitable temperature (Table 1.4) for processing and retain a solid state of matter after cooling. The molecular weights of thermoplastics are very high, and the polymeric chains are interconnected through intermolecular forces. The prime advantage of these polymers is that they can be reheated multiple times, without any major changes in the original properties for any kind of reformation. PP, PLA, PE, PS, PVC, and acrylonitrile butadiene styrene (ABS) are some common examples of thermoplastic polymers. Recently, some of the naturally-derived biodegradable polymers like PLA is also attaining popularity due to the increased sustainable features over synthetic polymers (Table 1.5).

Table 1.4: The melting temperature (T_m) and glass transition temperature (T_g) of some commonly used resins [1].

Resin	Melting Temperature (T_m) in °C	Glass Transition Temperature (T_g) in °C
PLA	150 to 162	58
PP	160 to 176	0.9 to 1.55
Nylon 6	222	40
Polyester	250 to 300	60
LDPE	105 to 116	120
HDPE	120 to 140	80
Epoxy	–	70 to 167
Starch	110 to 115	60
Polystyrene	–	100–135

Table 1.5: Different biodegradable polymers [49].

Naturally originated biodegradable polymers	Synthetic biodegradable polymers
(a) Polysaccharides – Chitin – Cellulose – Starch – Konjac – Levan	(a) Polyester – Poly (caprolactone) – Poly (lactic acid) – Poly (glycolic acid) – Poly (ortho esters)
(b) Polyester – Polyhydroxyalkanoates	(b) Poly (anhydrides)
(c) Lignin	(c) Poly (amides)
(d) Natural Rubber	(d) Poly (amide-enamines)
(e) Shellac	(e) Poly (vinyl alcohol)
(f) Proteins – Gelatin/collagen	(f) Poly (vinyl acetate)

– Silk, elastin, fibrogen, casein, albumin – Protein achieved from grains	
(g) Lignin	(g) Some poly (acrylates) (h) Some poly(urethanes)

The polymers which are are cooled from melted condition can be arranged into regular crystalline structures too but under a certain condition. However, as formed crystals provide less perfect structures compared to the crystals formed from low molecular weight copounds. A basic structure could be illustrated in terms of lamellae which is comprised of layered folded chains (Figure 1.10). A typical crystallite can be of 10 to 20 nm thickness [50]. Interestingly, as polymers do not contain uniform molecular weight, hence they can facilitate to manufacture only partially crystalline structures.

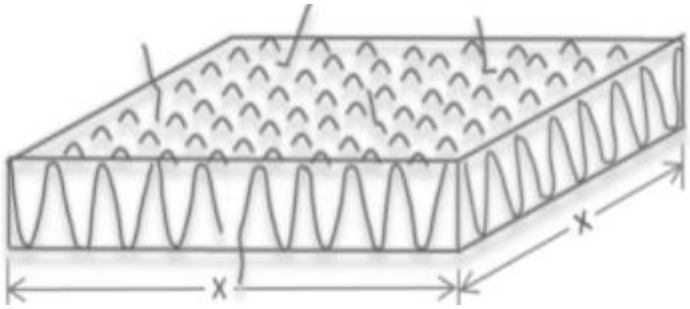

Figure 1.10: A basic structure of lamellae [50].

1.5. Nanomaterials

Besides the traditional thermoplastic and thermosetting polymers, nanoparticles are also receiving attention in terms of their potential to improve the functionality and mechanical performances of nanocomposites. These remarkable characteristics also have made nanocomposite materials convenient to apply in aerospace, mechanical, construction, automotive, marine, medical, packaging, and furniture industries, through providing environmental sustainability. Nanoparticles (TiO_2, carbon nanotube, reduced graphene oxide (rGO), ZnO, and SiO_2) are easily compatible with other ingredients (matrix polymer and biofibers) and can thus form nanocomposites. Nanocomposites are exhibiting a higher market volume with new technology and green approaches for utilizing natural fibers. The performances of nano-biocomposites depend on the manufacturing processes, types of natural fibers used, and the matrix polymer.

Nanocomposite materials are formed with two, three, or more components; one is in matrix form and the others are in particle or biofiber forms (Figure 1.11). Whenever any load is applied to nanocomposite materials, it is shared equivalently with every part. The greatest benefits of polymer-based nanocomposite materials are the higher productivity potential on an industrial scale, the ease of processing technology, and a reduction in manufacturing costs. Fibers, especially biofiber-reinforced composites and nanocomposite, offer better advantages compared to conventional composites.

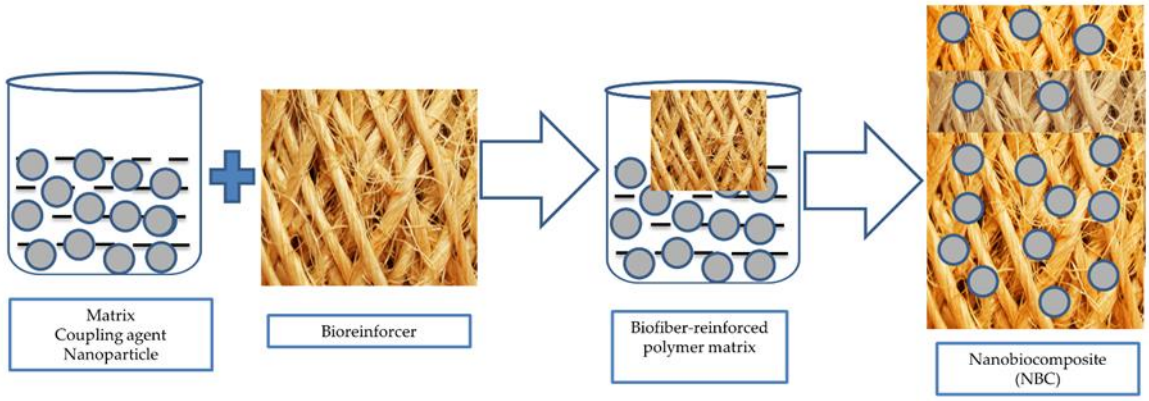

Figure 1.11: Formation mechanism of nanobiocomposites.

The combination of organic natural fibers and inorganic or organic polymers and nanoparticles has a high potential for improving mechanical performances thus expanding the areas of application. Some of the demerits regrading natural fiber reinforced composites and nanocomposites are 16ummarized in Table 1.6. Recently, various inorganic nanoparticles were studied for incorporating them with natural fibers in the matrix to form nanocomposite, especially for their biodegradability. This results in the development of an interfacial bond between the fibers and polymers in a composite, whereas the organic phase helps to form an inorganic matrix [51].

Table 1.6: A brief summary on the merits and demerits of natural fiber-reinforced composites and nanocomposite over traditional petroleum-based composites [1].

Number	Merits	Demerits
(a)	Comparatively lighter	Higher moisture absorption
(b)	Low cost	Low impact strength
I	Biodegradability	Poor flame retardancy
(d)	Renewability	Not suitable with a higher processing temperature
I	Better insulation and thermal performances	Poor resistance to microbial attack
(f)	Nontoxicity	Variation in quality
(g)	Environment-friendly	Complex supply chain of natural fibers for geographic locations and availability
(h)	No irritations with physical contact	/
(i)	Low energy consumption	/
(j)	Best alternatives for replacing synthetic fibers	

1.5.1. Various polymeric nanocomposites on silver nanoparticle treated fibers

Researchers are also nowadays getting interested on developing food packaging composite materals through treating the fiber materials with AgNPs before fabricating with thermosetting/thermoplastic polymers. In this regard, Khan et al. [52] developed nanocomposites for food packaging from AgNP treated hemp hurd and PLA polymers for antibacterial food products. The developed composites also provided significant thermal stability and mechanical properties [52]. Therefore, there is a significant potentiality for treating

various fibers with AgNPs and then to fabricate with suitable polymers for producing nanocomposites.

1.6. Mechanics of composites

The mechanics of composite materials deal with stress, strain, and deformations in structural engineering applications subjected to thermal, mechanical, physical, and fatigue loadings. The traditional composite mechanics were simply assumed as the homogeneous and isotropic materials like steel and aluminium. But, the fiber/ wood particles reinforced composites are generally not homogeneous and isotropic. Therefore, the dealing and analysis of such fiber/ wood particles reinforced composites are much more complex compared to traditional isotropic materials. However, the mechanics of fiber/ wood particles reinforced composites are studied mainly in two different ways: one is micromechanics level and another one is at macromechanics level [53].

(a) Micromechanisc level: The interaction of composite constituent materials are investigated in microscopic level. The distinct properties of the fiber and matrixes in the composite lamina system faicilitate to find the micromechanical properties like thermal, strength, stiffness, and moisture expansion coefficient.

(b) Macromechanisc level: The fiber/particle reinforced composites responses against thermal and mechanical loadings are studied on macroscopic level.

Kirchoffs hypothesis is popularly used as a classical lamination theory for anlyzing infinitesimal deformations of laminated structures (thin). There are several models available for predicting the short fiber and particle reinnforced composites. However the models could be grouped on five basic models [53]:

(a) law of mixtures
(b) Shear lag
(c) Laminated plate
(d) Vibrational principal, and
(e) Eshelbys model

In another study, Tabres et al. [54] has proposed three different models for tensile failure of the hybrid composites. The first model entailed the dry fiber bundles whiich depend on the fiber strengths statistics. Seond model entailed the multiple fragmentation of composite materials, and the last one is numerical modelling which warrant random distribution and stochastic nature of fibers.

1.6.1. Classical lamination plate theory

Classical lamination theory (CLT) evolved during 1960s which helped to undertsand the complex coupling effects in the laminated composites. This theory is helpful for predicting the strain, displacement, and curvature which generated when mechanical/thermal load is applied. In case of analytical method, some assumptiones are needed in order to solve the problem which builds the foundation of this theory. The following assumptions are considered to calculate the residual stresses under lamination plate theory [55]:

- The composite lamina is thinner plate (under plane stress consdition)
- The behavior pattern of the materail is linear elastic and remain unchanged over the time

- Microscopic residual stress calculation

It is reported that there is around 25% chemical shrinkage happened during the curation, therefore nearly 25% errors maybe found during the residual stress calculations [56]. The moisture and curing processes are two important factors for developing residual stresses in the composite. However, the residual stresses can be calculated numerically, analytically, and experimentally; whereas CLT is the most common and applicable theory to calculate the residual stresses. By using temperature-independent mechanical characteristics and CLT method the residual stresses could be measured most accurately. In some cases, like gradual failure in the applications like pressure vessels may happen due to fiber failure and inter fiber failure in the composites, which can not be precisely investigated using CLT. Therefore, Knops et al. [57] developed another model named Subu, where such kind of failure process in the fiber/polymer composite system could be more realistically calculated through quantifying the loss of stiffness [57].

1.7. Fiber to matrix adhesion

Natural fibers have inherent incompatibility with the polymers due to presence of some impurities like as oil, wax, and so on. Therefore, it is imperative to remove such unwanted impurities before the fabrication which will enhance the interaction in the composite system. Moreover, the treatments also break the atomic bonds from the fiber surfaces which will enable to functionalize them [58, 59]. However, the surfaces of the natural fibers could be modified in numerous ways like chemically, biologically, and physically.

1.7.1. Physical methods

There are several physical methods available for treating the plant-based fiber materials like as ultrasound, UV light, and plasma. In case of physical method, the bundle of fibers is separated, and the structure of the fiber surfaces are modified prior to composites fabrication. Among them plasma treatment is the widely used physical approach of surface modifications. This method is highly effective especially for the modifications of natural fibers surfaces. However, plasma method is also divided into two more groups: one is thermal and another is nonthermal methods [60]. Plasma is ionized gas (partially), comprising of radical, ionic, molecular, and excited atomic species along with the photons and free electrons [61].

1.7.2 Chemical methods

Alternative to the physical methods, chemical technology like silane treatment, mercerization/alkali, maleated coupling, acetylation, permanganate and peroxide, etherification, graft polymerization, benzoylation, isocyanate, and so on. The surface and mechanical properties of the fibers are improved through chemical-based modifications. A covalent bond is formed between the hydroxyl groups of cellulosic fibers and the chemical reagents used for pretreatment [62]. Crystalline structures of the natural fibers could also be improved through removing the weakly adhering polymers like as lignin from the fiber surfaces [11]. Moreover, water absorption and moisture contents of fibers and associated composites can be minimized through surface modifications for example using water repellent agents.

1.7.3 Biological methods

Although physical and chemical methods are widely used technologies nowadays, however there are still disadvantages for such approaches due to the usage of hazardous

chemicals, generation of wastages and pollutants, consumption of excessive energies, additional cost for purchasing of chemicals and machineries/equipment usages. Therefore, more eco-friendly and cost effective methods are also taken under considerations. In this regards, microorganisms like enzyme, bacteria, or fungi could facilitate to overcome such challenges through modifying the natural fiber surfaces even consuming comparatively lower energy [63, 64]. Hence, such kind of treatments are also called as "green" treatment methods. Like as, enzymatic treatments could remove the hydrophilic hemicellulose, lignin, and pectin from the surfaces of plant fibers through removing the hydrophilicity from the cellulose substances [65]. The principal behind this phenomenon of the catalytic process is the oxidoreductases and hydrolases [66].

1.8. Biodegradation of composites

Biodegradation means the chemical dissolution of respective materials/products by bacteria or any other biological agents (Figure 1.12). The principal reason behind the development of green composite is the biodegradations, beside the utilization of non-petroleum-based sustainable resources which in turn will not adversely effecting the environment. Moreover biodegradation has far distinct meanings than that of compostable materials as biodegradation is related with the degradation by microorganisms to ensure usual returning to the natural environment, whereas compostable indicates the breakdown of the objects in compost pile [67]. The organic materials are easy to be degraded aerobically in the presence of oxygen, or even anaerobically without oxygen. Petroleum-based hydrocarbons are relatively easier to degrade due to biological metabolism. The biodegradation depends on the presence of hydrocarbons. As different polymers, fibers, and versatile treatment of fibers are carried out in order to produce biocomposites, hence the exact determination of biodegradation is challenging. However, still there are several methods available for decompositions assessment like as the measurement of weight loss and mechanical properties, SEM analysis, FTIR spectroscopy, and so on [68]. Moreover, a realistic test is necessary to determine the perfect biodegradation test. Komal and his team [69] conducted a research on pretreated banana fiber (5% alkaline) reinforced composites with PP (extrusion-injection molding), where they found that although pretreatment had increased the mechanical properties in the compositesbut shown a decline whenever buried under the soil for 5 days. The buried samples shown a decline in 7.69% tensile, 12.06% flexural, and 3.27% impact strengths [69]. The same study [69] also investigated the effects of samples mechanical properties under the immersion in water, however, the significant changes were noticed in case of the soil buried samples. The similar effects (loss in mechanical properties) were also reported in the case of lignocellulosic fiber reinforced LDPE composites in anther study [70].

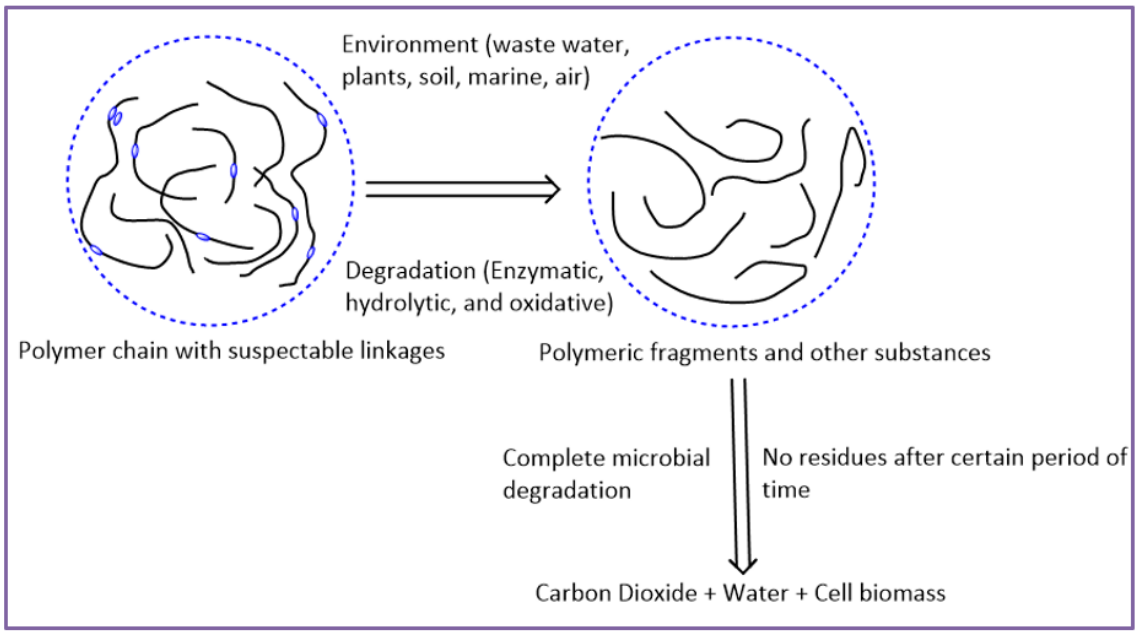

Figure 1.12: Biodegradation of biofiber-based composites. Adapted with permission from Reference [71]. Copyright Polymedia Publisher GmbH, 2009.

1.9. Fabrication of reinforcements (fiber and fabric) with matrix

The main raw materials of biocomposites are natural fibers or wood, either in virgin particles or saw dust from industry, see Figure 1.13**.** Biofillers provide higher stiffness and tensile strengths when reinforced with compatible polymers, which transmits shear stress to the matrix uniformly and protects the produced composites from external forces/destructions [72, 73]. However, the most compelling features of biocomposites are biodegradability and biocompatibility, in view of generating less burden and carbon footprint to the environment. Although natural fibers provide less durability but, when used with polymeric resin/synthetic fibers, they exhibit higher strength, stability, and significant performance. Additionally, durability and sustainable features of a composites, should be adjusted to the expected product life cycle [74].

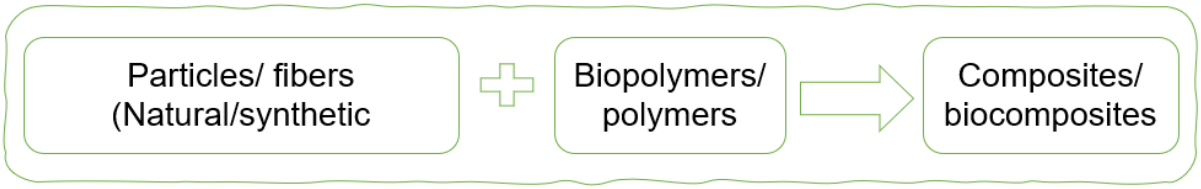

Figure 1.13: Normalized scheme for composite/ biocomposites production.

Generally, most of the cellulosic fibers contain cellulose, lignin, hemicellulose, and small proportions of impurities. The strength and stiffness of the fibers depend on their cellulose content [75]: the higher the cellulose content, the higher the strength. The degree of polymerization of cellulose and the microfibril angle of cellulose also influences the resultant mechanical properties [76]. Besides, cellulosic fiber-reinforced composites generate the highest renewable energy (6%) savings in contrast to glass-reinforced composites (2.9%) [77].

1.10. Design and fabrication of composites

The proper design of natural fiber reinforced composite is highly important to get the expected features and performances. The main purpose of scientific research, innovation, and

development is a part related to the life cycle of products. However, the actual engineering of the products starts with the development of science. The engineered design and fabrication could innovate a novel product or supplement to an available/existing item in the market through enhancing competitive advantage. The efficient design of composite trails numerous challenges along on account of the lack of available information, diverse fiber geometry, the orientation of fibers in the composites, variable characteristics of different thermosets and thermoplastic polymers, varied dimensions of fibers. There are several factors responsible for fruitful composite/ biocomposite/ nanocomposites design: (a) material selection, (b) fitness purpose, (c) ease of product manufacturing, (d) product cost, (e) production volume, (f) durability, (g) product quality, (h) maintenance feasibility, (i) operational cost, (j) efficiency, (k) environmental sustainability, and (l) safety aspects [78]. Some of the variable considered during composites manufacturing are pointed in Figure 1.14.

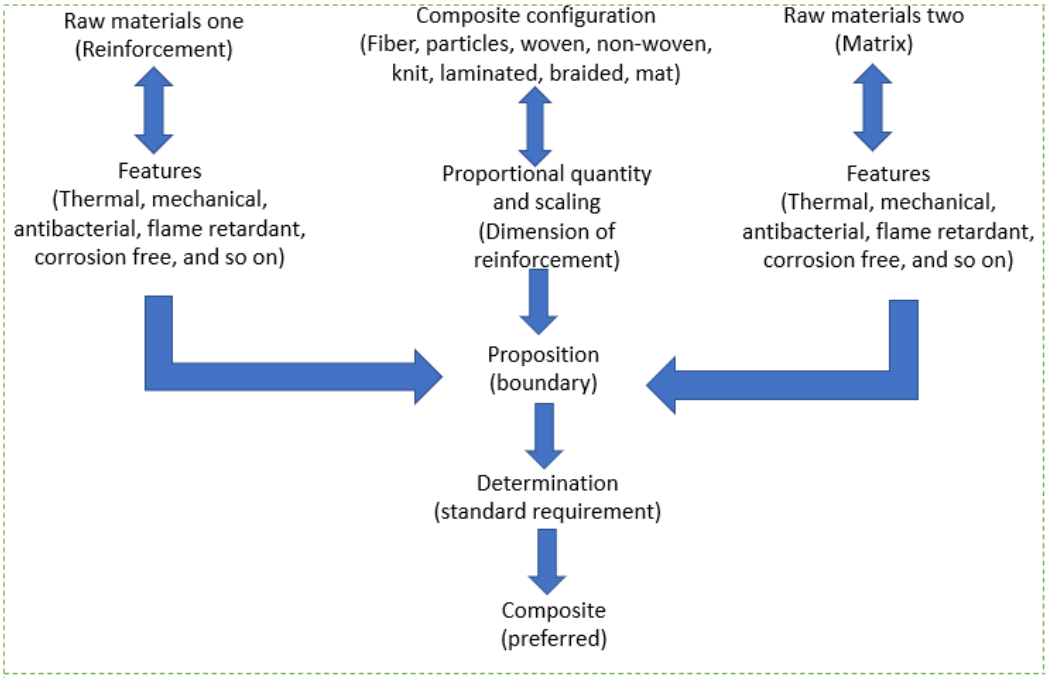

Figure 1.14: Different variables used for composite designing process.

Nowadays, probable experimental results of composite are also being predicted by FEA. Different software like ANSYS, Abaqus, and SolidWorks are used to serve this purpose. The ultimate results of the manufactured composite could be compared with the FEA results, and if needed, the model could be redesigned again according to the achieved output. SolidWorks is an efficient tool for the simulation of mechanical performances of composite with due respect to stress and strain [79]. So, this software has gained high reputation for predicting accurate results of the composite. The parameters used for experimental work could be used to simulate the data in advance through SolidWorks. Rosdi et al. [80] used SolidWorks for stress and strain analysis to enhance the durability of their materials produced. ANSYS is also used to simulate the mechanical structures through FEA to investigate the strength, temperature distribution, toughness, elasticity [81, 82], and so on. Sometimes assumptions are taken into consideration such as homogeneity and regular orientation of biobased fibers/wood materials, perfect bonding between the fiber and matrix, and the lack of voids for simplifying the FEA models [83].

1.10.1. Fabrication techniques of different fiber/paticle reinforced polymeric composites

There are several methods available for successful fabrications of fiber/paticle materials. The most known methods for composites fabrications are compression molding, injection molding, RTM, pultrusion, hand lay-up, calendering, extrusion, and so on (Figure 1.15). However, as we used pressing/hot pressing fabrication methods for most of our fabrication, hence processing parameters, functioning, and tools used for this technology is described in this section [84]. However, as pressing/ hot pressing technology was mainly used for producing the composites, hence a brief discussion is introduced here.

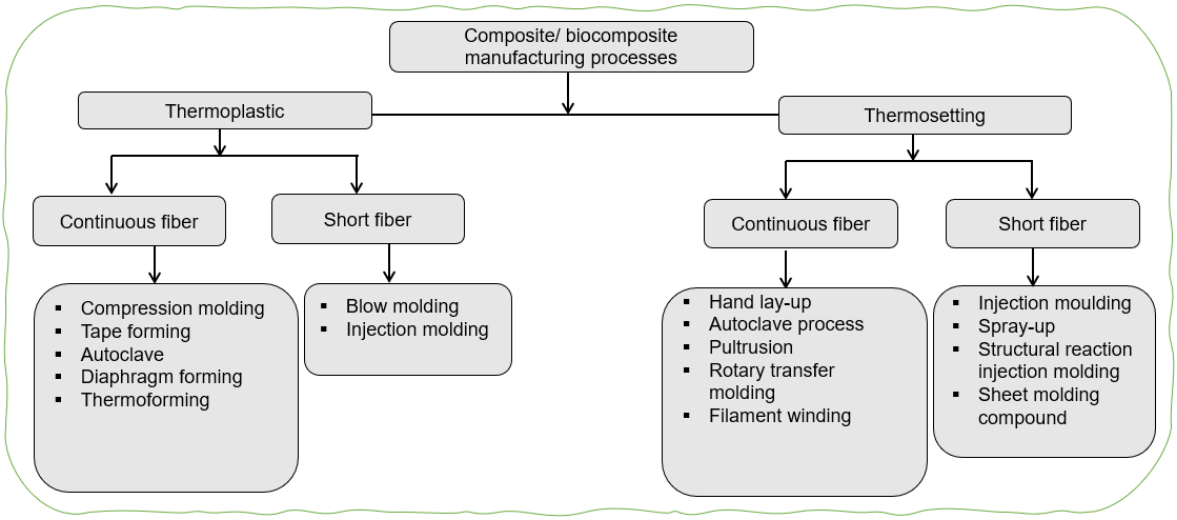

Figure 1.15: composite/ biocomposite manufacturing methods depending on thermosets and thermoplastics.

1.10.2. Pressing and hot pressing techniques

Hot pressing has become a very important process for composite/ biocomposite manufacturing, which effects the final products quality and performances significantly. The final shape and structure of the particle/fiber composites is given through compressing the mat with or without the application of high temperatures and pressure. The moisture content of the boards is reduced here along with the curation of adhesives. The key technologies of pressings could be:

- Pre-pressing or pressing
- Cold or hot pressing
- Continuous or discontinuous pressing
- Panel pressing or moulding

The pre-pressing of mat (50–60%) is easier for introducing the hot pressing. Besides, the time for hot pressing is also reduced along with less possibility of failure if the mat is pre-pressed. During the first stage of pre-pressing, air exits from the mat through the sieve belt, where the maximum linear pressure is 30 N/mm. In the second stage, compressive force on the belt is performed by four cylinders, where the maximum linear pressure is 250 N/mm. The belt speed could be adjusted within the range of 1 to 60 m/min.

In case of hot pressing, ways of heating of the mat can be as follows:

- Contact (heating through thermal oil/steam/hot water/electrical)

- Microwave and combined technique
- High frequency (in case of molded products or higher thicknesses)
- Steam injections (for higher thicknesses)

In case of fiberboard productions, (a) wet process and (b) dry processes are used. The moisture content of the mat is reduced from the last stage (wet process), whereas mat height could be reduced by applying dry methods.

The hot process can be divided into following categories:

- Continuous
  - Calender press (BISON–MENDE process)
  - Double belt flat bed system (Siempelkamp, Dieffenbacher, and Küsters)
- Discontinuous/batch [85]
  - Single daylight press
  - Multi daylight press

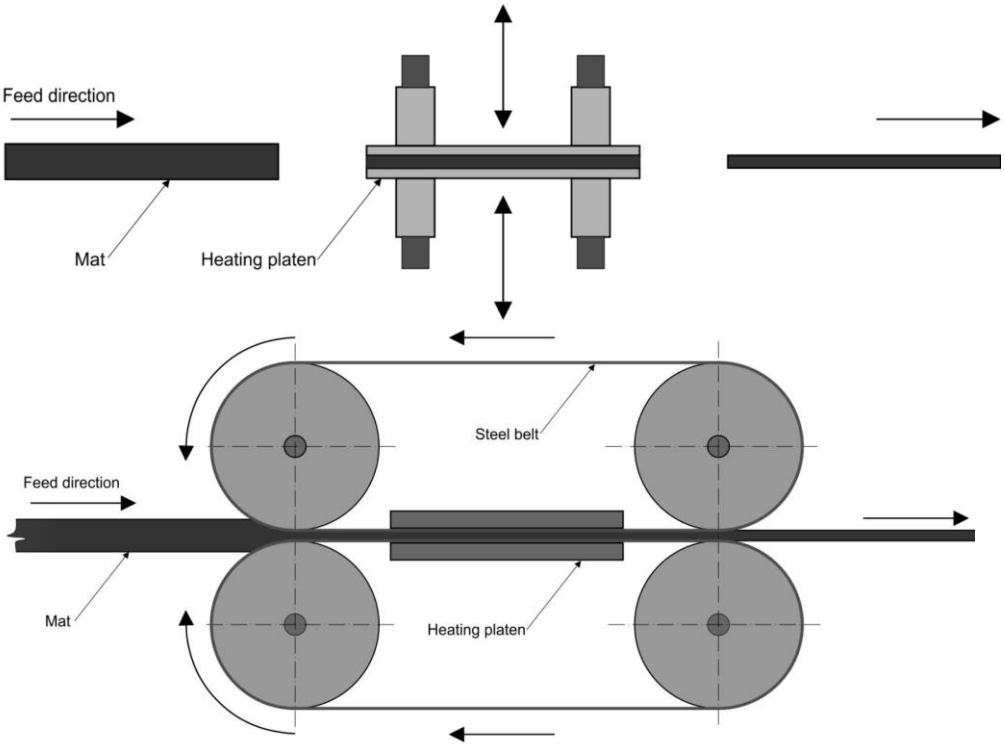

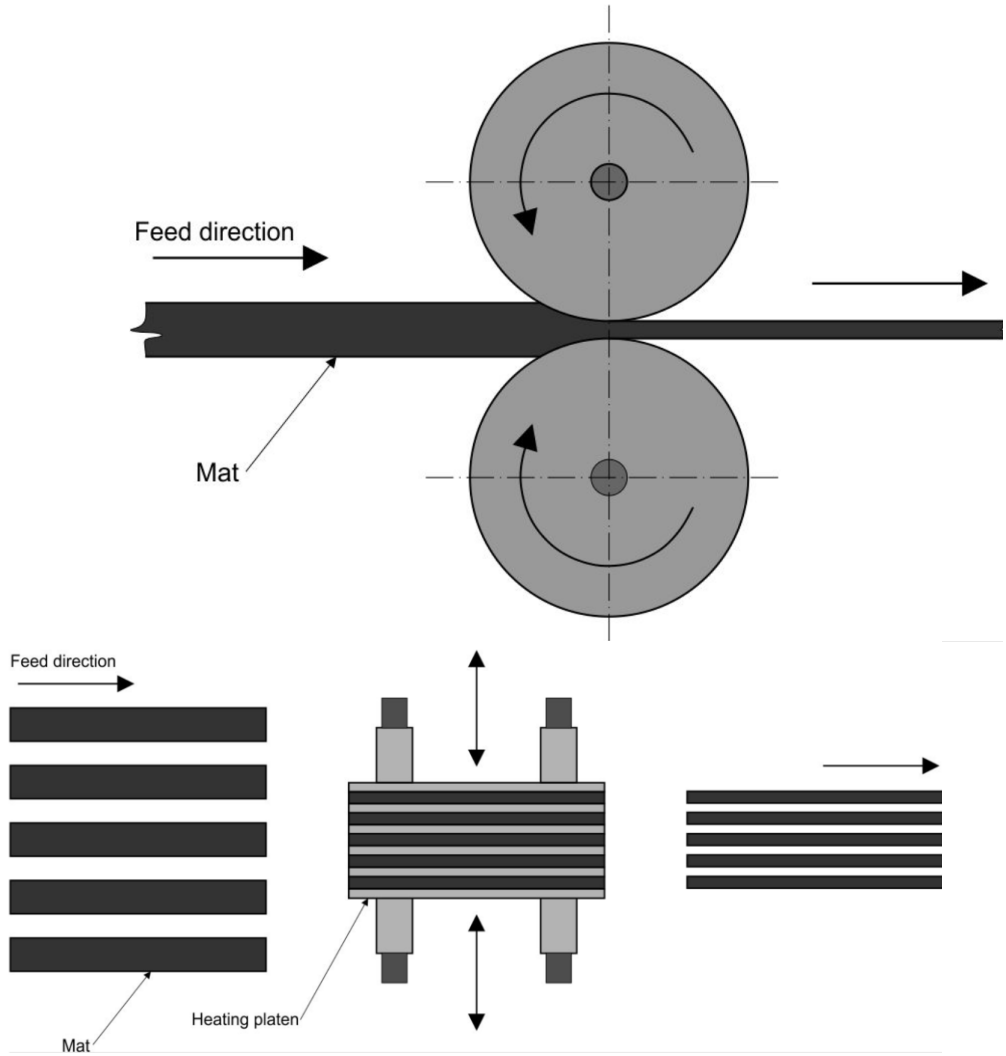

Figure 1.16: Different pressing and hot pressing mechanisms (drawing by Péter György Horváth).

Continuous common steel belt is used in batch production for transferring pressure and heat to the mat in the pre-pressing process (Figure 1.16). At the same time, the equipment needs to be able to transfer the mats from continuous to batch pressing. However, continuous process is simpler to produce particleboards. It is possible to manufacture diversified product items with wide range of size and thicknesses as the press is applied on longer piece of panels [85]. Larger boards are needed to produce for getting the maximum benefits of single daylight process. Most of the facilities installed are 25 m long or more [85]. However, a 52 m press was in operation in UK until 2009 [85]. After completion of this process, trims need to cut precisely for avoiding edge effects. In case of multi daylight pressing, up to 48 panels can be produced simultaneously. It is important to ensure the same temperature and pressures on all the boards. Generally, 4 to 8 boards (5 to 7 m long) are produced with 2.5 m width by using multidaylight process [85].

The pressing parameters are set in sections such as:

- Entering section,
- High pressure section,
- Medium pressure section,
- Cooling section.

Siempelkamp is a widely used hot press machine. Its typical design includes as follows:

- Flexible press table
- Rigid pressing head
- Upper and lower press plates
- Frame modules
- 2–4 hydraulic cylinders
- The whole volume should be heated above 100 °C temperature

The time for pressing depends on the technology. The required temperatures for curing should be reached over the whole cross-sections of the composite panel. Processes as bellow take place in the course of pressing:

- Heat transport
- Material transport
- Curing of adhesives
- Change of structure of mat

1.11. Composites characterizations

1.11.1. Tensile characterization of composites

Tensile properties of composites can be improved with the increase of fiber content but up to a certain level (optimum). After this level, tensile properties start to decline again [47]. The tensile tests are conducted as per different standards protocols as discussed in various articles [86, 87]. The surface modification of plant fibers also enhances the tensile properties of composites by ensuring better compatibility between the fiber and polymers. It was also found that the presence of non-cellulosic fibers is responsible for the poor tensile performance of composites. Compatible surface treatments can reduce the impurities present in natural fibers, thus enhance tensile strength and Young's modulus [88]. This finding was also confirmed by Ramraji et al. [89] whore ported that the alkaline treatment of flax fiber enhanced the tensile strength by 35% in polymeric composites. A simple tensile testing sample (ISO 527–1) and model are illustrated in Figure 1.17 and Figure 1.18. Mechanical properties of some natural fiber reinforced composites are listed in Table 1.7.

Figure 1.17: A schematic representation of tensile test samples

Figure 1.18: A tensile testing design for natural fiber reinforced composites sample using Instron testing machine [90].

Table 1.7: Mechanical properties of various cellulosic/artificial fiber/particle reinforced polymeric composites.

Reinforcement/ matrix	Tensile strength (MPa)	Tensile modulus (Gpa)	Flexural strength (Mpa)	Flexural modulus (Mpa)	Elongation at break (%)	Internal bonding strength (Mpa)	Method	Ref.
Flax/glass with phenolic resin	412.5±12.7–392.5±20.0	40.8±1.4 – 39.7±0.6	–	–	0.99±0.04 – 0.96±0.06	–	Compression molding	[21]
Hemp (35%)/ polyester	60.2	1.736	112.9	6.38	–	–	RTM	[91]
Jute/PP	56.71	1.82	77.32	4.34	–	–	Injection and extrusion molding	[92]
Ramie (5 layer)/ Epoxy	99.04±2.85	–	98.73±5.98	–	–	–	Compression molding	[93]
Kenaf/PP	24.67	2.35	45.56	2.37	–	–	Injection molding	[94]
Sisal/epoxy	83.96±6.94	1.58±0.08	252.39±12.11	11.32±1.02	–	–	Hand lay-up	[95]
Sugarcane bagasse/PU	–	–	14.9	1.53	–	1.18	Hot-pressing	[96]

Sugarcane bagasse/Portland cement	–	–	2.97	1.044	–	–	Pressing	[97]
Rice straw/LDPE	13.7	0.144	33.7	1.6	24.1	–	Injection molding	[98]
Bamboo/starch (C300)	45	–	58	–	–	–	Hot-pressing	[99]
Coir/polyester	16.46		29.22	–	–	–	Hand lay-up	[100]
Abaca-GFRP/epoxy	44.5	0.27	12.5	–	15.05	–	Hand lay-up	[101]
Pineapple/epoxy	80.12±2.23	8.15±0.23	~100	–	–	–	Hand lay-up	[102]
Coir/PLA	5	1.5	25	3.2	0.7	–	Hydraulic pressing	[103]
Rice straw/PP	33.2±0.5	1.66±0.025	36.5±0.5	1.28±0.027	23.9±2.9		Injection molding	[104]
Reed/citric acid	–	–	12.51	2.45	0.54	1 7.98	Hot-pressing	[105]

1.11.2. Flexural characterization of composites

Flexural strength and modulus are further significant parameters for assessing the composites performance. They indicate the capability of the composites to withstand bending load. The magnitude of reinforcement fiber loading influences the flexural strength. However, different loadings of fibers significantly influence the flexural properties (both the strength and modulus) [106]. There are different testing methods discussed and used by other scientists are followed for flexural properties analysis. Sathish et al. [107] found that in the case of flax and bamboo fiber reinforced epoxy, the flexural properties enhanced with the increase in flax fiber in the composite system. The highest flexural strength (298.37 Mpa) was attained when the proportion of flax and bamboo was 40:0 [107]. When the hemp fiber was bonded with PLA, the highest flexural strength was found at 30% fiber loading [108]. When cellulosic nanofibers were used with epoxy resin, the flexural strength was enhanced by 45 Mpa and the bending modulus by 3 Gpa [109]. A simple flexural testing model is illustrated in Figure 1.19 and Figure 1.20.

Figure 1.19: A flexural testing design for natural fiber reinforced composites using Instron universal testing equipment.

The modulus of rupture (MOR) is calculated as per Equation 1.1 [3]. Where, F indicates maximum load/force, l is span length (mm), b is specimen width, t is thickness, and a is deflection.

$$\mathrm{MOR} = \frac{3Fl}{bt^2} \qquad \text{Equation 1.1}$$

$$\mathrm{MOE}, \mathrm{E_m} = \frac{\mathrm{l_1^3} \times (\mathrm{F_2} - \mathrm{F_1})}{4\mathrm{bt^3} \times (\mathrm{a_2} - \mathrm{a_1})} \qquad \text{Equation 1.2}$$

MOE (Equation 1.2) demonstrates modulus of elasticity, l_1 is span support, increased load (N) on the straight direction of the curve ($F_2 - F_1$), F_1 stands for 10% of F_{max}, F_2 stands for 40% of F_{max}, $a_2 - a_1$ is the increased deflections measured from sample center related with the increased load $F_2 - F_1$.

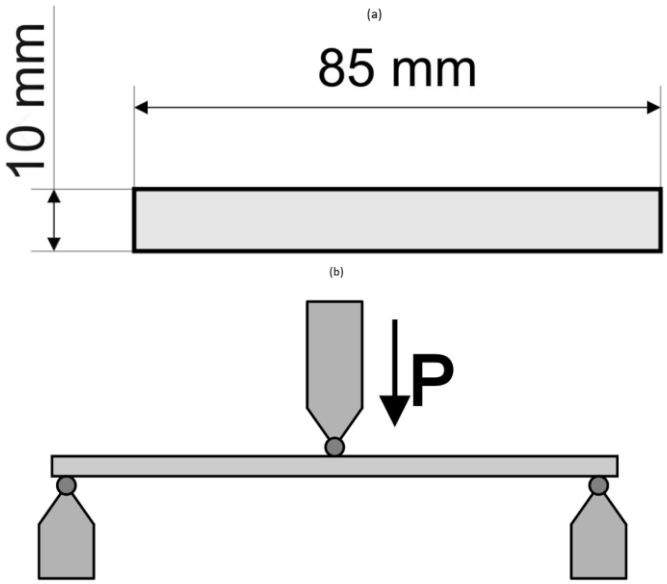

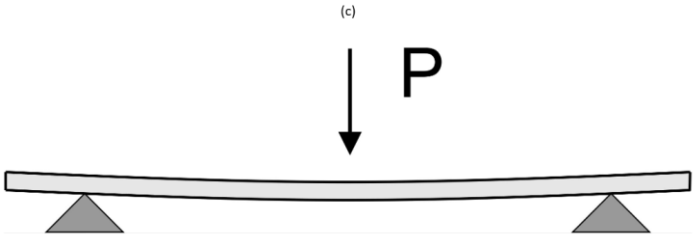

Figure 1.20: Flexural test: (a) samples geometry, (b) schematic diagram of three-point flexural test design and place samples in the system, and (c) schematic diagram of bent samples during the test. Drawn by Péter György Horváth.

1.11.3. Physical properties of composites

Studying physical properties of composite is important to investigate the dimensional stability of the developed products. Water absorption, thickness swelling, and moisture content of composites are considered as the principal physical properties. A schematic diagram of immersion of composite samples under the water is shown in Figure 1.21. The water absorption of composites entails the effect of moisture content characteristics and dimensional stability of composites, debonding between the fiber to matrix, and associated strength loss [110]. Furthermore, higher water absorption and poor thickness swelling results in decreased mechanical properties [111]. The natural fiber-oriented fabric reinforced polymeric composites provide higher moisture contents than artificial fiber-oriented composites because the natural fibers contain cellulosic polymers . The reason for the higher moisture contents of natural fiber-based [14] fabric composite is the presence of hydrophilic compounds like –OH, $–NH_2$, –COOH, and –CO groups. Furthermore, the pretreatment of fibers before composite formation could also lead to the increased moisture content, water absorbency, and thickness swelling properties [112]. Water absorbency of the composite samples is measured as per Equation 1.3, thickness swelling by Equation 1.4 and moisture contents by Equation 1.5.

$$W_a = \frac{W_{w-}W_d}{W_d} \qquad \text{Equation 1.3}$$

Where, W_a indicates water absorbency, W_d initial weight of specimens before submerging in water, W_w is the weight of specimens after the immersion in water.

$$T_s = \frac{T_{w-}T_d}{T_d} \qquad \text{Equation 1.4}$$

Where, T_s indicates thickness swelling, T_d initial thickness swelling of specimens before the immersion in water, T_w is the thickness swelling of specimens after the immersion in water.

$$M_c = \frac{M_{b-}M_d}{M_d} \qquad \text{Equation 1.5}$$

Where, M_c indicates moisture content, M_b initial weight of specimens before drying, M_d is the weight of specimens after drying.

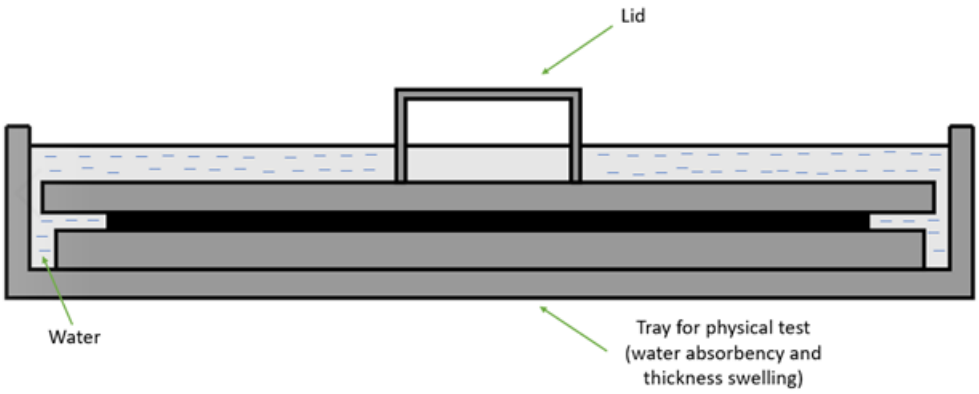

Figure 1.21: Schematic representation of water absorbency and thickness swelling test. Drawn by Péter György Horváth.

1.12. Application of composite/ biocomposites

The current global demand for composite products motivates manufacturers toward more decorative, advantageous, and diversified composite materials. Due to workforce availability and low material costs, China, Malaysia, Vietnam, Thailand, and Indonesia are currently the largest producers of laminated composites [113]. Manufacturers use natural fibers reinforced composites extensively, although they have some limitations regarding fracture/damage of composite systems, which reduces the structural, mechanical performances of the composites [114]. Due to their outstanding properties – such as being lightweight, anti-corrosion, superior thermo-mechanical characteristics, and the overall large volume of production capabilities – composites are extensively used in aircraft structural applications such as lightweight aircraft, helicopters, sailplanes, light machinery parts, bridges, construction, buildings, and commuter planes (Figure 1.22) [115]. Moreover, the shipbuilding sector also uses glass-reinforced laminated composites for smaller vessels like yachts and fishing boats [116]. Naval applications are also expanding from sustainable laminated composite panels [117]. Carbon-based laminates used in prominent vehicle parts are becoming more popular in the automotive sector [118] even in more than last 50 years. Composites from glass are also being implemented in areas where safety and security issues, such as in aerospace, defense, automotive windshields, and solar cell module materials, all of which are designed from structural and architectural points of view. Composites could provide higher mechanical performances, security, and environmental sustainability as structural materials [119]. In a most recent study, Chillara et al. [120] discussed morphing technology for laminated composites which could be used by soft robotics, aerospace, and automotive manufacturers as it could be shaped and tuned as per the desired performances over various ranges of operations. Defense industries are also using various types of composites (like synthetic fiber or natural fiber or natural/synthetic fiber hybridization with compatible polymers) [121, 122].

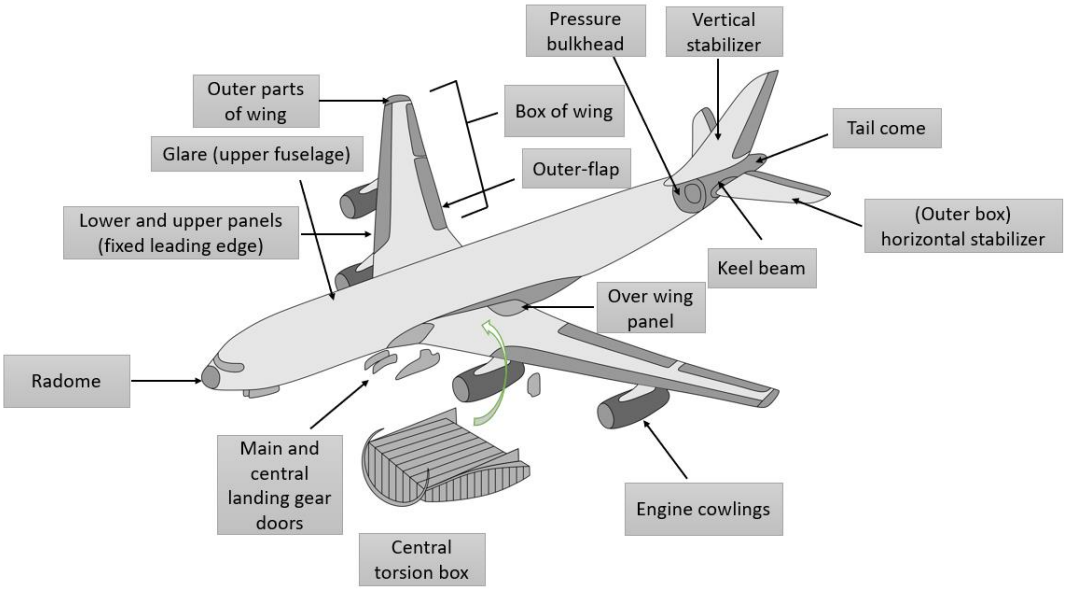

Figure 1.22: A schematic representation of where laminated composites could be used prominently on airplanes (A380 model of Airbus). Drawn by Péter György Horváth. Adapted with permission from Elsevier [123]. Copyright Elsevier 2011.

As natural fibers are replacing synthetic fibers through generating new routes of the use of green materials with enhanced sustainability, the proper design of composite becomes highly important. Furthermore, a business-friendly environment could nourish this sector significantly throughout the world. Different applications of natural fiber reinforced composites are shown in (Table 1.8). Composites show diverse potentiality to be the applicable product for multiple sectors from even in packaging to biomedical products (bone plates for fracture fixation) [124]. The interiors of cars and cabins of trucks are also made of composite [125]. The construction and building industries also use composite materials for floor beams, interior panelling and exterior siding of facades even with attractive appearances. The natural fiber reinforced composites are also used in the electronics sector (like circuit boards, mobile casing, and so on) [126]. In general, the natural fibers are comparatively cheaper, widely available, and environment-friendly materials. Biocomposite materials could be used for housing constructions, building, household materials, flooring, fences, automotive, aeronautical, decking, furniture (chair springs), power industry (housing of transformer), and sport materials. It is expected to reach the composites market 36.67 billion USD by 2022 throughout the world with a compound annual growth rate (CAGR) of 14.44% for a 5 years duration starting from 2017 to 2022 [127]. The safer product and recycling capability features are a few of the key indicators for this quick market expansion.

Table 1.8: Application, manufacturing method, and matrix materials of some potential natural fibers.

Reinforcing Fibers	Polymeric Matrix	Manufacturing Method	Application	References
Cotton	PLA, silane, and LDPE)	Extrusion and injection molding	Building, automotive, furniture, and food packaging	[128-131]
Jute	Polyester and PP	Compression/injection molding and hand lay-up	Door panels, ropes, roofing, durable chairs,	[132, 133]

			kitchen sinks, sanitary latrines (slab and rings), helmets, and chest guards	
Hemp	PE, PU, and PP	Compression molding and RTM	Automotives and furniture	[134, 135]
Flax	Epoxy, PLA, polyester, and PP	Vacuum infusion, RTM, and hand lay-up	Textile, automotive and structural	[136, 137]
Coir	PE, PP, and epoxy resin	Extrusion and injection molding	Building boards, insulation boards, roofing sheets, and automotive structural components	[138, 139]
Sisal	Polystyrene (PS), PP, and epoxy resin	Compression molding and hand lay-up	Body parts of automobiles and roofing sheets	[140, 141]
Kenaf	Epoxy resin, PLA, and PP	Pultrusion and compression molding	Bearings, automotive parts, and tooling	[142, 143]
Sugarcane Bagasse	HDPE and PVC	Compression molding, injection molding, and extrusion	Interior of automotives (side panels, seat frames, and central consuls)	[144, 145]
Bamboo	Epoxy resin and PLA	Compression molding	Hardware for electronics, furniture, and toys	[146, 147]
Ramie	PLA, PP, and polyolefin	Injection molding through extrusion	Civil and bulletproof vests	[148, 149]

In future, the efficient design and modelling of composites is going to play a revolutionary role, before going to production by using different computer-aided tools which could be a benchmark to produce more cost-effective and user-friendly products. Recently, lots of green composite-based products have been available in the market. This market has a higher potentiality to be increased further significantly for the regulations imposed by the governments/organizations in different countries/regions around the globe.

Chapter II: Workpackages

The overall research reported in this thesis are divided into four work packages as we produced various types of composite panels from different polymers and cements which are published in different journal. The work packages are named in terms of work package 1, 2, 3, and 4. The title of each work packages are provided bellow:

Work package 1: Rice straw and energy reed fmaterials reinforced phenol formaldehyde resin polymeric biocomposites.

Work package 2: Semi-dry technology-mediated coir fiber and scots pine particle-reinforced sustainable cementitious composite panels.

Work package 3: Thermomechanical behavior of Methylene Diphenyl Diisocyanate-bonded flax/glass woven fabric reinforced laminated composites.

Work package 4: Hemp/glass woven fabric reinforced laminated nanocomposites via in-situ synthesized silver nanoparticles from *Tilia cordata* leaf extract.

Chapter III: General Introduction and Hypothesis

3.1. Work package 1: Rice straw and energy reed materials reinforced phenol formaldehyde resin polymeric biocomposites

Still now, the research on hybrid composites development through utilizing energy reeds and rice straws are not studied yet to make them usable as a prominent biocomposite material. Chemical composition of both energy reed and rice straw is shown in Table 3.1. According to the composition, it is seen that both of them are prominent lignocellulosic materials enriched with cellulose, hemicellulose, and lignin. Energy reed plants are grown nearby the lake shores and sea. There are some organizations like Energianövény-Team Kft., company (Lengyeltóti, Hungary) which is working since 2006 for harvesting energy reeds in eastern and central European countries [157]. However, the same company is also taking initiatives to expand the energy reeds cultivation in some other neighboring countries of Hungary like in Romania, Slovakia, and so on from 2017 [157]. The energy reed plants materials could potentially be used as suitable raw materials for food packaging, biomass heat power, and afterall, high strength composite panels [157]. The energy reeds are used to produce bioenergy in some European countries like in Finland [158], however, the potential applications on composite fields is needed more attempts to explore. In this regard, it could be interesting work to explore more viable options of fiber materials and processing methods to enhance the performance characteristics of sustainable products. Interfacial bonding between the fiber and polymer is extremely important. However, one of the possible reason behind the poor internal bonding strengths maybe the poor interfacial adhesion between the fibers and matrix. However, the pretreatment could facilitate with the improved fiber to matrix interactions [73] which could consequently increase the mechanical performances of the biocomposites as well. In this regard, pretreated energy reed is attempted to reinforce with PF resin through hybridized with another prominent natural resources like rice straw. It is found that the performance of the biocomposite panels increased with the increase of energy reeds fiber content in the composite systems. However, unfortunately, according to our knowledge, still now no research on energy reed fiber reinforced polymeric composites are found yet to carry on with the comparative study.

Table 3.1: Chemical components present in reeds fiber and rice husk material.

Constituent polymers	Energy reed fiber [159]	Rice straw fiber [160]
Cellulose	50.3	35.6
Hemicellulose	21.7	20.5
Lignin	15.0	16.8
Mineral ash	4.0	15
Moisture content	–	12.1

Rice is extensively grown throughout the world as a popular agricultural products. Rice straw is a common agricultural byproduct which is inexpensive and abundantly available as the naturally derived waste material having no commercial values that is why generally burnt or thrown away in the field for disposal after the extractions of rice [161, 162]. However, the burning and associated disposals create some extra burdening effects to the environments through generating CO_2. Nevertheless, the rice straws generated from rice milling industries could be utilized as the prominent biocomposite material. There is around 20% of total rice product is considered as the byproduct materials [163]. The polymeric components present in

rice husk (Table 3.1) demonstrates that cellulose is the main chemical component here like as other natural fibers. There are also significant presence of lignin and hemicellulose in the polymeric structures of rice husk. However, the as-mentioned rice straw could be conveniently used for biocomposites productions too. El-Kassa et al. [164] reported about the rice straw reinforced urea formaldehyde resin composites where they found 24.00 MPa MOR (modulus of rupture), 2850 MPa MOE (modulus of elasticity), and 0.50 MPa IBS (internal bonding strength). Zhang et al. [165] developed hybrid composites from rice straw and coir fibers reinforced with PF resin and found 30.23 MPa MOR, 4.55 GPa MOE, 0.41 MPa IBS, and 13.09 % TS (thickness swelling) for 100% rice straw and 27.16 MPa MOR, 2.92 GPa MOE, 1.00 MPa IBS, and 8.06% TS for 50% rice straw and 50% coir fibers for medium density fiberboards (728 kg/m^3). However, still now, no researches performed yet on energy reeds and rice straw reinforced hybrid polymeric composites.

Moreover, the pretreatment of natural fibers could facilitate with the enhancements in thermomechanical performances in the composite systems through improving the fiber to matrix interactions. There are different pretreatment methods like mercerization, acetylation, etherification, peroxide treatment, graft copolymerization, benzoylation, and so on for natural fibers surface modification . However, the alkaline pretreatment method is used for this research to treat the energy reed and rice straw materials before the fabrications. In order to achieve the better performance characteristics through fiber treatment, it is required to use an optimum concentrations of alkaline reagents like NaOH or Na_2CO_3 [166, 167]. The possible reaction mechanism of energy reed and rice straw materials are shown in Equation 3.1 and Equation 3.2. On the other hand, in European countries, medium density fiber boards (MDFs) are widely produced and used composite materials. In this regards, both the rice straw and energy reeds are collected from central European regions to find out more diversified renewable materials for medium density biocomposite panels production.

$$Rice\ straw - OH + Na - OH \rightarrow Rice\ straw - O^- - Na^+ + H_2O \quad \text{Equation 3.1}$$

$$Energy\ reeds - OH + Na - OH \rightarrow Energy\ reeds - O^- - Na^+ + H_2O \quad \text{Equation 3.2}$$

The mechanical properties found from rice husk reinforcement is lower compared to energy reeds. However, the incorporations of energy reeds with the rice straw1 enhanced the performances of developed biocomposite panels due to the attribution of positive hybrid reinforcement effects. Moreover, this research work would facilitate the biocomposite panel manufacturers with a sustainable and novel materials from renewable sources, where energy reed fibers could function as a new reinforcement biomaterial.

3.2. Work package 2: Semi-dry technology-mediated coir fiber and scots pine particle-reinforced sustainable cementitious composite panels

Plant-based renewable materials exhibit notable potential to help shift the world from synthetic products to green and eco-friendly products. Cementitious materials are extensive in building, construction, and structural applications; however, the increasing global demand for sustainable products has intensified the pressure on scientists and manufacturers to keep up with demand. In this regard, plant-based renewable lignocellulosic materials like coir, jute, sisal, abaca, hemp, flax, ramie, spruce, Scots pine, beech, and Turkey oak could all be crucial choices. The chemical constituents of naturally derived plant materials like lignin, cellulose, hemicellulose, and other materials are all potential candidates for cementitious reinforcements with reagents like OPC. Current efforts to develop OPC bonded lignocellulosic composite materials are tremendous. However, drawbacks continue to linger, particularly in selecting

optimal reinforcement materials (lignocellulosic) to achieve satisfactory thermo-mechanical performances. Our previous study [168] attempted to utilize lignocellulosic saw dust (industrial byproducts) to develop cementitious materials, but our experiments could not attain internal bonding strengths higher than 0.5 MPa. Consequently, we began investigating lignocellulosic materials that are more convenient and discovered the following: both coir fiber and pine particles provide internal bonding strengths higher than 0.5 MPa when mixed together. Moreover, cement incompatibility with lignocellulosic materials [169] is another significant drawback that needs to be overcome to attain satisfactory performances. Generally, cement is alkaline in nature and on its surface it possesses the hydroxyl (–OH) group, which intensifies in wet conditions that have higher pH values [168, 170]. This phenomenon is responsible for the decay of hemicellulose from the polymeric structures of plant-based materials, resulting in significant strength loss.

Additionally, clinker materials like dicalcium silicate and tricalcium silicate help the cement setting by creating calcium silicate hydrate through exothermic reactions in the presence of water. Water-soluble polymeric compounds like hemicellulose, sugar, and tannin also restrict the compatibility between the cements and plant-derived lignocellulosic materials. Hence, it is better to use additive materials like Na_2SiO_3 (water glass/ sodium silicate), $MgCl_2$ (magnesium chloride), $CaCl_2$ (calcium chloride), and $Al_2(SO)_4)_3$ (aluminum silicate) [169, 171]. The pretreatment of the lignocellulosic materials could help to facilitate with improved compatibility between natural fiber/wood and cements. However, pretreatment is unnecessary if the reinforcement materials have no impurities or are below the acceptable limits of 0.4% for tannin content and 0.5% for sugar content [169]. These limits necessitate the examination of sugar and tannin contents of the materials prior to composite panel manufacturing. However, the minimized inhibition between lignocellulosic materials and cement facilitates higher strengths in the composite panels. Moreover, two ratios – the type of wood species/lignocellulosic materials and cement ratio, and the water to cement ratio – also play vital roles in cementitious composite panels [172].

The proper selection of lignocellulosic materials like plants is important as not all plant-derived materials are suitable for cementitious materials production due to the differing chemical structures of various plants. Additionally, plant growth, plant maturity, and the harvesting period/season also determine the strengths of lignocellulosic materials and composited materials. Research studies exploring the reinforcement possibilities of Scots pine with OPC [171, 173] have been conducted. However, according to our knowledge, no research studies concentrating on the hybridization of Scots pine with natural lignocellulosic fibers like coir have been completed yet. Scots pine is extensively available in central European countries like Hungary. Scots pine represent a large group of Hungarian forested area [174]. On the other hand, coir fibers are also popular seed fibers that have been widely grown in some Asian countries for a long time. Coconuts are primarily grown for their water and fruit, not their shells. Once the water and fruit have been extracted from the coconut, the husks, which do not biodegrade quickly or easily, are conventionally disposed of as waste. This practice creates numerous environmental burdens. However, coconut husks could be used as a potential raw material for biocomposite and cementitious materials as well. It has been reported that coconut husks contain around 30% fiber materials and 70% coir piths [175]. Coir has significant potentiality to improve the thermomechanical properties of hybrid composite panels when mixed with scots pine and OPC, which is the focus of the current research study. Moreover, both coir and scots pine contain significant amounts of cellulose, hemicellulose, lignin, and pectin in their polymeric structures (Table 3.2). As Table 3.2 shows, coir fiber contains more lignin (41 to 45%) than scots pine (27 to 29%), which may facilitate coir with higher mechanical

properties in the produced composite panels. Moreover, the higher lignin content in coir also makes it more durable, rot-resistant, and elastic [175].

Many different types of cements – such as Portland, aluminate, sulfate, phosphate, and sulfo-aluminate – are currently available [176]. Some derivatives of Portland, like OPC, Portland blast furnace, Portland pozzolana, fly ash, etc., are among the most widely and commonly used cement matrixes [176]. OPC is a widely used binding reagent due to its cost effectiveness and availability [177]. The current study used OPC type I cement to develop the composite materials. CaO and SiO_2 are the two main chemical constituents of cements and comprise 64.18% and 21.02%, respectively. Al_2O_3, Fe_2O_3, MgO, SO_3, Na_2O, K_2O, TiO_2, Cl, P_2O_5, and Cr_2O_3 are also present in varying proportions (Table 3.3).

Moreover, the utilization of renewable lignocellulosic materials for flooring, wall, and roofing application in the building and construction sector could expedite lower costs, lower energy consumption, lower environmental burdens, and thermal comfort. Consequently, cementitious materials developed from renewable plant-derived resources and OPC could encourage construction that is more environmentally sustainable. Though forested areas in the world continue to shrink, the combination of natural fibers with plants [178] could accelerate potential alternative lignocellulosic materials for OPC bonding via hybrid composite production. The current study implemented a semi-dry technology to produce composite panels from coir fibers and Scots pine particles and their associated composites. These are similar to the wood particle/cement composite panels used by the manufacturing industry. Comparatively, semi-dry technology is cheaper and more convenient as it is less capital intensive and less labor intensive [3, 179]. However, research on semi-dry technology oriented natural fiber-reinforced cementitious materials remains limited. In this regard, the current research developed cementitious composite panels using semi-dry technology, which is a novel and innovative fabrication method for scots pine/coir fiber and OPC that, to our knowledge, has not been reported yet. Moreover, this research will facilitate manufacturers of engineered construction materials by means of an economic, green, and feasible method of hybrid production as well as composite panel production.

Table 3.2. Chemical components present in coir fiber and Scots pine material.

Constituent polymers	**Coir fiber (wt%) [180]**	**Scots pine (wt%) [181]**
Cellulose	36–43	44–46
Hemicellulose	10–20	25–28
Lignin	41–45	27–29
Pectin	3–4	15
Moisture content	8	12.1
Others	–	3–4

Table 3.3: Chemical compositions of OPC materials.

Chemical component	**OPC type I (wt%) by Ferreiro et al. [182]**
CaO	64.49
SiO_2	19.01
Al_2O_3	5.51

Fe_2O_3	3.81
MgO	0.99
SO_3	3.69
K_2O	0.43
Na_2O	0.28
Loss in ignition	2.34
TiO_2	0.27
Cl	0.01
P_2O_5	0.35
Cr_2O_3	0.01

*OPC– Ordinary Portland cement; PC– Portland cement

3.3. Work package 3: Thermomechanical behavior of Methylene Diphenyl Diisocyanate-bonded flax/glass woven fabric reinforced laminated composites

Polyurethane (PU)-based resins are derived from vegetable/petroleum-based oils [183] having widespread applications such as coating materials, adhesives, automotive parts, and different infrastructures. However, they are more popular for producing durable, lightweight, and cost-effective composite products [184]. PU is highly compatible with plant-based fibers as isocyanate group present in PU interacts with the –OH (hydroxyl group) of natural fibers [183, 185]. Besides, PU also exhibit some outstanding properties like zero VOC (volatile organic compound) emission, comparatively cheaper price, feasible processing technology, higher reactivity, and so on. In this regard, MDI is widely used for particle board productions by manufacturers. But, it is not yet getting attentions for laminated multilayered hybrid composites productions. So, researches are needed to find out novel routes of producing economical and feasible laminated composite panels manufacturing.

Although there are enormous advantages of using plant fibers, still there are some limitations for the inherent structural properties. The polymeric resins are hydrophobic and non-polar but while the natural fibers contain –OH groups so they are hydrophilic and polar in nature [186, 187]. The compatibility problem hampers the bonding when these two different properties of materials are mixed together in the polymeric matrix. The mechanical properties of natural fiber reinforced composites are affected by this kind of incompatibility, because the affinity towards the water is enhanced. The incorporation of synthetic fibers like glass or carbon with the natural fibers (like flax, hemp, kenaf, coir, jute, and so on) could overcome this challenge. Kumar et al. [187] have reported that when the hybrid composites are developed through reinforcing glass with flax, the tensile strength was increased from 85.6 MPa to 143.21 MPa. The same study also found a significant improvement in impact strength and flexural properties of the hybrid composites. Bajpai et al. [188] described in another study that, the reinforcement of three layered jute and single layer glass with epoxy resin provided the highest flexural strength (107.78 MPa), and impact strength (72.24 J/m) making it useful for safety helmets in industrial applications.

Besides, composites made from woven fabrics are also getting importance to the researchers and industrialists for better comfort, dimensional stability, strength, stiffness, lower fabrication cost, and so on [189, 190]. Glass and flax woven fabrics were selected for this research. Some studies also revealed, that pretreatment of both the flax and glass fibers could improve the interfacial bonding in the polymeric composite [73]; so both the flax and glass woven fabrics were treated with NaOH and silane, respectively before producing the hybrid composite. Different percentages of flax and glass woven fabrics were used as reinforcement

to fabricate the composites through reinforcing with MDI matrix. According to our knowledge, no researches have been conducted yet on pretreated flax and glass woven fabric-based laminated composites reinforced with MDI polymeric resin. As MDI is used widely in industrial particle board manufacturing process, I hope this current research could facilitate the bulk productions of glass/flax reinforced MDI composites. The mechanical, physical, morphological, thermal, and statistical analysis have provided significant information on the produced hybrid composites.

3.4. Work package 4: Hemp/glass woven fabric reinforced laminated nanocomposites via in-situ synthesized silver nanoparticles from *Tilia cordata* leaf extract.

The hybridization of natural fibers with synthetic materials like glass could solve the problems of lower mechanical/physical properties obtained through cellulosic fibers reinforcements. The glass fiber is made compatible with the help of silane coupling agents with different thermosetting polymers. However, the strengths of the produced composite materials finally depends on the strengths and modulus of elasticity of both the fiber and the polymeric matrix, and after all on the bonding capability between the fiber to matrix [191].

As much effort is being made to improve the thermal and mechanical performances of composites. In this regard, pretreatment of glass and flax also have been reported by the researchers to enhance interfacial adhesion between the fiber and polymeric matrix. Furthermore, the development of nanocomposites for improving the thermal and mechanical performance of natural and synthetic fiber reinforced composites [192] is also getting significant attention nowadays. The NPs commonly used for producing nanocomposites are Ag, SiO_2, ZnO, TiO_2, carbon nanotube, and so on. Although the application of biosynthesized AgNPs were reported for textile and associated materials substantially with improved functionalities like coloration, thermal, and mechanical properties, UV-protection, antibacterial effect, and so on [6, 193-195], they are not yet researched extensively for developing nanocomposites. The world is turning to produce more sustainable products through avoiding/minimizing traditional ones not free from hazardous materials or environmentally harmful ingredients, in this regard the biosynthesized AgNPs could be a benchmark for developing hybrid nanocomposites.

Biosynthesized AgNPs possess low toxicity; hence they are safe for the environment. There are different approaches used for synthesizing AgNPs like physical, biological, and chemical methods. However, the physical and chemical approaches could generate hazardous by-product materials. In this regards, bio-based synthesizing methods and protocols are favored to minimize the harmful effects. The green synthesis of AgNPs is also practiced by the researchers through using different bio-based plant extracts as potential reducing and stabilizing agents through applying "Green Chemistry". The leaves from *Tilia Cordata* could be a good choice in this context as the leaves can be directly collected from the trees which grow in abundance in central European countries like Hungary [196, 197]. The extracts from *Tilia Cordata* could also function as a potential reducing and stabilizing agent for synthesizing green AgNPs like as other plant extracts [198]. It was reported by researchers that the cellulosic fiber could adsorb the Ag^+ ion on the surface because of its –OH functional groups, which behave as seeds when in situ synthesized with the natural fibers; hence it deposited successfully on cellulosic fibers [199, 200]. Besides, glass fibers also demonstrate very good interaction with AgNPs synthesized by using biobased stabilizing and reducing agents [6]. Conversely, most of the chemical reducing agents possess N,N-dimethylformamide and hydrazine which are harmful for the environment [201]. In this context, natural plant-based stabilizing agents could minimize the toxic effects of solvents associated with AgNP preparation. Overall, greenly

synthesized AgNPs bear superior potentiality for developing nanosilver treated glass/hemp woven fabric reinforced hybrid composites.

The woven fabrics had been treated with AgNPs first before going to composites production which could bring a revolutionary development on the colorful laminated composites manufacturing houses. The presence of green AgNP was tested and confirmed by using XRF and ICP OES test. The developed hybrid composites were characterized for thermal, mechanical, physical, and morphological performance and found satisfactory. The colorimetric studies also ensured the presence of brilliant color appearances on the developed composite materials. Mechanical properties of these composites were tested on specimens prepared from the panels. Statistical analysis of the test results confirmed the positive influence of nanosilver loading on hybrid composites. According to our knowledge however, until now no research has been performed on biosynthesized AgNP treated thermoset polymeric hybrid composites with glass and hemp woven fabrics reinforcements. Moreover, the synthesis of nanoparticles from *Tilia cordata* leaf extracts to treat glass and hemp woven fabrics also not yet studied for producing hybrid nanocomposites although having superior potentiality. Hence, there is an urgent necessity is urged to explore the reinforcement effects of nanosilver treated glass and hemp woven fabric reinforced epoxy composites. The current research could facilitate the industrial production units with new route of nanosilver loaded laminated hybrid composite products.

Chapter IV: Methods and Materials

4.1. Work package 1

4.1.1. Materials

The energy reeds were obtained from Energianövény-Team Kft., company located in Lengyeltóti, Hungary. The rice straw was received from local areas of central Europe (Hungary). However, both the rice straw and energy reeds were dried at ambient temperature and defibrated using a defibrating machine. The fiber materials were sieved for ensuring homogeneous fiber dimensions before going to composite productions. The physical image and micrographs of both fiber types are shown in Figure 4.1. Phenolic resin-like PF was supplied by Chemco, a. s. in Slovakia for the purpose of research. The PF is reddish-brown in appearance, liquid. The dynamic viscosity of the PF resin was within 240 to 1080 mPa.s, density 1210±20 kg/m^3, dry matter content minimum 48 wt%, pH 10–12, and maximum free phenol content 0.1 (wt%).

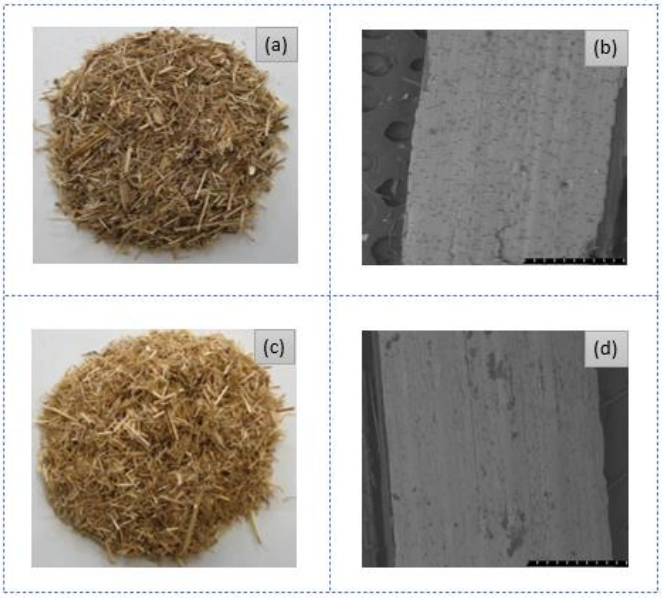

Figure 4.1: Physical and morphological photographs/micrographs of energy reeds and rice straw: (a) Physical photographs of energy reeds; (b) SEM micrograph of energy reeds; (c) Physical photographs of rice straw; (d) SEM micrograph of rice straw.

4.1.2. Methods

4.1.2.1. Preparation of rice straw and energy reed materials

The rice straw and energy reeds are long stem plant materials which were chopped around 30 to 40 mm in length by using circular cutting equipment (DCS570N XJ model, Pennsylvania, United States). After that, both the rice straw and energy reeds were pretreated with 5% (w/v) of NaOH for removing any impurities present in the raw plant materials. The excessive usage of alkaline reagents could damage the cells of cellulosic substrates [202, 203], hence an optimum values of NaOH was used for this pretreatment [204]. The materials were soaked in cold water for 24 h at basic pH medium (around 12.0). The treated rice straw and energy reeds were then washed with tap water for removing the excess impurities and mucus from the surfaces and dried in an oven for 30 min at 100 °C. The pH of energy reed and rice straws were checked again after the treatments with pH paper and found was around 7.0. Moisture contents of the rice straw and energy reeds were checked after the drying and found

to have around 9.3%. Later, the rice straw and energy reed stems were cut using a cutting machine (VZ 23412, Dinamo Budapest, Hungary) without destroying the fibrils of the materials through adjusting the grain and grinders distance. The particles of the sellulosic materials were then defibrated. All the fibrous materials were sieved using a Sieve analyzer from Fritsch GmbH (ANALYSETTE 3Pro, Germany) having different dimensions from 0.1 to 3.55 mm for rice straws and 0.5 to 1.66 mm for energy reeds (Figure 4.2). The amplitude vibrations of the sieve analyzers were 1.0 for a 15 min duration of time for 100.0 g (randomly chosen) rice straw and energy reeds, respectively. It is found that the highest dimension of rice straw materials were 44.1% and energy reeds were 44.6% as per sieve analysis. However, 5.7% rice straw fibers dimension were within 2.55 mm, 27.6% fibers 3.55 mm, 10.6% fibers 0.5 mm, 11.1% fibers 0.1 mm. On the other hand, 26.7% energy reeds were within 1.25 mm, 13.8% fibers 1.0 mm, 14.8% fibers were 0.5 mm in dimensions. Overall, the prepared sieved materials from rice straw and energy reeds were termed as the fiber materials.

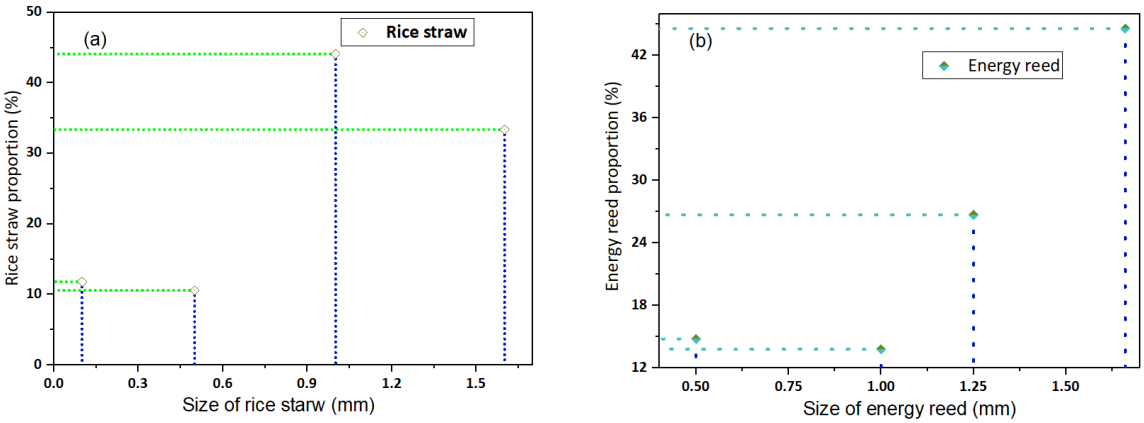

Figure 4.2: Sieve analysis and size distribution of rice straw and energy reed materials.

4.1.2.2. Production of biocomposites panels

The hot pressing technology was implemented for manufacturing biocomposites from rice straw and energy reed fibers. Initially, the PF resin as per the recipe mentioned in Table 4.1 was sprayed uniformly to the fibers in a rotating drum blender for nearly 5 min each. The drum was a custom made by the university technical stuffs for mixing the fiber/particles with thermosetting polymers. The motor of the blender was developed by DOKKER- DOMETAL Kft. (0.42 kw, RMI 141-753/93, RPM 30, Hungary). In case of first biocomposite panel (EH1) 90% rice straw fibers were used but for the biocomposite panel 4 (EH4) 90% energy reed fibers were used. The biocomposite panel 2 (EH2) was produced from 54% rice straw and 36% energy reeds, whereas the biocomposite panel 3 (EH3) by 36% rice straw and 54% energy reed fibers. However, there were just only 10% PF used for all the biocomposite panels. The moisture contents of the mat were considered as 12% and resin by 34% to calculate the recipe from the fractions. The mixed fibers were placed in a 400 mm x 400 mm wooden frame through ensuring uniform spreading. Later, two 10 mm thickness steel rods were placed in the two sides of the mats for providing a certain thickness to the ultimate biocomposite panels. A hot press machine (G. Siempelkamp GmbH and Co., Kg., Germany) was used for hot pressing the composites. The platen temperature was set to 135 °C, whereas the initial pressure applied to the biocomposite panels were 7.1 MPa for a period of 2 min, which was reduced to 4.7 MPa after another 2 min and 3.2 MPa after following the similar time durations (2 min) (Figure 4.3). Later, the temperature is minimized to the environmental conditions through providing a cold water flow in the machine and the pressure was then totally released. The reason behind the extended time of pressing is performed for achieving the perfect curing of PF resin with the rice straw and energy reeds fiber. The extended duration of curing was also reported by another

researcher where pMDI and UF bonded rice straw boards were produced [205]. However, the total time used for this current research to produce each biocomposite was 6 min which is much lower than reported by another recent study (20 min) [165]. On the other hand, reason behind the gradual decrease in pressure is to ensure crack free and uniform composite panels. Otherwise, the panels could be destroyed if the pressure is released instantly. Finally, biocomposite panels were removed from the machine and kept in normal atmospheric conditions (25 °C temperature and 65% relative humidity). However, there were four biocomposite panels (Figure 4.4) which were produced alike following the same operation protocols.

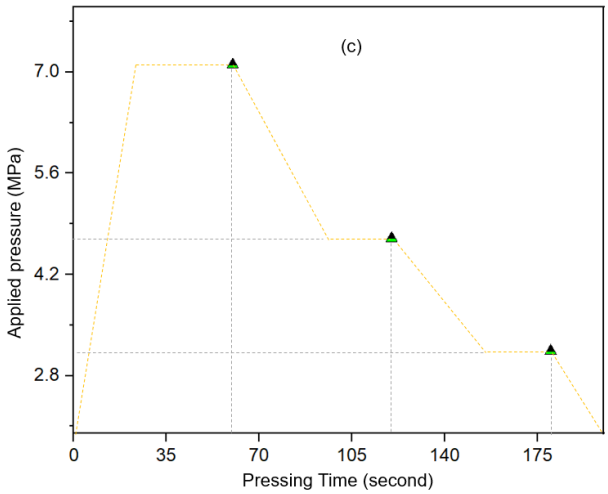

Figure 4.3: Pressure versus time used for biocomposites production

Table 4.1: Experimental design for rice straw and energy reed fibers reinforced PF biocomposite panels production.

Biocomposite materials	RS (%)	ER (%)	PF (%)
EH1	90	0	10
EH2	54	36	10
EH3	36	54	10
EH4	0	90	10

*RS– Rice straw, ER– Energy reeds, and PF– Phenol formaldehyde resin

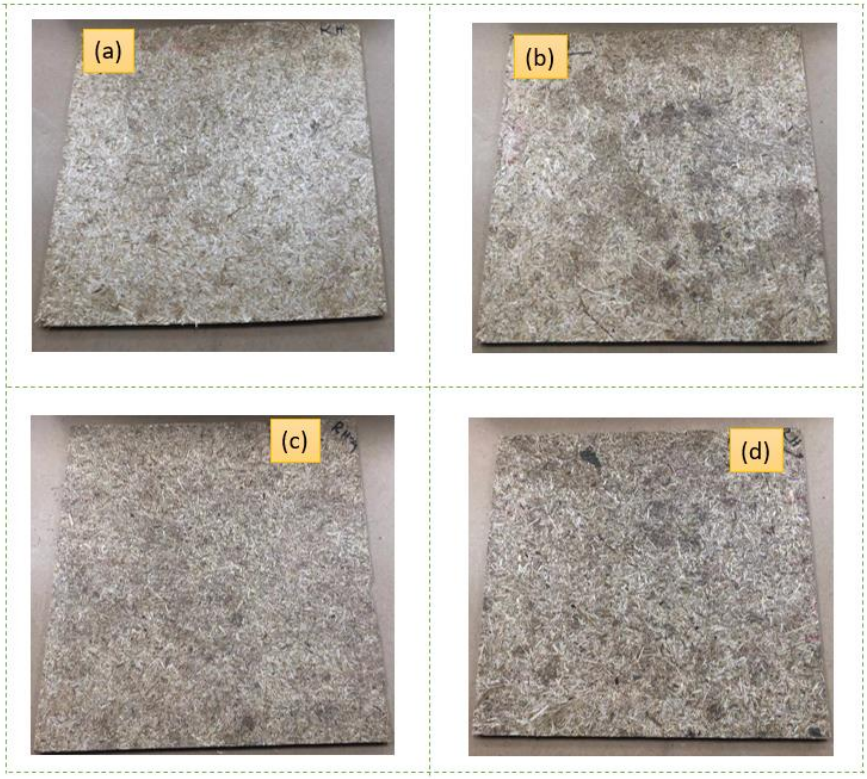

Figure 4.4: Photographs of produced biocomposite panels produced from rice straw and energy reed fibers reinforced PF composites: (a) EH1, (b) EH2, (c) EH3, and (d) EH4.

4.1.2.3. Characterizations

A moisture analyzer (Kern ULB 50–3 N, KERN AND SOHN GmbH, Germany) was used for investigating the moisture contents of fiber materials. However, accuracy of the equipment was 0.001 g, whereas the temperature was 105±0.3 °C. The standard EN 322:1993 was followed for moisture content investigations. Nearly around 1 g of scots pine and coir materials each were taken for this test. Thermal conductivity of rice straw and energy reed fiber reinforced PF composites were investigated as per EN ISO 10456:2012 standard through following hot plate method at ambient atmospheric conditions (relative humidity 65±5% and temperature 20±2 °C). The size of the tested samples was 350 mm by 350 mm, whereas the thickness was 10 mm. 100 readings were taken for each plates. The panels were placed between the hot and cold plates. However, the temperature gradient was kept 10 °C during the test. The mechanical performances of biocomposite panels were tested in terms of flexural properties (strength and modulus) and internal bonding strengths through Instron testing machine (4208, United States). The size of samples for flexural properties were determined by 20t+50, where t is thickness. In this regard, the length of the samples was 10×20+50 = 250 mm and the width was 50 mm. There were six samples from each composite type prepared and taken for the respective tests as per the standards. The standard EN 310 was followed for flexural properties investigation and EN 319 for internal bonding strength. The length and width of the samples prepared for internal bonding strength and physical properties were 50 mm by 50 mm whereas thickness was constant (similar with composite plate). Furthermore, morphological studies were conducted through a SEM equipment (S 3400 N, High Technologies Co., Ltd., Hitachi, Japan) by means of 100x and 200x times magnifications at 15.0 kV for both unfractured and fractured samples. The sizes of the test samples for SEM were nearly around 5 × 5 × 2 mm^3. In order to test FTIR, the samples were prepared nearly around 10 × 10 mm^2 dimension (length × width).

4.2. Work package 2

4.2.1. Materials

The Scots pine (*Pinus sylvestris*) particles were provided by FALCO Woodworking Co., in Szombathely, Hungary. The coir (*cocos nucifera*) fibrous chips were obtained from a local company named Pro Horto Ltd., located in Szentes, Hungary. The scots pine particles were used as received from the company, while the coir fibrous chips were defibrated before they were fabricated into composite panels (Figure 4.5). Typical OPC CEM I 42.5 was used as the cement matrix for reinforcing Scots pine and coir fibers in order to manufacture the composite panels. The FALCO Woodworking Co., also provided the cement, which was manufactured by Duna-Dráva Cement Kft., in Vác, Hungary. Figure 4.5 presents the physical and morphological tphoographs/micrographs of the Scots pine, coir fibers, and OPC. The additive reagent (water glass, Na_2SiO_3) was procured from Sigma Aldrich, Hungary.

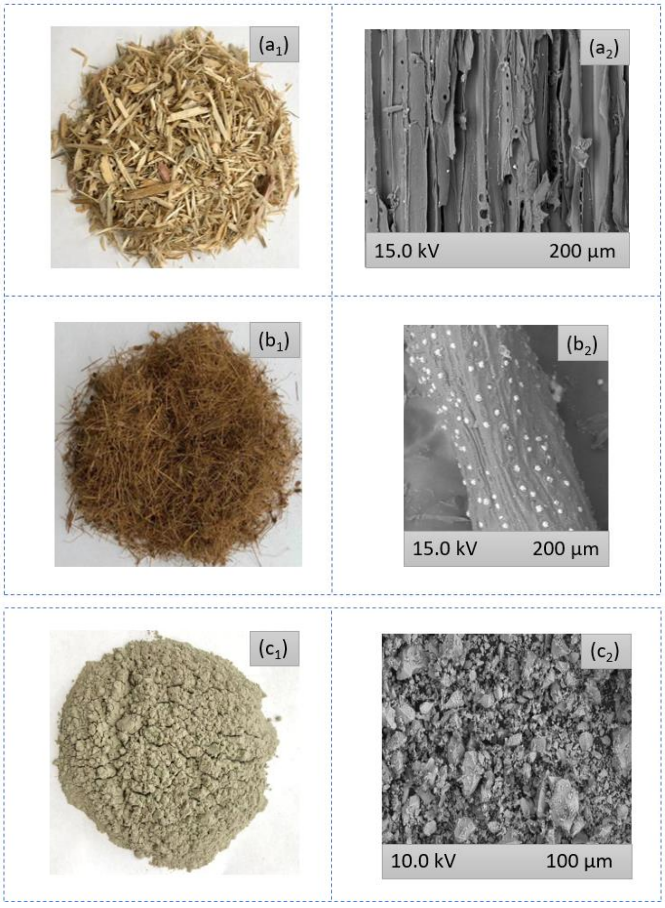

Figure 4.5: Physical and morphological photographs/micrograph of coir fiber, scots pine, and OPC material: (a_1) Physical photographs of scots pine material; (a_2) SEM micrograph of coir fiber; (b_1) Physical photographs of Scots pine; (b_2) SEM micrograph of coir fiber; (c_1) Physical photographs of OPC; (c_2) SEM micrograph of OPC.

4.2.2. Method

4.2.2.1. Preparation of coir fiber from chips and sieving of coir fiber and scots pine

The coir fibrous chips were cut with a VZ 23412 model defibrating machine (Dinamo Budapest, Hungary). Later, the defibration procedure was performed carefully by adjusting the

grinders and grain distance to protect the extracted fibers from damage. Later, both the extracted fibers and Scots pines were sieved (sieve analyzer, ANALYSETTE 3Pro, Fritsch, Germany) to ensure uniform lengths for composite panel production. Our previous studies discuss the detailed sieving protocol for fiber/chips materials [3, 202]. The length of the sieved coir fibers ranged within 0.1–2.25 mm, and for scots pine this range was 0.355 to 1.6 mm. The sieve test revealed that around 42.3% of the coir fibers possessed a length of 1.25 mm (highest value), whereas the lowest proportion was 7.4%, corresponding to a 0.8 mm length (Figure 4.6). However, two types of fiber lengths, 0.355 mm (26.6%) and 0.1 mm (22.5%), were also present. Conversely, the highest length obtained for scots pine particles was 1.6 mm, which comprised 33.4% of the particles, whereas the lowest portions of scots pine were 0.5 mm in lengths, comprising 10.6%. Two other scots pine lengths included 1.0 mm, which made up 44.1%, and 0.1 mm, which encompassed 11.8%. Overall, the dominant lignocellulosic material size for coir fiber was 1.25 mm and 1.00 mm for scots pine.

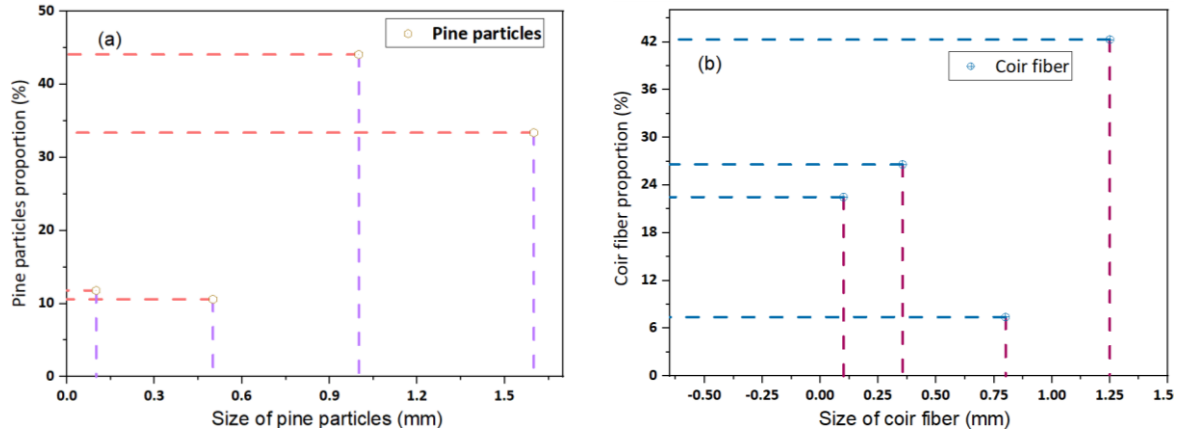

Figure 4.6: Size distribution of scots pine particle and coir fiber (a and b, respectively).

4.2.2.2 Production of composites panels

The moisture contents of both types of sieved materials were measured as per EN 322:1993 standards. The accuracy of the measurement was 0.001 g and dry temperature was 105±0.3 °C. The investigated moisture content for coir was 11.8 (0.01%) and for scots pine it was 35.8 (0.3%) for six consecutive tests. Later, all the lignocellulosic materials, OPC, Na_2SiO_3 were measured proportionately, as noted in Table 4.2. Composite panel 1, denoted by P@C1, is made of 100% Scots pine, while composite panel 5, C@C5, is 100% coir fiber. The hybrid composites were denoted by PC@C2, PC@C3, and PC@C4, respectively and the proportions of Scots pine and coir fibers were 0.6/0.4, 0.5/0.5, 0.4/0.6, respectively. Since a main focus areas of this research was to investigate the effects of increased loading of coir fiber with scots pine in the composites system, the proportions of OPC, Na_2siO_3, and cement stones were kept constant for all the recipes at 2.6, 0.052, and 0.52, respectively. Though the materials mentioned in Table 4.2 were weighed in g, they are reported here as proportions for all the composite panels, individually. Another important material in this research is mixing water (H_2O), which was weighed by 50% of total dry matter content in every recipe. The water content was further measured in terms of composite panel density, dimensions, moisture content of scots pine and coir fibers, and water glass. The nominal densities of the composite panels were set to 1200 kg/m^3 each and the dimensions were 400 x 400 x 12 mm^3. Later, the slurry was prepared by uniformly mixing lignocellulosic materials, OPC, water glass, and cement stone. To prepare the slurry, the lignocellulosic materials were placed into a steel drum into which the OPC was gradually poured while being constantly stirred with a magnetic stirrer. Once the OPC and lignocellulosic materials were optimally mixed, the water glass and water solution was poured in following the same protocol used for the cement additions. Water glass facilitates the perfect

setting of OPC with lignocellulosic materials. Finally, the mixed ingredients in the drum were stirred for another 3 min to confirm the even mixing of all the materials to ensure a superior slurry. Later, a wooden frame of 400 x 400 mm^2 was placed on a table over a long polybag where the prepared slurry was uniformly spread. When the slurry spreading was complete, another wooden lid was used to manually press the materials in the mat to ensure they adhered without any deformations. After that, the material proceeded to mechanical pressing. Subsequently, the frame was withdrawn from the mat and covered by the same polybag. Two 12 mm steel rods were placed at the two sides of the mat and a steel plate was inserted over it. Finally, the mat containing the steel plate was placed to the platen of the pressing machine where 7.2 MPa pressure was applied on the mat. Pressure was applied constantly for 24 h durations at environmental temperature and humidity. Later, the pressure was gradually decreased and the panel was removed from the plate. A 28-day curing period followed. All the composite panels (Figure 4.7) were manufactured following the same protocols.

Table 4.2: Experimental design of scots pine and coir fiber-reinforced OPC composite panel manufacturing.

Composite materials	**SP (proportion)**	**CF (proportion)**	**OPC (proportion)**	**Na_2SiO_3 (proportion)**	**CS (proportion)**
P@C1	1.00	0	2.6	0.052	0.52
PC@C2	0.60	0.40	2.6	0.052	0.52
PC@C3	0.50	0.50	2.6	0.052	0.52
PC@C4	0.40	0.60	2.6	0.052	0.52
C@C5	0	1.00	2.6	0.052	0.52

*SP– Scots pine, CF– Coir fiber, and OPC– Ordinary Portland cement, Na_2SiO_3– Water glass, CS–Cement stone

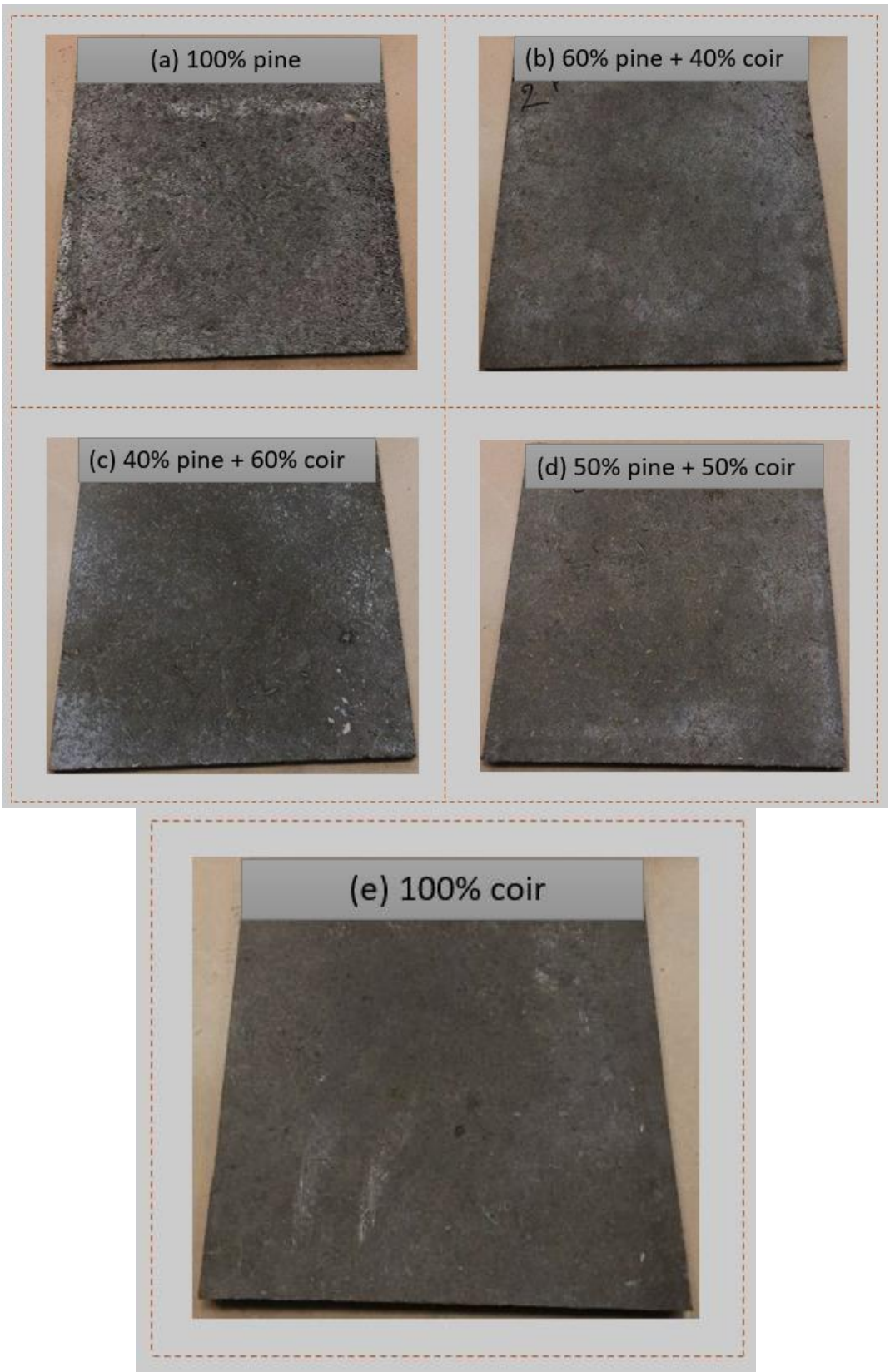

Figure 4.7: Photographs of produced composite panels from coir fiber and scots pines reinforced with OPC: (a) P@C1, (b) PC@C2, (c) PC@C3, (d) PC@C4, and (e) C@C5.

4.2.2.3 Characterizations

The sugar and tannin contents of the fibers were investigated by following analytical methods in the laboratory. A sand bath was used for boiling the water with coir fiber and scots pine during the tannin and sugar contents testing protocol. The thermal conductivity of the developed cementitious composites was tested according to the EN ISO 10456:2012 standard. The detailed testing protocol was discussed in our previous studies [202, 206]. In brief, the composite panel trims were evenly cut. The panel surfaces needed to be flat and uniform to conduct this test. Once this was complete, the composites were placed in a standard atmospheric condition (65±5% relative humidity and 20±5 °C temperature) to ensure that all the panels reached an equilibrium moisture level. It is necessary to secure uniform heat flow transfer; hence, the composites were surrounded by insulation boards (15 cm). The size of the panels were 300 × 300 mm^2. The measurement readings were taken at steady rate and at least 100 data points were found to have less than 0.002 W/(m.K). The measurements were taken every minute and ultimate thermal conductivity was considered from the last 100 measurement readings. The internal bonding strengths and flexural performances of the developed cementitious composites were characterized by Instron testing equipment (4208 model, United States) as per EN 319 and EN 310, respectively. The test specimens were prepared by cutting the samples with a circular saw (saw cut instruments, DCS570N XJ model, Pennsylvania, USA). The speed of crosshead movement for internal bonding strength was 0.8 mm/min and flexural properties were tested at 5.0 mm/min. Furthermore, the SEM micrographs were taken by SEM instruments (S 3400 N model manufactured by High Technologies Co., Ltd., Hitachi, Tokyo, Japan) at 15.0 kV and different magnifications. The EDX analysis was also performed by the same SEM machine. The FTIR analysis was conducted using FT/IR-6300 model instruments made by Jasco, Tokyo, Japan within a 4000 to 400 cm^{-1} wavenumber. Moreover, TGA (Thermogravimetric analysis) and DTG (Derivative thermogravimetric analysis) analysis was performed by a Themys thermal analyzer instrument made by Setaram Instrumentation, France, under nitrogen atmosphere at 10 °C/min within 25 to 800 °C. The sizes of all the tests specimens were prepared through following the similar protocol with work package 1.

4.3. Work package 3

4.3.1. Materials

The flax woven fabrics (article number: LV06506, density: 230 g/m^2, composition: 100% flax, Twill structure) were purchased from Malitext (Pécs, Hungary). The glass woven fabric (with measured density of 255 g/m^2, 100% glass, plain weave structure (grid size 4.4 × 4.2 mm^2)) was procured from Tolnatext company located in Tolna, Hungary. The alkaline NaOH was bought from VWR international Kft., (Debrecen, Hungary) and Vinyltrimethoxysilane, $C_5H_{12}O_3Si$ (L#MKBZ5796V, 98%, molecular weight (M_W) 148.23 g/mol) from Sigma-Aldrich Co., (St. Luis, MO, USA). The MDI (Ongronat XP-1161) was purchased from Borsodchem Zrt. (Kazincbarcika, Hungary). The Formula Five type mold release wax was procured from Novia (Hungary) to use as a coating material between the composites and teflon sheet to avoid stickiness of the resin with the teflon.

4.3.2. Methods

Initially, the flax woven fabrics were pretreated with 0.5% NaOH solution (material: liquor ratio was 1: 20) for 30 min at 100 °C temperature to enhance the fibers interaction to polymeric resin. The reaction mechanism is shown in Equation 4.1. The glass fabrics were treated by vinyltrimethoxysilane at room temperature for 30 min (material: liquor ratio was 1: 10). After the pretreatment, the fabrics were rinsed and washed three times to remove the alkaline mucus,

Vinyltrimethoxysilane solutions, and other impurities from the surface. The fabric samples were then dried in an oven at 60 °C for 6 min. After that, six layers (Table 4.3) of glass (G)/flax (F) woven fabrics (G1, GF2, GF3, and F4) coated with MDI resin were stacked up by hand-layup method. The sequence of layers in the laminates were (G,G,G,G,G,G/ G,G,F,G,G,G/ G,F,G,F,G,F/ F,F,F,F,F,F) with thicknesses of 1.56, 1.9, 2.58, and 3.6 mm for G1, GF2, GF3, and F4 composites, respectively (Table 4.3). The produced laminates were pressed (3.5 MPa pressure) by a pressing machine for 15 min at room temperature. Later on, the composites were then cured for 24 h at ambient conditions.

$$Flax - OH + Na^{+} - OH^{-} \rightarrow Flax - O - Na^{+} + H_2O \qquad \text{Equation 4.1}$$

Table 4.3: Stacking sequence, thickness, and density of developed hybrid composites (G1, GF2, GF3, and F4). Composites were developed with different densities and thickness. (Mean values with standard deviations in parentheses).

Laminates	Sequence of stacking	Thickness (mm)	Ultimate thickness (mm)	Density (kg/m^3)
G1 (100% glass)	G,G,G,G,G,G	1.56 (0.012)	1.06 (0.004)	1727.62 (29.01)
GF2 (83.33% glass/ 16.67% flax)	G,G,F,G,G,G	1.9 (0.005)	1.52 (0.014)	1401.32 (60.28)
GF3 (50% glass/ 50% flax)	G,F,G,F,G,F	2.58 (0.007)	2.23 (0.007)	1091.53 (146.7)
F4 (100% flax)	F,F,F,F,F,F	3.6 (0.19)	2.51 (0.005)	1195.02 (32.10)

*G-glass, F-flax.

4.3.3.1. Characterization of the composites

The tensile and flexural properties of the produced composites were measured by using universal testing equipment Instron 4208 (Instron corporation, USA). The tensile test was conducted as per ISO 527–1:11996 procedures whereas flexural properties were adopted from the ISO 178:2019 standard. The dumbbell shaped test specimens as shown in Figure 1.18 was used for tensile testing (length 175 mm and width 20 mm), whereas sample sizes of 85 mm in length and 10 mm in width were used for flexural properties test (Figure 1.19). Six samples from each composite were selected for conducting the test. The crosshead movement of tensile test was 10 mm/min and flexural test 5 mm/min. The FTIR characterization of the composites were performed using FTIR–6300 (Jasco, Japan) spectrometer at 4000–500 cm^{-1}. The morphological investigation was performed by using a SEM equipment (SEM, S 3400N, Hitachi, Japan) at 15.0 kV voltage with 2000x and 1000x magnifications. The similar testing protocol and dimensions of work packages 1 and 2 were followed for SEM, TGA/DTG, and FTIR tests. The TGA and DTG analysis was conducted using Themys thermal analyzer (Setaram Instrumentation, France) within 25 °C to 850 °C at 10 °C/min temperature gradient under nitrogen (N_2) atmosphere. The water absorbency was tested at 2 h, 24 h, and 240 h time intervals as per MSZ 13336-4:13379 method. Samples of 50 mm by 50 mm dimensions were prepared to execute this test. The composite samples were immerged into 30 mm depth of water.

The moisture content of the composite boards was investigated in line with EN 322 methods. The dimensions of the samples were kept the same (50 mm by 50 mm).

4.4. Work package 4

4.4.1. Materials

Glass and hemp woven fabrics being prominent reinforcement materials and epoxy resin polymeric matrix materials were selected for our experiments. The images/micrographs of physical and morphological appearance of the glass and hemp woven fabrics are shown in Figure 4.8. Hand woven hemp fabrics (density: 75 g/yard, organic fiber, and milky grey color) were purchased from Rambutan, Vietnam. The fabrics were made by tribes women in northern Vietnam. The E-glass plain woven fabrics (100% glass, 4.2 mm × 4.5 mm grid size, 255 g/m^2 measured fabric density) were purchased from Tolnatext (Tolna, Hungary). Metallic silver precursor ($AgNO_3$, purity 99.98%) was purchased from Sigma Aldrich (St. Luis, MA, United States). Leaves of *Tilia cordata* tree were collected from the garden of University of Sopron, Sopron, Hungary. The epoxy resin (modified bisphenol A) and crosslinkers (hardener, modified cycloaliphatic amine) were purchased from Novia Kft., located in Hungary. The viscosity of the epoxy resin is within 800 to 1200 mPa.S, equivalent weight 175 to 190 g/equiv., and density 1100 to 1110 kg/m^3, whereas the hardener contains 40 to 70 mPa.S viscosity and 950 kg/m^3 density, equivalent weight 60 g/equiv. The epoxy resin and hardener were mixed by proportion of 100 to 33 in laboratory standard environment (65% relative humidity and 25 °C temperature).

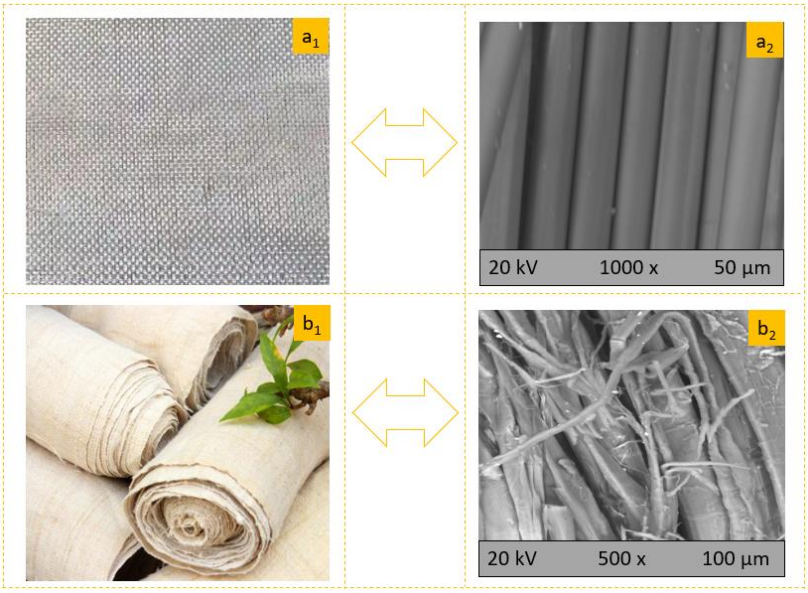

Figure 4.8: Macroscopic and SEM morphologies of glass and hemp woven fabrics: a_1 and a_2: glass woven fabric; b_1 and b_2: hemp woven fabric. SEM micrographs of hemp woven fabric is collected from the seller of this fabric that is used in this research [207].

Figure 4.9: Schematic representation of synthesis and application of green AgNPs: (a) dried *Tilia cordata* leaves; (b) crushed *Tilia cordata* leaves powder; (c_1 and c_2) $AgNO_3$ precursor in distilled water (1.0 and 5.0 mM concentration, respectively); (d_1 and d_2) synthesized green AgNPs solutions for different precursor; (e_1 and e_2) bending test species of produced composites from greenly synthesized AgNPs treated woven fabrics.

4.4.2. Green synthesis of AgNPs (in situ) on glass and hemp woven fabrics

Generally, bioreduction of metallic salts like $AgNO_3$ requires a solution of a plant extract in case of plant- mediated nanomaterial synthesis as stabilizing and reducing agents. The collected *Tilia cordata* leaves were washed and cleaned with distilled water for removing all the contaminating materials and debris from the surfaces of leaves and dried at ambient temperature (around 25 °C). The dried *Tilia* leaves were crushed by a grinder to make fine particles before the extraction process. The powders (200 g for 2.0 L solution) were then boiled for 60 min at 80 °C. The extracts were filtered using filter paper after cooling down the aqueous solution and stored at refrigerator at 4 °C. The green AgNPs were prepared in a beaker for 1.0 and 5.0 mM $AgNO_3$ precursor along with 1% (v/v) leaf extracts. The hemp woven fabrics were first put into the beaker as well. A color change was observed from colorless/milky color to brown/darker brown which confirmed the successful reduction of metallic Ag^+ to Ag^0 [208]. The darkness of the color solutions varied on the addition of $AgNO_3$ precursor into the aqueous solutions. The as discussed *in situ* synthesis of green AgNPs is shown in Figure 4.9. The similar synthesis protocols were also performed in case of glass woven fabrics. The glass and hemp woven fabrics were washed three times with tap water to remove any undeposited nanosilver from the surfaces. The nanotreated samples were then dried at 80 °C for 10 min.

4.4.3. Lamination of the hybrid composites

Hand lay-up process in combination with compression molding was used for manufacturing the hybrid composites from nanosilver treated glass and hemp woven fabrics. Before starting the composite production, a teflon paper coated with wax was used, which was placed under the bottom layer. The waxy layer ensured a barrier between the teflon paper and epoxy coated laminated composites. The five-ply laminated hybrid composites were produced by stacking the glass as top and bottom layer where hemp was put under every glass layer as shown in Table 4.4 (stacking sequence G,H,G,H,G), where G stands for glass and H for hemp.

The epoxy resin and hardener mix was sprayed over each layer in the laminates with rotating roller. Two nanocomposite laminates (NC1 produced through using 1mM $AgNO_3$ and NC2 produced using 5 mM $AgNO_3$) and 1 control laminate without any nanotreatment were stacked up (CC3), followed by pressing. Approximately 300 mL of mixed polymers were used for every individual laminated composite. Another teflon paper coated with wax was placed over the laminated composites. The dimensions of the samples were maintained 400 by 400 mm^2. The laminated composites were then dried at room temperature (25 °C) for 24 h.

4.4.4. Characterization of hybrid composites

Scanning electron microscope (SEM, Hitachi, Tokyo, Japan) of S 3400N model was used for morphological investigation of the developed composites at an accelerating voltage of 15.0 kV through different magnifications. The presence of AgNPs on nanocolloid and treated materials were confirmed by using ICP OES instrument (Thermofisher Scientific, 6000 series, Cambridge, United Kingdom) and XRF (X-ray fluorescence) equipment (Niton TM XL2, Thermoscientific™, United States), respectively. AgNPs also exhibit bright color appearances on the surfaces of the treated materials. In this regard, the color properties of the developed composites were also further investigated. Themys thermal analyzer made by Setaram Instrumentation (France) was used for investigating the thermal properties by TGA and DTG. This characterization was performed under nitrogen atmosphere (purging rate was 50 mL/min) at 10 °C/min heating rate from 10 to 800 °C. The mechanical properties of the developed composites were performed in terms of tensile and flexural properties. Mechanical performance of the composites was characterized by testing tensile and flexural properties tested according to the ISO 527–1:1996 and ISO 178:2010, respectively using an Instron machine (Instron 4208, Instron Corporation, United States). For these tests, the composite panels were cut into six test-pieces and tested accordingly for each types of mechanical and physical properties. Among the physical properties water absorbency and thickness swelling were studied according to the standard MSZ 13336-4:13379 and EN 317:1998, respectively while moisture content according to (EN 322). The thickness swelling characteristics were measured by a Mitutoyo 543-551D Digimatic indicator, manufactured by Mitutoyo Europe GmbH located in Neuss, Germany. All the samples were prepared by using laser cutting instrument (Universal ILS9.150D, United States) according to the different standards. All the sample dimensions are similar with work package 3.

Table 4.4: Parameters for NC1, NC2, and CC3 composites.

Laminates	$AgNO_3$ (mM)	*Tilia cordata* leaf extract % (v/v)	Sequence of stacking	Thickness (mm)	Density (kg/m^3)
NC1	1	3	G,H,G,H,G	2.34 (0.1)	1374 (32.1)
NC2	5	3	G,H,G,H,G	3.62 (0.3)	1298.4 (23.6)
CC3	0	0	G,H,G,H,G	2.81 (0.1)	1052.5 (31.3)

*NC1 – nanocomposite 1 where 1 mM $AgNO_3$ used; NC2 – nanocomposite 2 where 5 mM $AgNO_3$ used; CC3 – control composite where no $AgNO_3$ used.

Chapter V: Reseults and Discussions

5.1. Work package 1

5.1.1. Density and mechanical properties

Density of the thermosetting polymer reinforced biocomposites play a significant role for determining thermomechanical properties of the products. Hence the densities of the biocomposites were also investigated. Although, the nominal densities were calculated to be 680 kg/m^3, but the actual densities found after the biocomposite formations were 713.66, 725, 742.79, and 764.49 kg/m^3. Interestingly, it is observed that with the increase of energy reed fibers in the composites, density also started to increase whereas highest value was found for 100% energy reeds reinforced composite (with a 12.43% increase compared to the nominal density) whilst the lowest value was noticed for rice straw reinforced composite panels (with a 4.94% increase compared to nominal density). It maybe that the energy reed fibers are comparatively stronger than the rice straw, hence increased the density of the composites.

The load versus displacement curves of biocomposite panels are plotted in Figure 5.1(a and b) both for flexural properties (flexural strength and modulus) and IBS (Internal bonding strength) characteristics. The highest load was displayed by composite panel 4 (2096 N), whereas composite panel 1, 2, and 3 showed 673, 1019, and 1114 N loads, respectively. Conversely, in case of flexural properties, the values of load corresponding to the composite panel 1, 2, 3 and 4 are 194, 225, 341, and 261 N, respectively. However, after showing the maximum load for cracking of the test samples, still the load continues with the extended delaminations until the biocomposite panels total failure occurs. It is found that the 100% energy reed fiber reinforced biocomposites with PF resin requires the highest load for breaking/bending the biocomposite panels compared to rice straw reinforced polymeric biocomposite panels. The similar effects were also reported in the previous studies for different natural fiber reinforced hybrid polymeric composites [209-211].

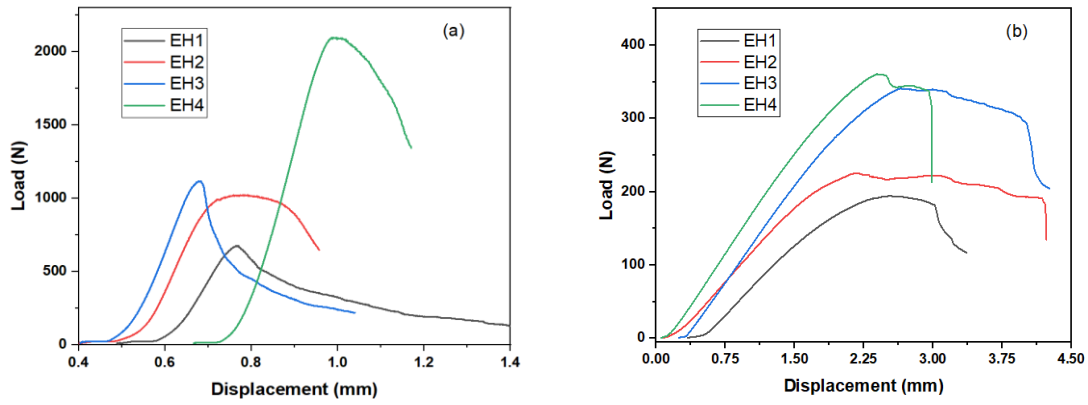

Figure 5.1: Load versus displacement curves for energy reed and rice straw fibers reinforced PF composites: (a) IBS and (b) flexural properties.

Mechanical characteristics of the developed composite panels from rice straw and energy reed fiber reinforced PF composites are tabulated in Table 5.1. The maximum value for MOR was seen for composite material 4 by 21.47 (2.12) MPa, whereas the lowest value was

observed for composite material 1 just only 11.18 (1.91) MPa with a 47.9 % decline from the composite 1. However, other two composite panels also showed the moderate results, whereas composite 2 provided 15.65 (3.91) MPa and composite 3 by 16.94 (2.02) MPa. The differences in flexural strengths started to increase with the increase in energy reeds proportions in the composite systems. The similar trends are also noticed for the MOE and IBS properties. Likewise, composite 4 showed the highest MOE 8.73 (0.16) MPa and composite 1 by 5.42 (0.69) MPa. Just except composite 2 (thickness value 9.52 (0.18) MPa), all other panels were showing the decreasing pattern of thicknesses (9.85 (0.31), 9.85 (0.11), and 9.58 (0.04) MPa) (Table 5.1) with the increase in rice straws in composite system. It seems rice straws provided higher thickness compared to the energy reeds. The associated elongation at break (EBS) for flexural studies also showing dissimilar results, although the lowest value was found for composite 1 by 0.396 (0.04)%, and highest values for composite 3 by 0.53 (0.056)%. However, still composite 4 is showing higher values (0.41 (0.08)%) compared to composite 1 panel.

Table 5.1: Mechanical characteristics of produced biocomposite panels from rice straw and energy reed fibers reinforced PF composites.

BCs	D (kg/m^3)	MOR (MPa)	MOE (GPa)	IBS (MPa)	T (mm)	EBS (%)
EH1	713.66 (30.45)	11.18 (1.91)	5.42 (0.69)	0.25 (0.02)	9.85 (0.31)	0.396 (0.04)
EH2	725 (21.01)	15.65 (3.91)	6.64 (0.66)	0.31 (0.09)	9.52 (0.18)	0.523 (0.066)
EH3	742.79 (16.51)	16.94 (2.02)	7.85 (0.25)	0.34 (0.04)	9.85 (0.11)	0.53 (0.056)
EH4	764.49 (8.28)	21.47 (2.12)	8.73 (0.16)	0.52 (0.04)	9.58 (0.04)	0.41 (0.08)
R^2	0.50	0.64	0.85	0.41	0.49	0.46

*D–Density; MOR–Modulus of Rupture; MOE–Modulus of Elasticity; IBS–Internal Bonding Strength; T– Thickness; EBS– Elongation at bending stress.

IBS is another most important parameter to consider for the biocomposites performance analysis. The highest performances against internal bonding failure are displayed by the energy reed fiber reinforced composite panels (0.52 (0.04) MPa) compared to all other types of panel (0.25 (0.02), 0.31 (0.09), and 0.34 (0.04) MPa) for composite 1, 2, and 3). The composite panel 4 showed a higher strength by 108% compared to composite 1, 67.7% compared to composite 2, and 52.9% compared to composite panel 3. Likewise, other mechanical properties (flexural strengths and modulus), IBS also provided the similar trends: the increase in performances depend on the increased loading of energy reed fibers proportion in hybrid composite system. However, still we could not find any report regarding the reinforcement of rice straw and energy reeds fiber reinforced hybrid composites to compare the performances, however the perceived results are providing satisfactory mechanical properties in case of medium density composite panels. Statistically, mechanical properties of the manufactured composite panels were tested further using coefficient of variation (R^2) in terms of energy reeds fiber proportions in composite systems. The R^2 values for density, MOR, and MOE are higher than 0.5, whereas the values of IBS, T and E@BS are also higher than 0.41. The R^2 values of all the mechanical properties (Table 5.1) demonstrating a significant influence of energy reeds on the flexural properties of the developed materials. Hence, it could be stated that, the increased loading of energy reeds fibers in the composite system possesses a positive attributions for determining the different characteristics of biocomposite panels.

5.1.2. Morphological properties and EDX analysis

The morphological observations of rice straw and energy reed fibers provide a deep insight of both material types (Figure 5.2). However, the surfaces of fiber materials are seem to be rougher, which is happened maybe for the alkaline pretreatment of the materials before the fabrication, which also agrees with some other previous studies by the researchers [165]. Furthermore, the rougher surfaces obtained through treatment of the materials could also provide better mechanical properties to the composites as the impurities like oil, wax, etc., are removed from the cellulosic materials. The morphological micrographs of unfractured surfaces (Figure 5.2) display flat and uniform coating of PF resins over the fiber surfaces, demonstrating a stronger bonding in the composite systems. The reason behind the strong reinforcement effects between the fiber and polymers is mediated by the pretreatment of the rice straw [212] and energy reeds materials. Although the fibers somehow appear in the unfractured surfaces, the clear representative fibers could be seen explicitly in fractured surfaces (Figure 5.3). Overall, it could be summarized that a better reinforcement effect is achieved through pretreating rice straw and energy reeds before the defibration and fabrications which is also in agreement with the previous reports by the researchers [213].

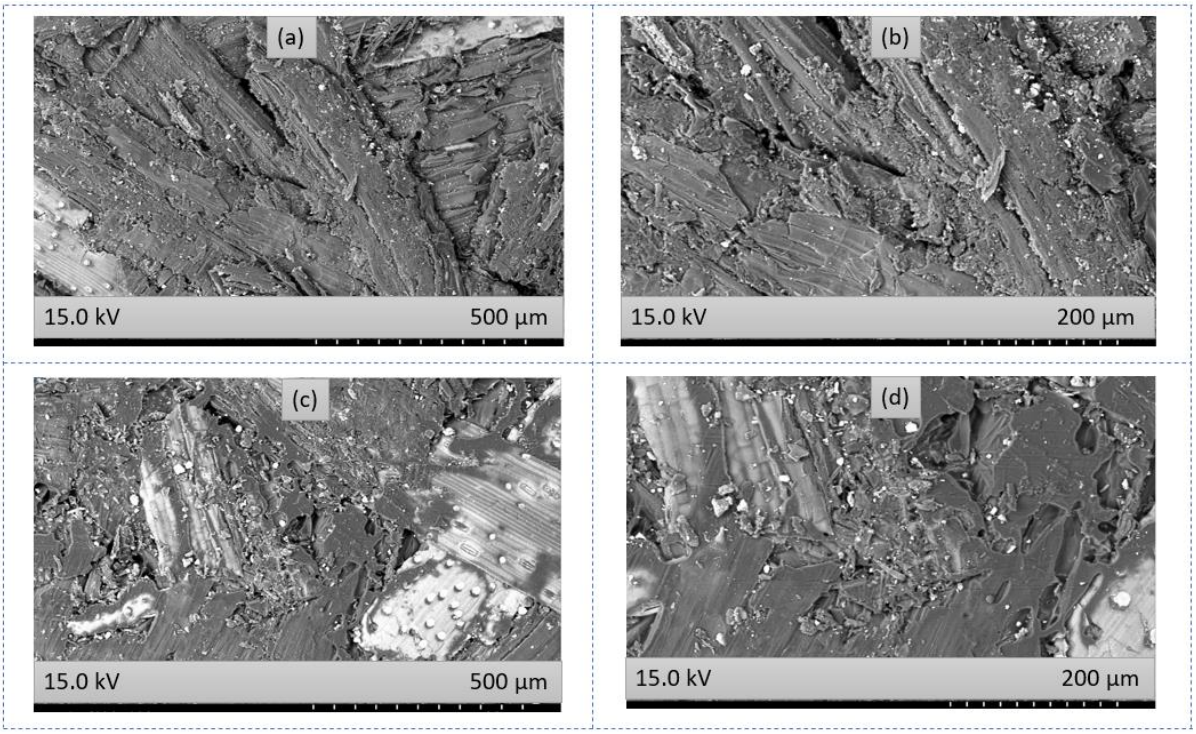

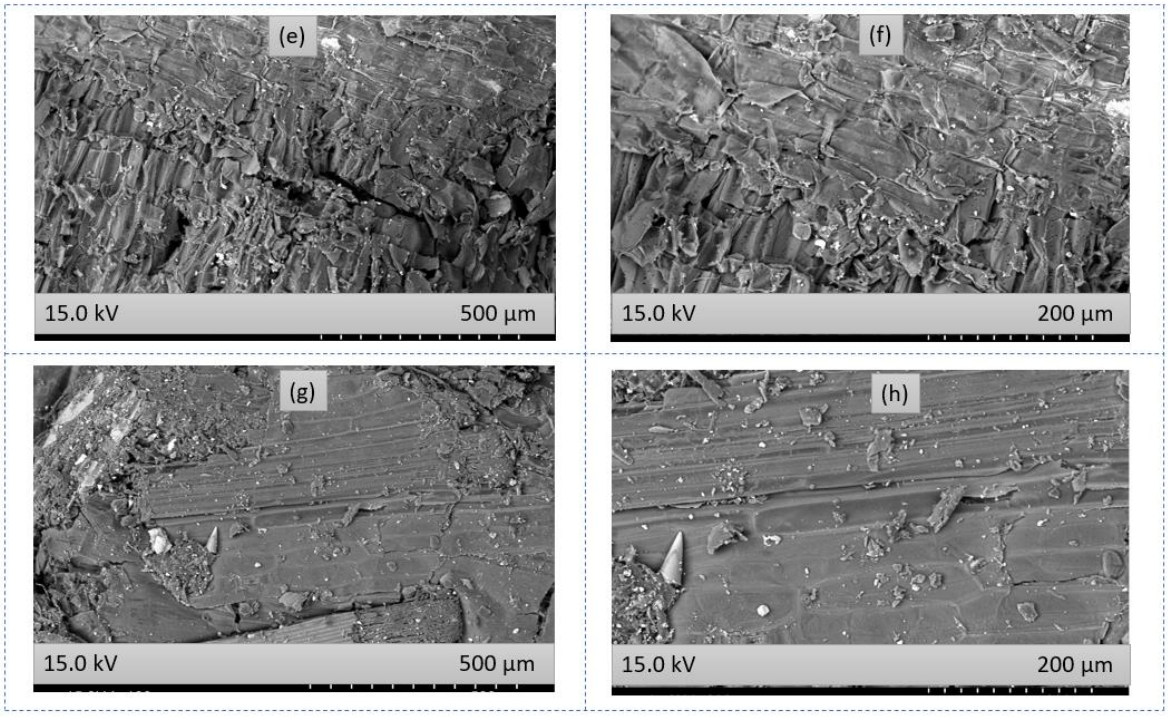

Figure 5.2: SEM micrographs of biocomposite panels (before fracture) from rice straw and energy reed fibers reinforced PF composites at different magnifications (a and b) EH1; (c and d) EH2; (e and f) EH3; (g and h) EH4.

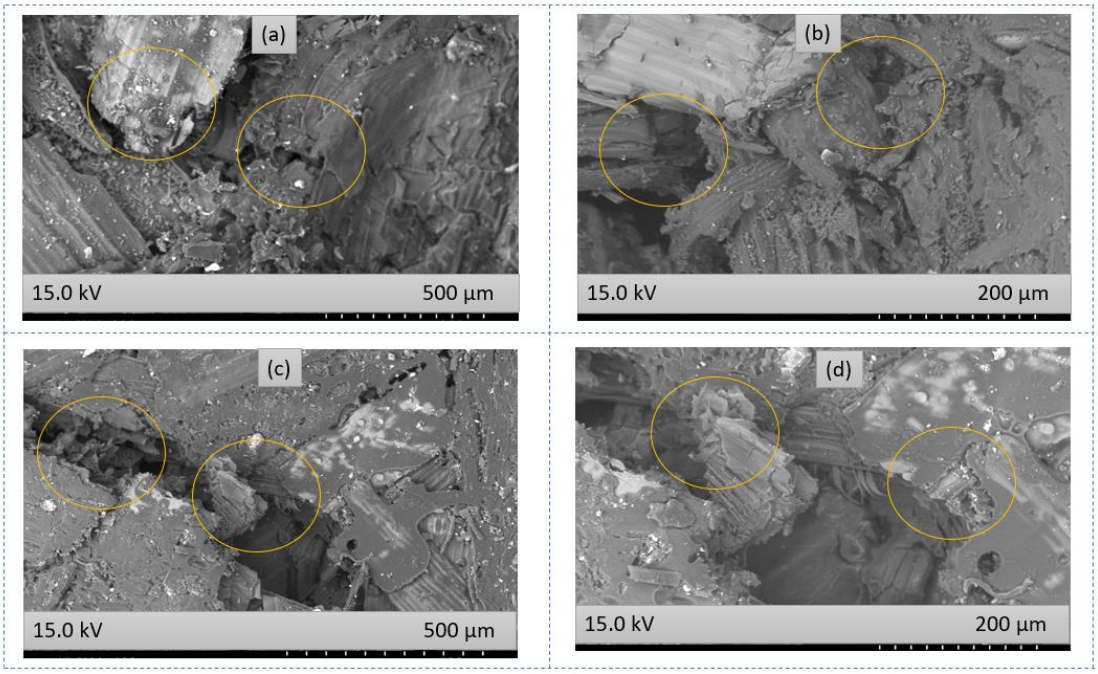

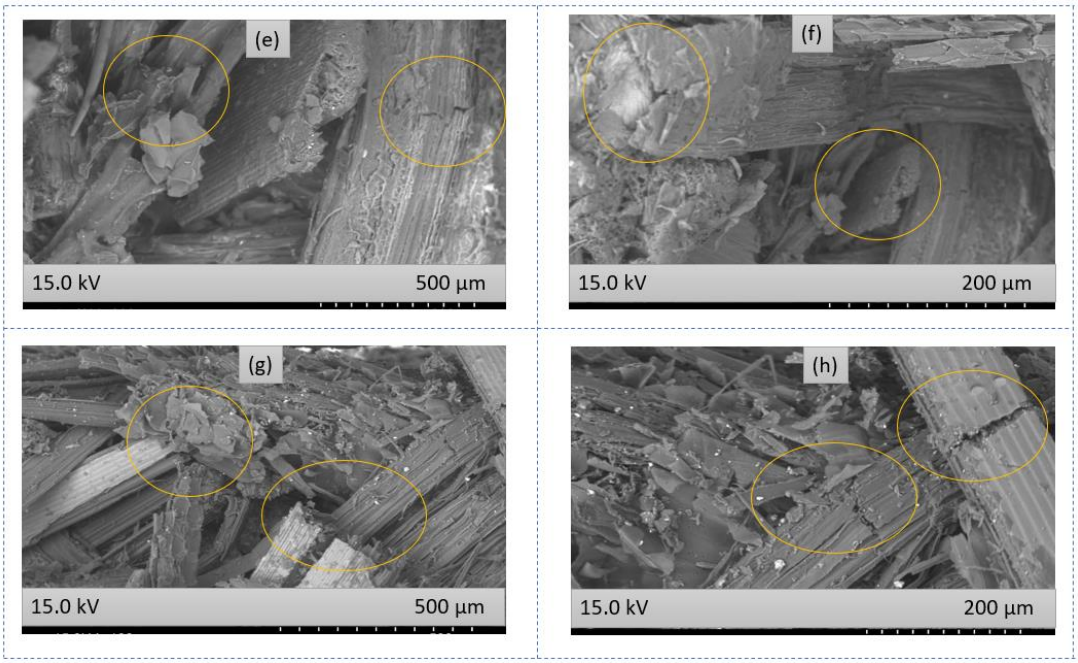

Figure 5.3: SEM micrographs of fractured biocomposite panels from rice straw and energy reed fibers reinforced with PF resin at different magnifications: (a and b) EH1; (c and d) EH2; (e and f) EH3; (g and h) EH4 .

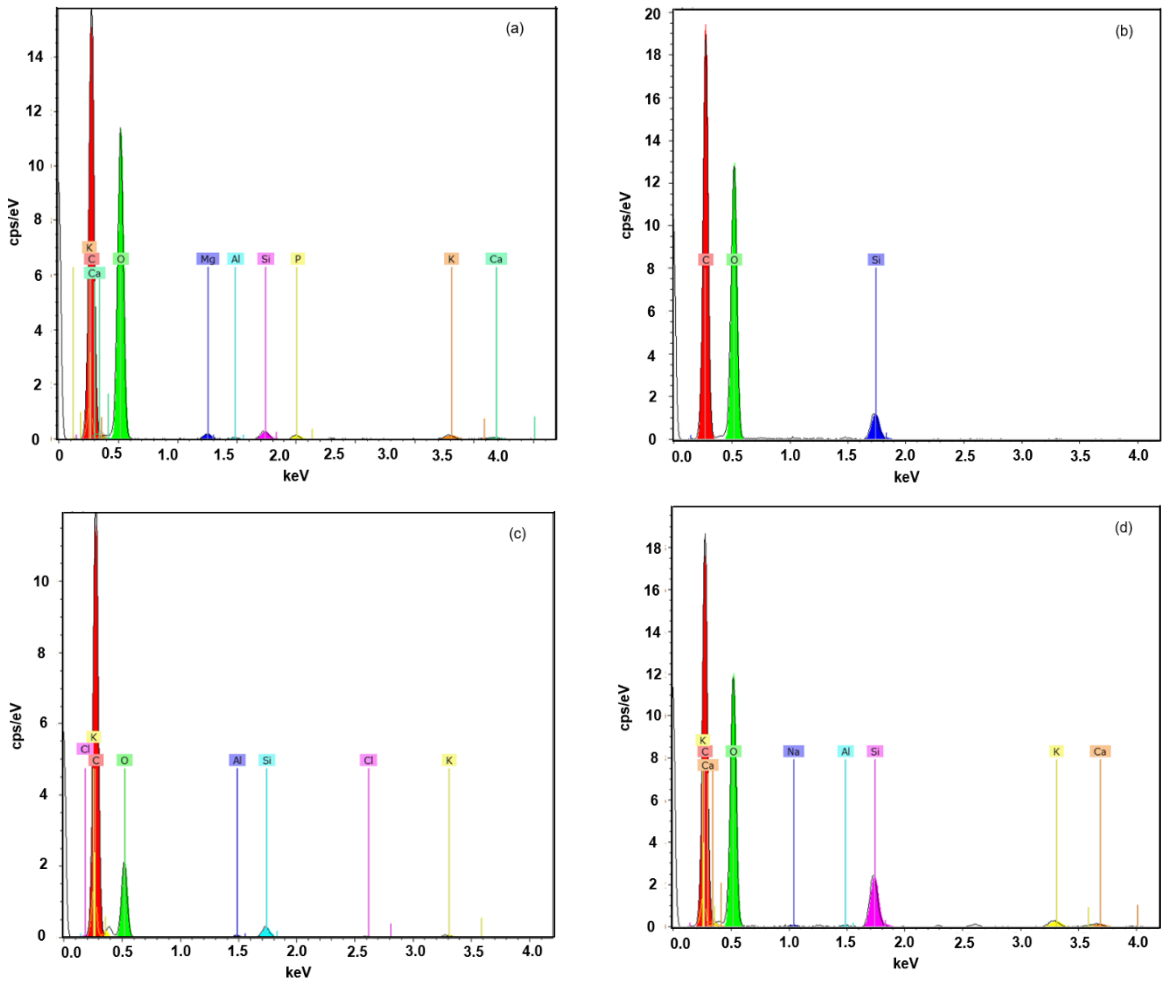

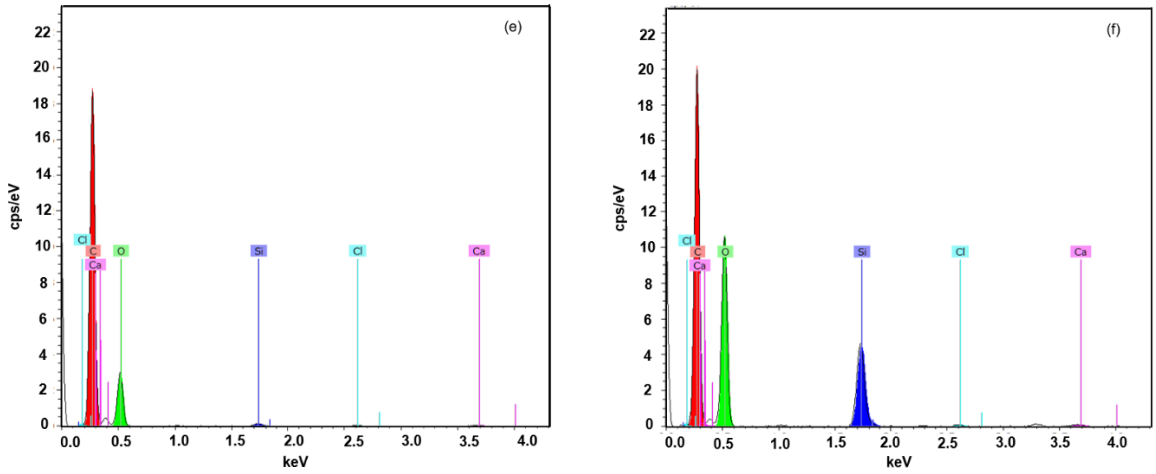

Figure 5.4: EDX spectra of produced biocomposite panels from rice straw and energy reed fibers reinforced with PF resin: (a) energy reeds fiber; b) rice straw fiber; (c) EH1; (d) EH2; (e) EH3; (f) EH4.

Furthermore, the presence of chemical elements in the biocomposite panels were also studied in terms of SEM mediated EDX (energy-dispursive X-ray) spectra to investigate the constituents of the materials. The main chemical elements of natural fibers are carbon (C) and oxygen (O) [155, 214] which are detected as the broad peaks in Figure 5.4 (a and b). However, the presence of C and O could also be observed for all the composites as well (Figure 5.4 c, d, e, and f). Moreover, there is also a signal detected for the presence of chlorine (Cl), Aluminum (Al), and potassium (K) in the composite panels which is maybe responsible for using the tap waters or processing equipments during preparing the materials in different stages appeared as impurities. However, the prominence of C and O is found to have increased especially for Figure 5.4 (E and H) compared to Figure 5.4 (a and b). The PF resin also contains O (oxygen) and carbon similar to natural fibers in their polymeric structures which may have consequence for this changes in the composite systems and their weight%.

5.1.3. Thermal conductivity

Thermal conductivity is a critical performance and reliability assessment parameter of polymeric composite panels for structural and construction materials. The types of finer and associated volume fraction of fiber materials play a significant role for the improved thermal conductivity of natural fiber reinforced composites [215]. It is found that composite panel 1 displayed the lowest values of thermal conductivity (0.061 (0.00083)) W/(m.K), whereas the highest values were found for 100% energy reed fibers reinforced composites (0.104790 (0.000571)). Moreover, the values of EH@2 and EH@3 composites provide 0.10383 (0.00061) and 0.10447 (0.00069) W/(m.K) thermal conductivity. It is noticed that thermal conductivity also shows increasing trends like mechanical properties with the increased loading of energy reeds (Figure 5.5). In our previous study [216] for coir fiber and fibrous chips reinforced with MUF polymeric composite panels (medium density), we found the thermal conductivity values between 0.09302±0.00999 to 0.1078±0.0072 W/(m.K). In another study by Ramanaiah et al. [217] for *Typha angustifolia* reinforced polyester composites (high density) showed the thermal conductivity between 0.137 to 0.432 W/(mK). However, the obtained thermal conductivity reported in this current study is found to provide comparatively better results demonstrating the produced biocomposite panels could perform as prominent insulation materials. However, the density could be enhanced from medium to higher for attaining lower values of thermal conductivity, which could be utilized as a potential building material. Additionally, rice straw reinforced composites provided better thermal conductivity values in terms of insulation

performances, although the mechanical properties found were not competitive compared to energy reed fibers reinforced panels.

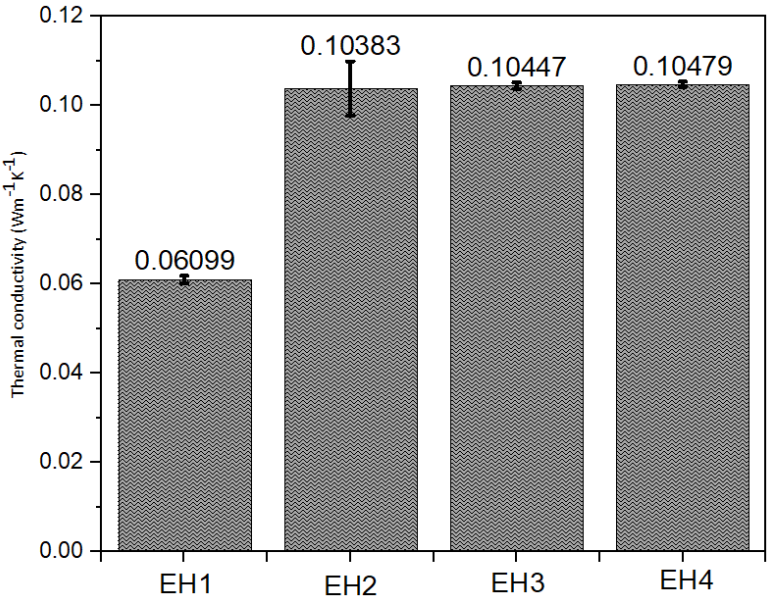

Figure 5.5: Thermal conductivity of produced biocomposite panels from rice straw and energy reed materials reinforced with PF resin

5.1.4. FTIR investigation

The functional groups of cellulosic materials used in this research were detected in terms of FTIR spectra (Figure 5.6). Both the rice straw and energy reeds are displaying broad absorption peaks within 3600 to 3200 cm^{-1} wavelength demonstrating the presence of –OH groups in their polymeric structures [218, 219]. However, similar peaks also could still be noticed after the fabrication of biocomposites. The peaks become broader after the reinforcement maybe due to the reinforcement with PF resin. The peaks at around 2921 and 2852 cm^{-1} are indicating the C═H stretching vibrations [218, 220]. Moreover, peaks at 1733 cm^{-1} are related to the lignin fractions present in the naturally derived materials. The absorption band at 1507 cm^{-1} is assigned for the aromatic ring vibrations. The presence of primary alcohol is confirmed by the peaks at 1032 cm^{-1} [221]. The presence of different functional groups present in control and produced products are seen according to different peaks. It seems even after reinforcement the changes in their inherent polymeric structures are not degraded, hence providing better performances even after reinforcement among the natural fibers and PF resin.

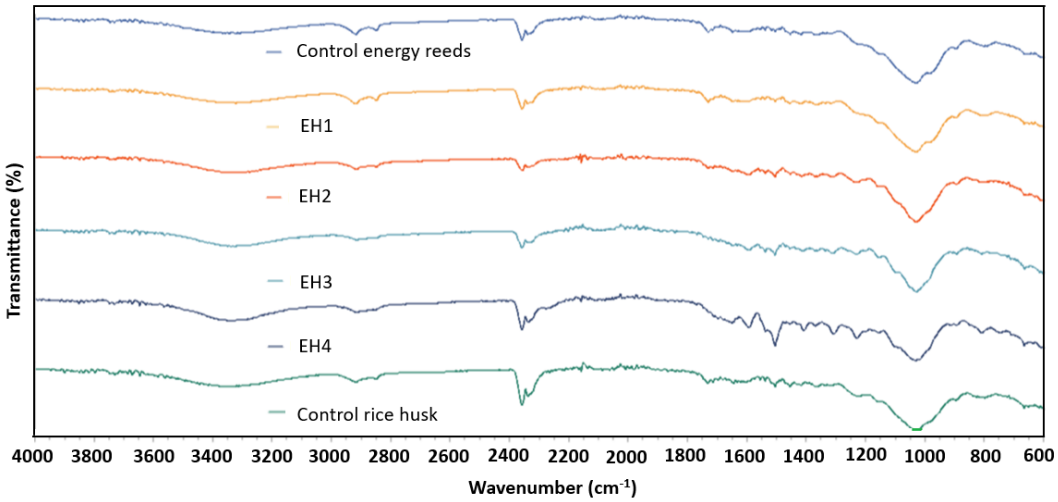

Figure 5.6 : FTIR spectra of control energy reed, rice straw, and associated biocomposites.

5.1.5. Physical properties test

The water absorbency, thickness swelling, and physical properties are the key parameters for investigating the physical properties of biocomposite materials (Figure. 5.7). All the properties were measured after 2 and 24 h. The water absorbency and thickness swelling properties were tested after immersion of the hybrid biocomposite samples under the water. Compared to artificial fibers, natural fiber reinforced composites in general absorb higher water and moisture from the surrounding atmosphere [155]. The cause of higher water absorption is due to the presence of some hydrophilic chemical compounds like –CO, –COOH, –NH_2, and –OH, in the natural fibers polymeric structures [155, 222]. The water absorption, thickness swelling, and moisture content studies of the developed hybrid biocomposite panels shown that 100% rice straw reinforced composites provided the maximum values (54.284 (2.6580)% for water absorbency, 38.572 (0.1744)% for thickness swelling, and 5.92 (0.6464)% for moisture content) whereas the energy reed fiber (100%) reinforced composites provided the lowest values (7.746 (0.3391)% for water absorbency, 9.383 (0.5115)% for thickness swelling, and 5.11 (0.2423)% for moisture content) after 2 h. However, the similar trend is also noticed after 24 h although the absorption rates started to decline gradually after 2 h. The sequence of the physical properties in terms of higher values is EH1> EH2> EH3> EH4 for the composite panels. It is seen that energy reed fiber loaded biocomposites absorb less moisture and water compared to the rice straw loaded biocomposites. However, the moisture content in the hybrid composite systems start to decrease with the increased loading of energy reeds in the proportions. The similar phenomenon were also discussed by the researchers in previous studies for different natural fiber reinforced polymeric composites [167, 223, 224].

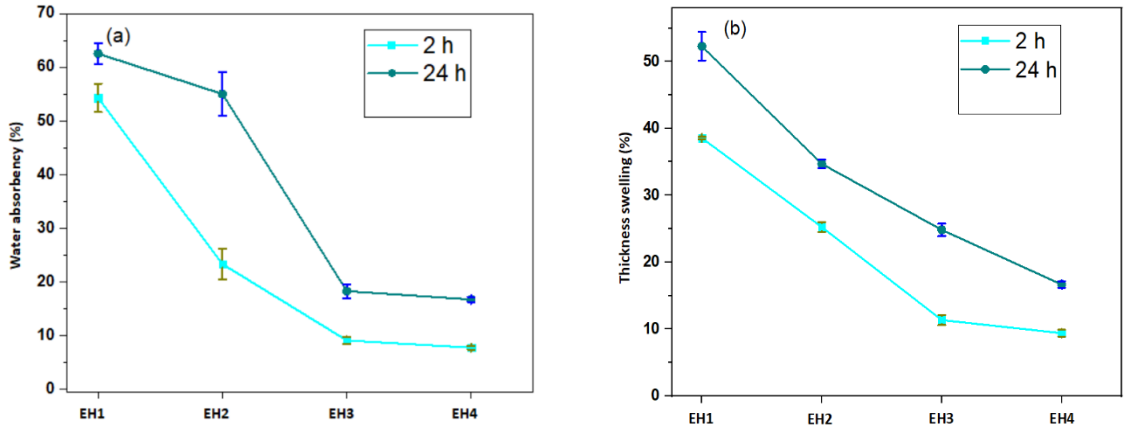

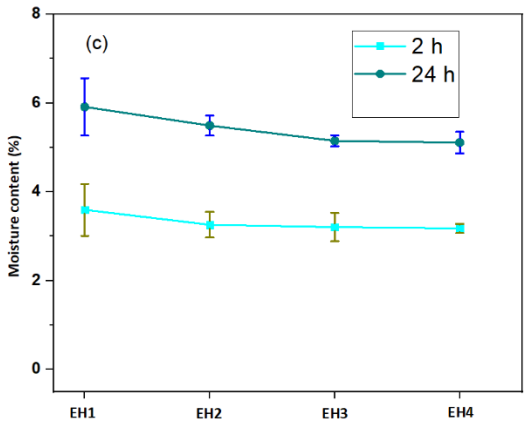

Figure. 5.7: Physical properties of the developed biocomposites: (a) water absorbency, (b) thickness swelling, and (c) moisture content.

5.2. Work package 2

5.2.1. Sugar and tannin contents

Sugar and tannin contents of both scots pine and coir fibers were investigated before composite panel fabrications began in order to keep the presence of inhibiting materials in the lignocellulosic materials within an acceptable range. By applying analytical method in the laboratory both sugar and tannin contents were measured. In case of sugar content test, the sealed test tube was used for this investigation which was Ø 16 mm in dimensions. The electric balance was used for the measurements of the chemical ingredients and fibers having the accuracy of 0.01 g. A sand bed was used for the heating of test tubes. Erlenmayer flask was used with 250 and 600 cm^3 volume. Some other flasks of 100 and 200 cm^3 were also used. The adjustable pipette (1-5 cm^3) with 20 and 100 cm^3 volume were also used for this study. The funnel size was Ø 16 mm and beaker dimensions were 100 cm^3. The filter and pH papers were used throughout the test for filtering and checking the pH of the solutions, respectively. The required chemicals used for this investigation were Lead acetate, concentrated H_2SO_4, granular NaOH, Fehling's solution (mixture of two solutions). The solution (A) was prepared from 6.39 g of $CuSO_4.5H_2O$ mixed in 100 cm^3 volume. The solution (B) was prepared by mixing 34.6 gm of potassium sodium tartrate and 10 gm of NaOH in 100 cm^3 distilled water. These two solutions were mixed equally before the usage. The lignocellulosic materials were weighed (10 g) by using an electric balance and transferred to a Erlenmayer flask containing 200 cm^3 distilled water. The flask was then placed in the sand bed and heated at 90-100 °C for 30 minutes. The solution was then filled with more hot distilled water to ensure 200 cm^3 volume for the filtration of aqueous extractions. In case of tannin content, 20 cm^3 of aqueous extracts were placed in another beaker. Then, 0.7 gm calcium lead acetate was added and waited for 24 h. The results were interpreted from the graph. However, the obtained tannin content was less than 0.25% as we found no change in the color for the solutions.

Finally, 100 cm^3 of aqueous extracts were transferred to another 250 cm^3 Erlenmayer flask, where 1 g of lead acetate was added. The existing tannin contents were dissolved and precipitated after the reactions. This is required for higher amount of tannin (because the tannin is cleaved by hydrolysis with H_2SO_4 and gallic acid in d-glucose and therefore having a sugar content in Fehlings solution reduction). The dissolved tannin is filtered and washed for twice

in a 250 cm^3 Erlenmayer flask. 5 cm^3 concentrated H_2SO_4 was added to that solutions. The resulted white lead sulphate precipitation was filtered off again quantitatively. The resulting filtrate was heated by sand bed at 90-100 °C for 30 min (the plant fiber sugars were reduced to monosaccharides in this stage). It was then poured into a 100 cm^3 standard flask. The pH was adjusted to the range 8-9 carefully by using NaOH after cooling. It could be mentioned that, the addition of NaOH particles to the solution should be performed/adjusted carefully as if the volume could not be exceeded from 100 cm^3. It was then poured into a 100 cm^3 standard flask. This solution was then equally distributed to 5 test tubes (20 cm^3 of each). After that, 1 cm^3 of Fehling solutions were added to each test tubes. The mixtures were then boiled for 2 min. As the solution to color change, so the wood fiber contains less than 0.5% sugar in this stage which is acceptable in terms of technological point of view.

The perceived sugar content of scots pine was nearly 0.415% and tannin content was less than 0.225%. Conversely, the assessed values of coir fibers were found to be nearly 0.25% for tannin content and the sugar content was also found to be lower than 0.5%. However, the standard range of sugar content should be less than 0.5%, whereas the standards for tannin content also found 0.3% [169]. The current research skipped the pretreatment step to save on energy, associated chemicals, and costs.

5.2.2. Mechanical properties

Figure 5.8 shows the load-displacement curves in terms of internal bonding strength and flexural properties. The pulling out strengths for 100% coir/OPC composite was the highest compared to all other types, whereas 100% pine/OPC composites had the lowest value in this current study. However, the strengths started to increase with the increased coir fiber loading in the composite systems. It seems that coir fiber possesses higher bonding with the OPC matrix, which requires the highest loads for displacement compared to other composite panels. Furthermore, the increased values of load also demonstrate an effective and uniform transfer of stress throughout the composite materials. Moreover, a creation of hydrogen bonding between the fibers and OPC also facilitates the creation of a stronger interface in cementitious matrix systems. It is also worth mentioning that coir fibers developed stronger bonding with the OPC than the Scots pine materials did. This was also discussed by the scientists for different fiber-reinforced cementitious composites [225]. Accordingly, the highest value for loading, 1973.6 N, was observed in C@C5 composite panels and lowest, 1468.3 N, in P@C1 composites. The highest loads exposed by different composite panels are as follows: PC@C2, 1507.3; PC@C3, 1575.3; and PC@C4, 1676.54 N for the pulling out of the test samples. Similar trends are also observed for flexural load-displacement curves. The highest load required to bend the specimen was in C@C5 samples (217.2 N) and the lowest load in P@C1 composites (81.2 N). Conversely, other composite panels also showed increasing trends from P@C1, which increases with the increase of coir fiber loading in the cementitious systems. Additionally, the stresses continued with the extended displacements until total failure occurred.

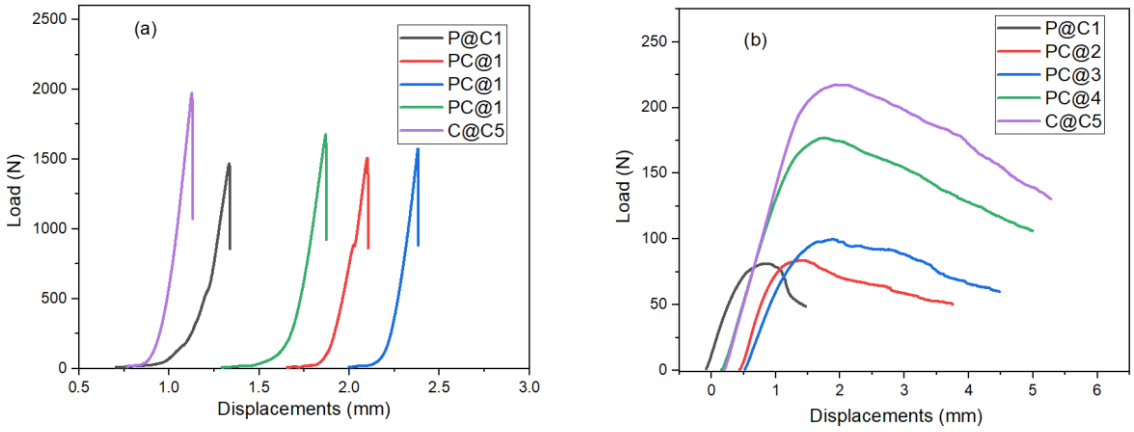

Figure 5.8: Load versus displacement curves of composite panels produced from coir fiber and scots pines reinforced with OPC: (a) Internal bonding strength and (b) flexural properties.

The nominal densities of the composite panels were considered 1200 kg/m^3; however, actual panel densities were 1176.1 (35.76), 1021.03 (38.95), 1337.47 (65.64), 1118.4 (6.94), and 1150.17 (18.81) kg/m^3. The same operation protocol was maintained for all the composite panels, but the discrepancies may have been due to the manual mixing of materials, in-homogeneous mixing of materials to the form mat, the compression of mats, and the manual cutting of test specimens. On the other hand, the mechanical properties of the developed composites also displayed the same pattern with the load-displacement curve. The flexural strengths obtained for the five composite panels were 6.22 (0.78), 6.77 (0.12), 6.78 (0.73), 7.97 (0.8), and 8.02 (0.87) MPa (Table 5.2) after 28 days of air curing in the laboratory. The flexural strengths of 100% scots pine was the lowest, whereas the patterns increase with the increase of coir fiber contents. Finally, 100% coir fiber-reinforced OPC composites exposed the highest values. A 29% increase was found in C@C5 compared to P@C1s. A similar trend was also observed for MOE results, with the exception of the PC@C2 composites. The reason behind the enhanced flexural properties could be the strong chemical and physical bonding [226] between the lignocellulosic materials and cement reagents (OPC). The incorporations of wood-based materials could play a significant role for the developed flexural properties in wood materials/cement composites [227].

Table 5.2: Mechanical characteristics of produced composite panels from coir fiber and scots pines reinforced with OPC: (a) P@C1, (b) PC@2, (c) PC@3, (d) PC@4, and (e) C@C5.

BCs	D (kg/m^3)	MOR (MPa)	MOE (GPa)	IBS (MPa)
P@C1	1176.1 (35.76)	6.22 (0.78)	6.78 (0.72)	0.63 (0.08)
PC@C2	1021.03 (38.95)	6.77 (0.12)	5.54 (0.74)	0.64 (0.03)
PC@C3	1337.47 (65.64)	6.78 (0.73)	7.62 (0.73)	0.66 (0.02)
PC@C4	1118.4 (6.94)	7.97 (0.8)	7.81 (0.42)	0.68 (0.03)
C@C5	1150.17 (18.81)	8.02 (0.87)	7.52 (0.87)	0.72 (0.06)

*BC–Biocomposites; D–Density; MOR–Modulus of rupture; MOE–Modulus of elasticity; IBS–Internal bonding strength.

The composite panels were also tested for internal bonding strengths (Table 5.2). P@C1 displayed 0.63 (0.08) MPa, whereas PC@C2 was 0.64 (0.03), PC@C3 was 0.66 (0.02), PC@C4 was 0.68 (0.03) MPa, and C@C5 was 0.72 (0.06) MPa. Similarly, the properties shown improved performances when coir fiber was induced in the composite systems. The most interesting finding is that all the panels show values higher than 0.5 MPa, which is the standard bottom line for internal bonding strengths [171]. Nevertheless, Ghofrani et al. [228] notes that the standard of internal bonding strengths as per ISO (the International Organization for Standardizations) system is 0.45 MPa. In this regard, the produced biocomposite panels could be implemented as prominent materials in the construction and building sector. Moreover, the 100% coir fiber-reinforced composite provided values that were roughly 14% higher than 100% scots pine reinforced cementitious materials. Although density is a significant parameter for determining the mechanical performances of composite panels [229], however the incorporation of different lignocellulosic materials played a key role in determining the ultimate performances of the composite materials in this current study.

5.2.3. Morphological observation

In addition to the thermomechanical and physical properties of cementitious materials, morphological photographs were also investigated. Figure 5.9 contains the SEM pictures of the composite panels, where the interface zones of coir fiber and Scots pines bonded OPCs are explicitly noticeable. Two phases could be observed in the composites: (a) a continuous fiber like layer (attributed to lignocellulosic materials) and (b) aggregated particle-like appearances (corresponding to OPC) [230]. Similar fiber-like appearances also appeared in the developed composites; see Figure 5.9 (a_1 and a_2). Furthermore, other images also displayed both the fiber and particle like aggregates in the composite systems. The appearances of lignocellulosic materials appeared more in P@C1 and PC@C2 than in other composites. This could be because the bigger scots pine particle contents were higher (100 and 60%) in these panels than they were in the other three types of panels. Conversely, the coir fibers were used here in fiber forms, which is why they were in closer contact with the OPC (due to smaller fiber-like materials); hence, they are nearly disappeared in the strongest bonding in the composite systems. This phenomenon also illustrates that lignocellulosic materials are compatible with OPCs. The strongest bonding could also be proved by the increased mechanical properties of the composite panels with higher loadings of coir fibers. However, the presence of lignocellulosic materials could be clearly seen in the fractured surfaces of composites, although OPC was strongly adhered in the surfaces of lignocellulosic materials (Figure 5.10). That is why more load is required to break the composites. This is also reflected in load versus displacement curves (Figure 5.8) and internal bonding strengths (Table 5.2). In addition, the interaction between the lignocellulosic materials and the OPC matrix plays a significant role for the initiation and determinations of crack propagations [231].

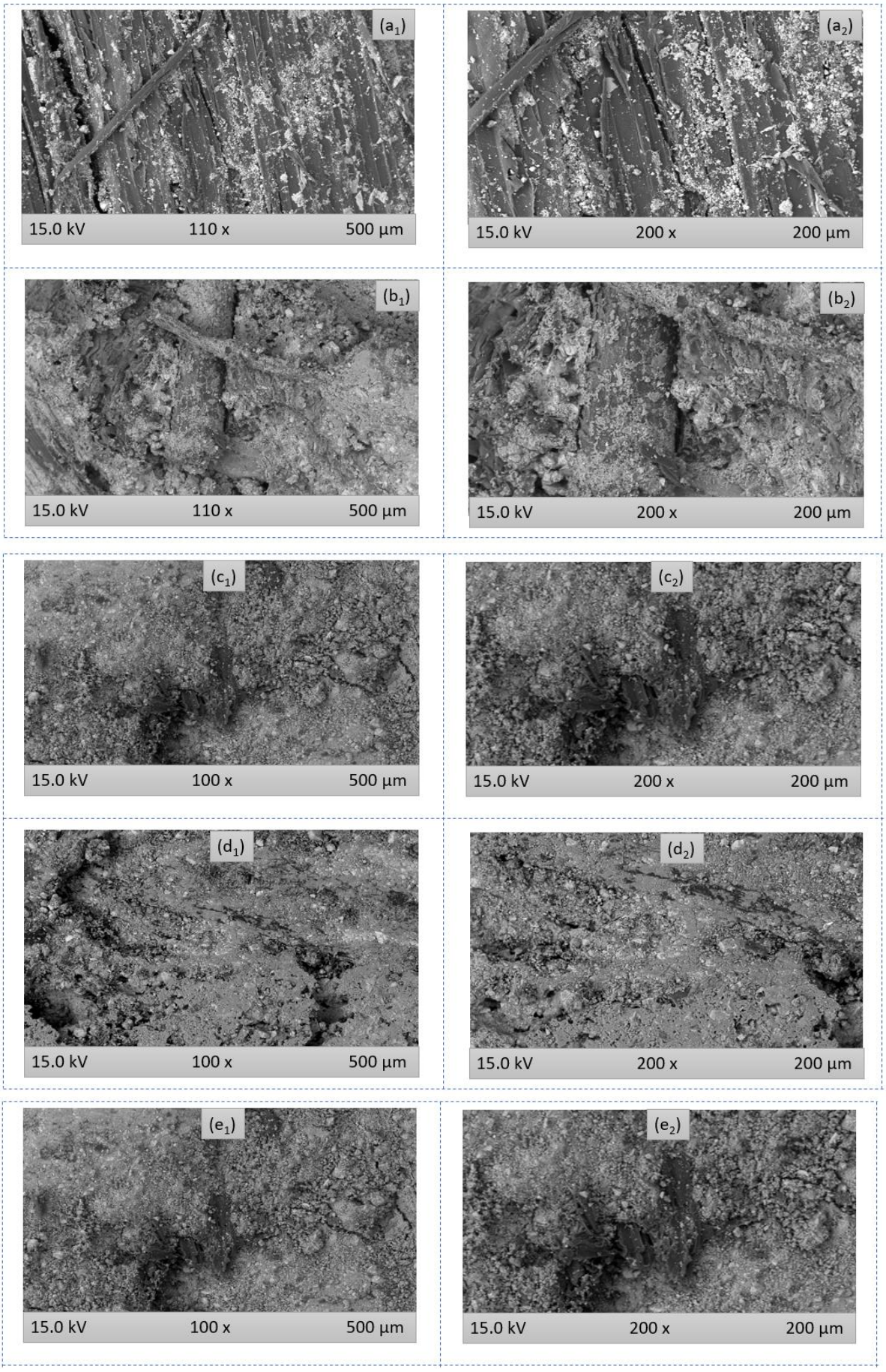
(a1)
15.0 kV 110 x 500 µm
(a2)
15.0 kV 200 x 200 µm
(b1)
15.0 kV 110 x 500 µm
(b2)
15.0 kV 200 x 200 µm
(c1)
15.0 kV 100 x 500 µm
(c2)
15.0 kV 200 x 200 µm
(d1)
15.0 kV 100 x 500 µm
(d2)
15.0 kV 200 x 200 µm
(e1)
15.0 kV 100 x 500 µm
(e2)
15.0 kV 200 x 200 µm

Figure 5.9: SEM micrographs of specimens (before fracture) of produced composite panels from coir fiber and scots pines reinforced with OPC: P@C1 (a_1 and a_2), PC@C2 (b_1 and b_2), PC@C3 (c_1 and c_2), PC@C4 (d_1 and d_2), and C@C5 (e_1 and e_2).

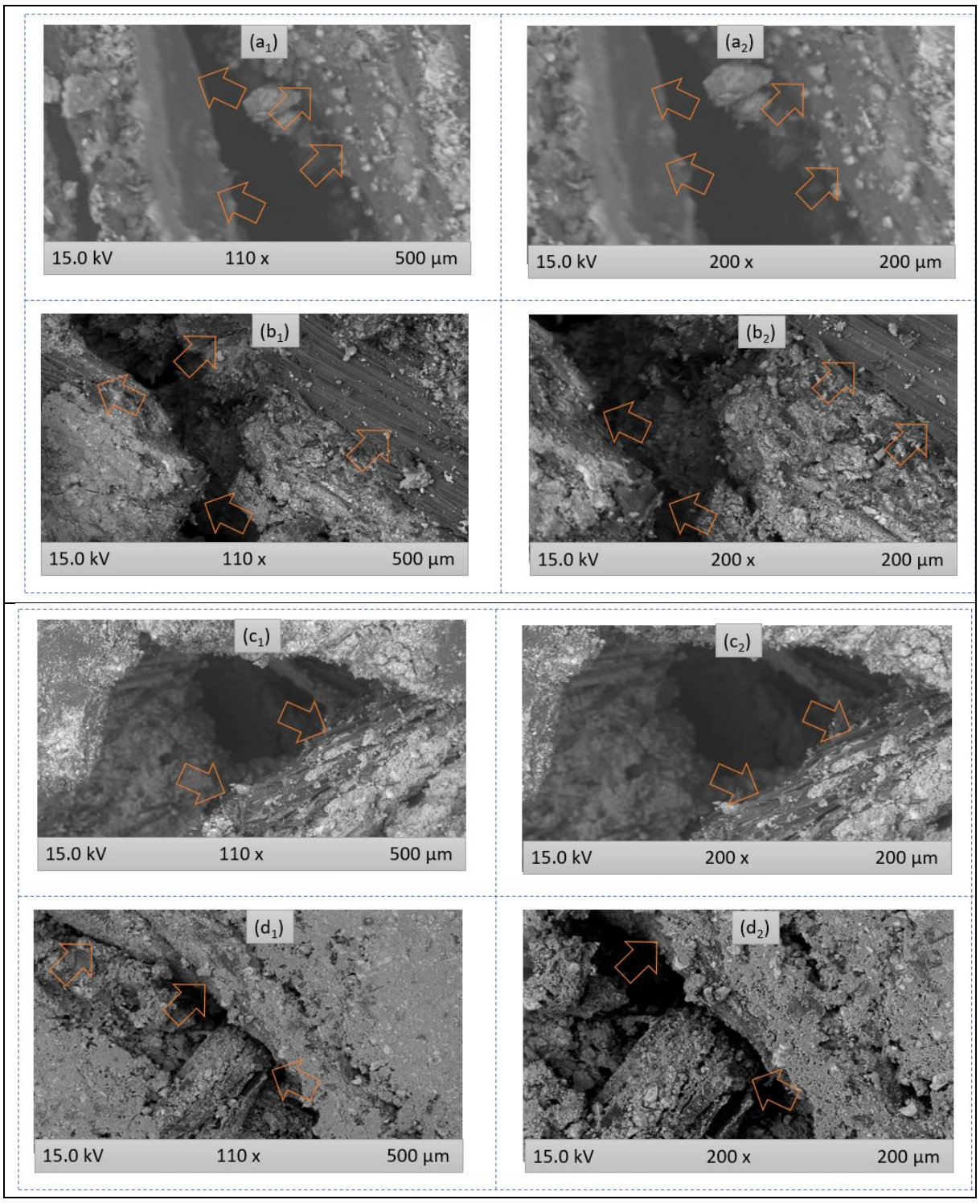

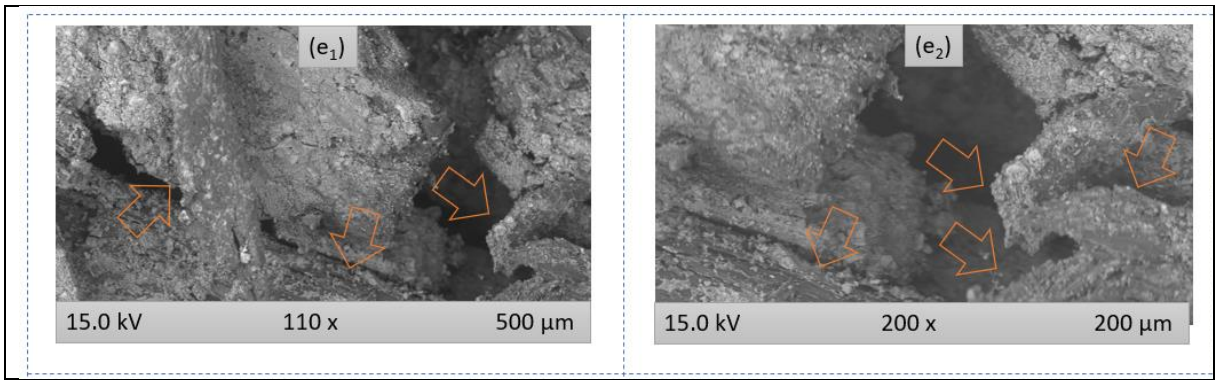

Figure 5.10: SEM micrographs of specimens (after fracture) of produced composite panels from coir fiber and scots pines reinforced with OPC: P@C1 (a_1 and a_2), PC@C2 (b_1 and b_2), PC@C3 (c_1 and c_2), and PC@C4 (d_1 and d_2), and C@C5 (e_1 and e_2).

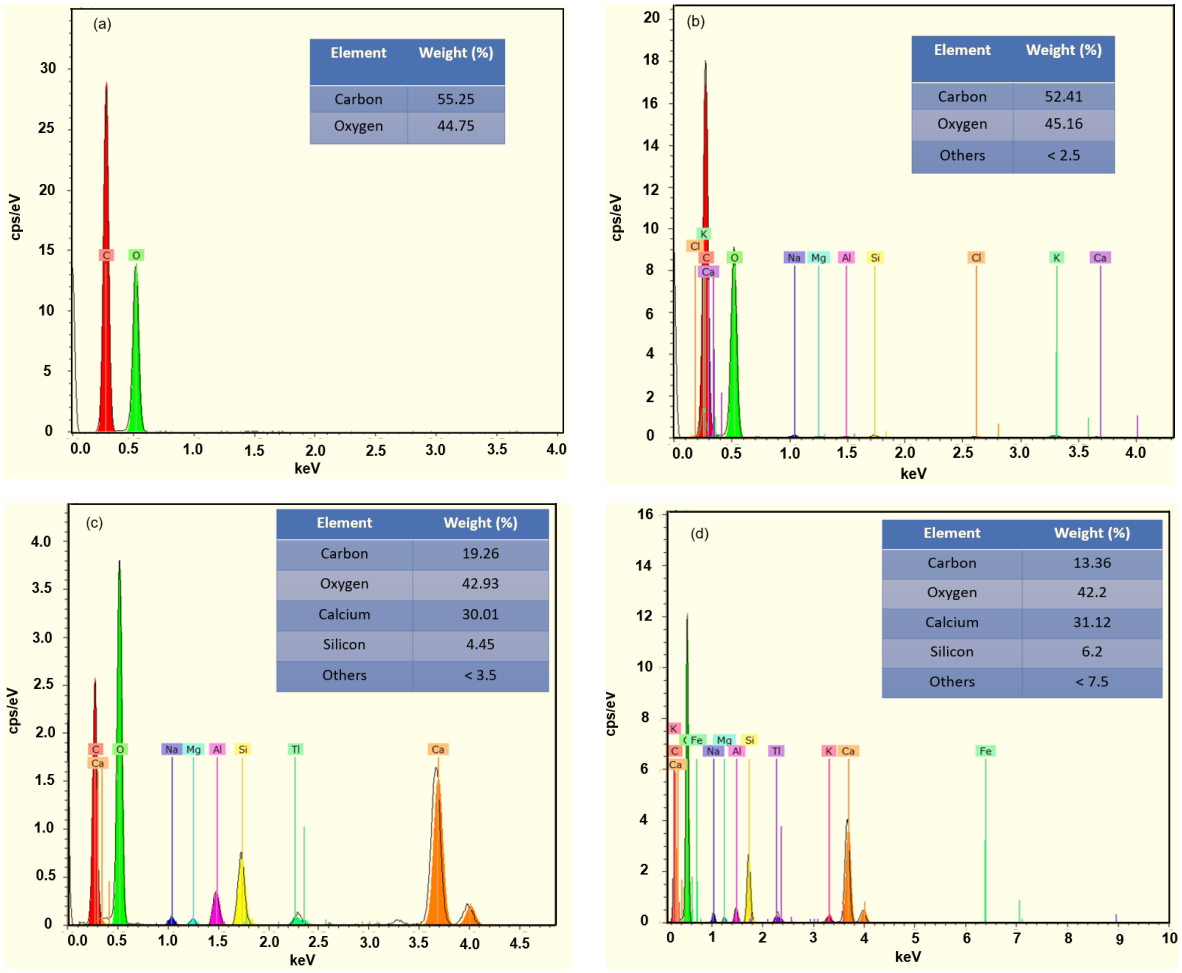

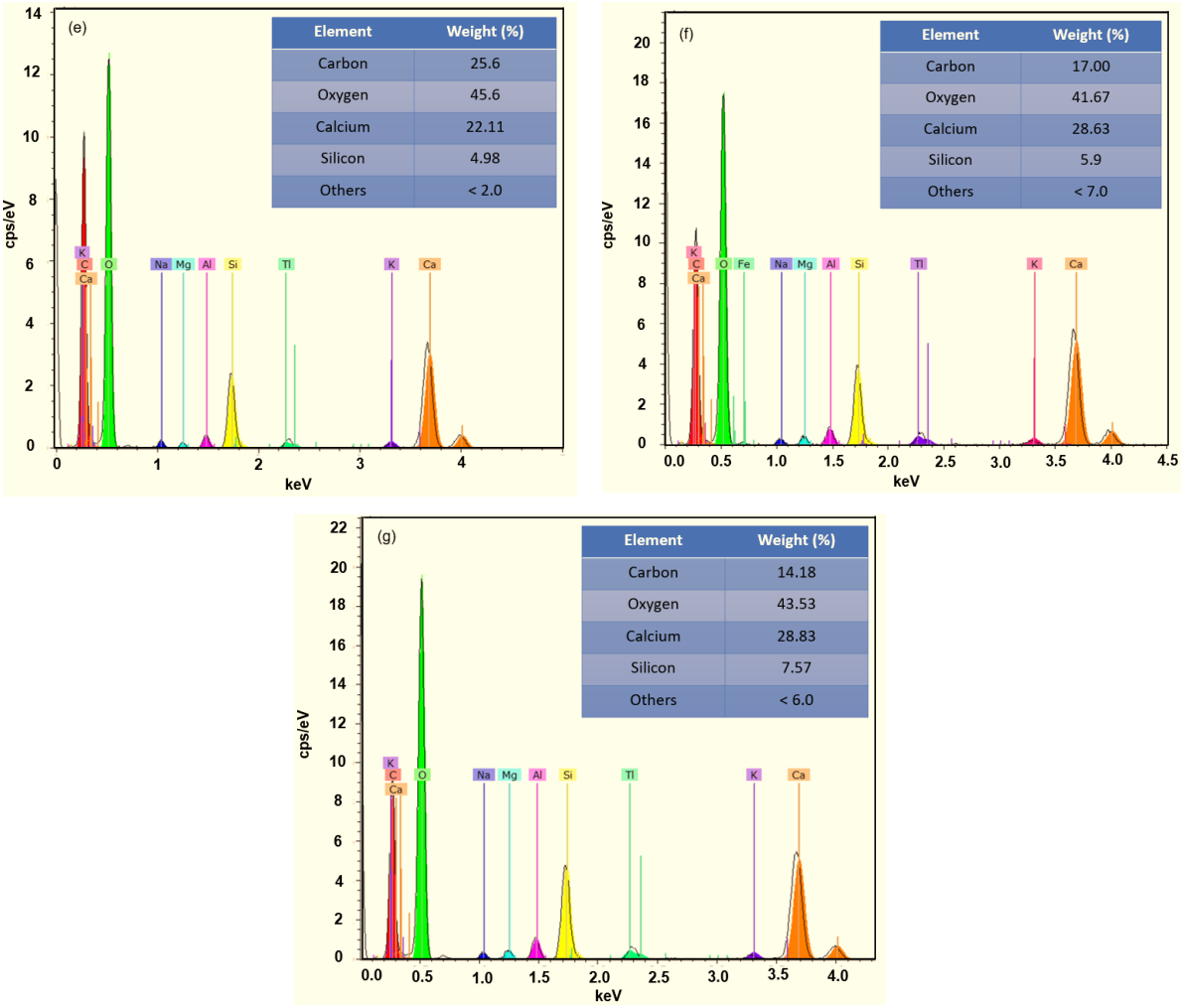

Figure 5.11: EDX spectrum of produced composite panels from coir fiber and scots pines reinforced with OPC: (a) 100% Scots pine, (b) 100% coir fiber, (c) P@C1, (d) PC@2, € PC@3, (f) PC@4, and (g) C@C5.

5.2.4. EDX analysis

The detected chemical elements in the cementitious composites could be easily discerned by differently colored scaling of EDX spectra. The EDX analysis of the cementitious composite exhibits the distribution of Ca and Si in different fragments that are the principal chemical constituents of OPC. The presence of Si and Ca signals were also detected by Wei et al. [232] for wood/cement composite panels at their interface. Furthermore, the significant presence of some other chemical elements like as Na, Mg, Al, Ti, K, and Fe, also reflects a successful bonding of OPC with the lignocellulosic Scots pine and coir fiber materials. The presence of these materials also corresponds with the constituent materials of OPC as shown previously in Table 3.3. The presence of C and O at different fragments in Scots pine and coir fiber control (Figure 5.11) was also notable, even after the bonding with OPC. Furthermore, the bonding of lignocellulosic materials with OPC could also be further confirmed by the FTIR analysis. Interestingly, the presence of C is higher in Scots pine (55.25%) than in coir fiber (52.41), which also applies to the associated composite panels at 100% Scots pine-reinforced OPC composite. In addition, this shows that the presence of C that is higher than it was in the 100% coir fiber-reinforced cementitious materials. Alternatively, a similar effect was noticeable in O, which was higher in coir fibers and associated composites. Moreover, the coir fiber and Scots pine controls displayed the dominance of C and O in their polymeric structure, but the phenomenon changed after the bonding with OPC for all the five composite panels,

where the dominance of Si and Ca is also apparent due to the strong influence of OPC in the composite systems. The presence of cementitious chemical agents in the composite systems also accords with the reports of other scientists [230, 233, 234].

5.2.5. Thermal conductivity investigation

Thermal conductivity values of different cementitious composite panels (Figure 5.12) were also investigated to assess their insulation performances. The thermal conductivity of air is 0.026 W/(m.K), water 0.6 W/(m.K), and the cement stones is 1 to 3 W/(m.K) [235]. Natural plant fibers contain a thermal conductivity of around 0.2 W/(m.K) [226]. The distribution and volumes of pores in the cementitious composite also affect the thermal conductivity. As the thermal conductivity of water and cement is also excessively higher than air, they also significantly influence the thermal conductivity of lignocellulosic materials bonded with OPC composite panels. However, thermal conductivity values obtained in our current study exhibited values of 0.17045 (0.00352) W/(m.K) for P@C1, whereas PC@C2 was 0.16651 (0.00265), PC@C3 was 0.11646 (0.00263), PC@C4 was 0.11265 (0.00409), and C@C5 was 0.10547 (0.00657) W/(m.K). Notably, when the coir fiber was induced in composite systems, the thermal conductivity values started to decline. That is why our study reveals the 100% coir fiber-reinforced cementitious composite to be the best insulation material, whereas 100% scots pine displayed the lowest thermal conductivity values according to the performance perspectives. Another highly impressive finding of this research is that the cementitious composite panels also provided competitive thermal conductivity with MUF polymeric composites with coir fiber and fibrous chips, which in our previous study ranged within 0.09302 (0.00999) to 0.1078 (0.0072) W/(m.K) [202]. In another study by He et al. [226], the lowest thermal conductivity value was obtained for wood/magnesium-oxychloride cement composite by 0.97 W/(m.K), whereas the results explained in this current study are within 0.17045 (0.00352) to 0.10547 (0.00657) W/(m.K), demonstrating better thermal insulation capability of the panels.

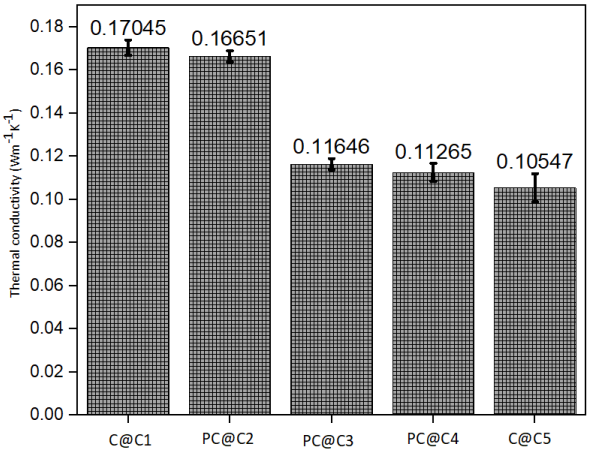

Figure 5.12: Thermal conductivity of coir fiber and Scots pines reinforced with OPC composites.

5.2.6. FTIR analysis

The FTIR analysis of the developed composite panels from coir fiber and scots pines reinforced with OPC matrix is shown within 4000 to 400 cm^{-1} wavelengths (Figure 5.13). The peaks within 3200 to 3400 cm^{-1} represents the stretching vibrations of O–H and C–H bands of hemicellulose [236, 237]. The peaks around 1000 cm^{-1} is associated with the stretching vibrations of Si–O [237] and C–O bands (cellulose and hemicellulose). The spectrum within

873 to 1418 cm^{-1} are related with the carbonations of different hydrates in the composite systems [237, 238]. Furthermore, the absorption band at 1418 cm^{-1} is attributed to the CH bending of aromatic rings of lignin polymers [239], which is broader with coir-based materials as coir possesses higher lignin contents when compared to scots pine. Moreover, the peaks at 573 cm^{-1} is attributed to the cementitious matrix that is absent from the coir fiber and scots pine controls, but is present in the cementitious materials [170]. The overall discussions demonstrate a successful bonding of coir fiber and Scots pines with the OPC matrix, which adds better thermal and mechanical properties to the composite panels.

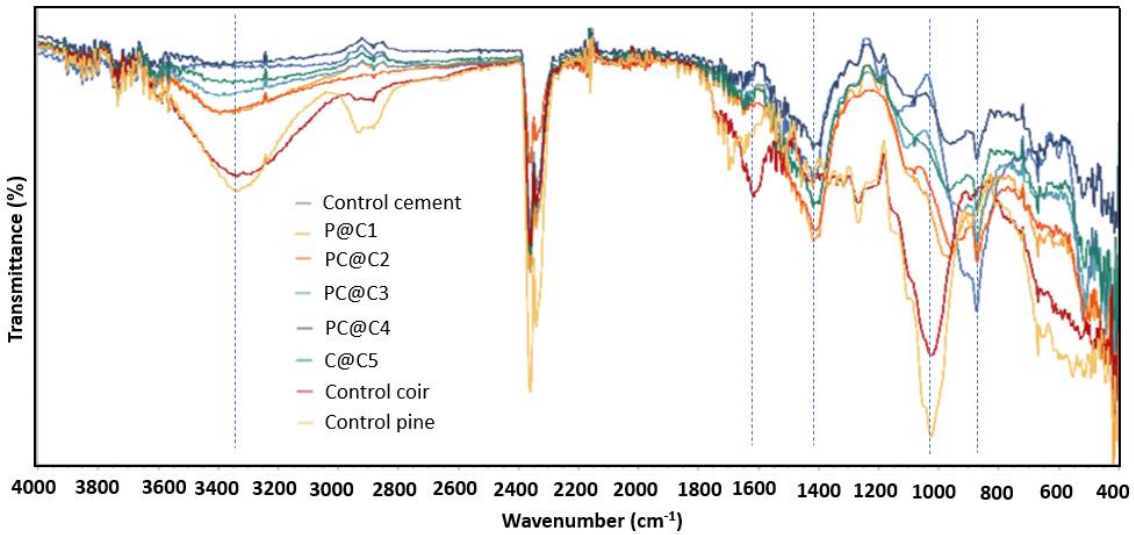

Figure 5.13: FTIR analysis of produced control ligncellulosic materials, OPC, and associated composite panels from reinforced with OPC.

5.2.7. Physical properties investigation

The physical effects of different lignocellulosic materials on cementitious materials are shown in Figure 5.14, in order to investigate the dimensional stabilities for 2 and 24 h periods. It is evident that the incorporation of coir fiber leads to decreased moisture content as well as decreased water uptake. This is because fiber materials could achieve closer contact with the cements, thereby reducing the possibility of void creations. This, in turn, led to less water absorption [226] than in the porous Scots pine particle reinforcements. Moreover, plant materials are hydrophilic in nature due to the presence of –OH groups in their polymeric structures; hence, a hydrogen bond is created when they come in contact with water. This phenomenon is also responsible for moisture contents and water absorbency as well as thickness swelling (Figure 5.14 b). Coir fiber also possesses high resistance against moisture, which helps it to withstand water [19]. As is the case with other thermal and mechanical properties, 100% coir fiber-reinforced cementitious materials also exhibited better stability against water compared to 100% scots pine reinforced cementitious composite panels. The moisture content for composite 1 was 5.3 (0.4)% and 3.9 (0.9)% for composite 5. The sequence of moisture contents, water absorbency, and thickness swelling in terms of better stability is seen from the figure from coir reinforcement to pine in the composite system. A similar trend was also observed for water absorption, where the values varied from 19.1 (0.9)% for composite panel 1 to 14.6 (0.9)% for composite panel 5 after 2 h of water immersion. After 24 h of immersion, the values increased slightly by 30.3 (0.4)% for composite 1 and 25.1 (0.3)% for composite 5. The other panels showed water absorption values between composite panel 1 and 5 as they are made of different proportions of Scots pine and coir. Composite panel 1 displayed a thickness swelling value of 1.9 (0.02) and composite 5 displayed a value of 1.1 (0.07)% after 2 h. After 24 h, the values increased slightly to 2.6 (0.06) and 1.9 (0.06)%, respectively. The other

composites demonstrated thickness swelling values that ranged between composite 1 and 5. A similar phenomenon of physical properties was also reported by other researchers for lignocellulosic fiber-reinforced cementitious composites [228, 231, 240]. However, the developed composite panels could also be used for indoor applications due to their improved physical properties.

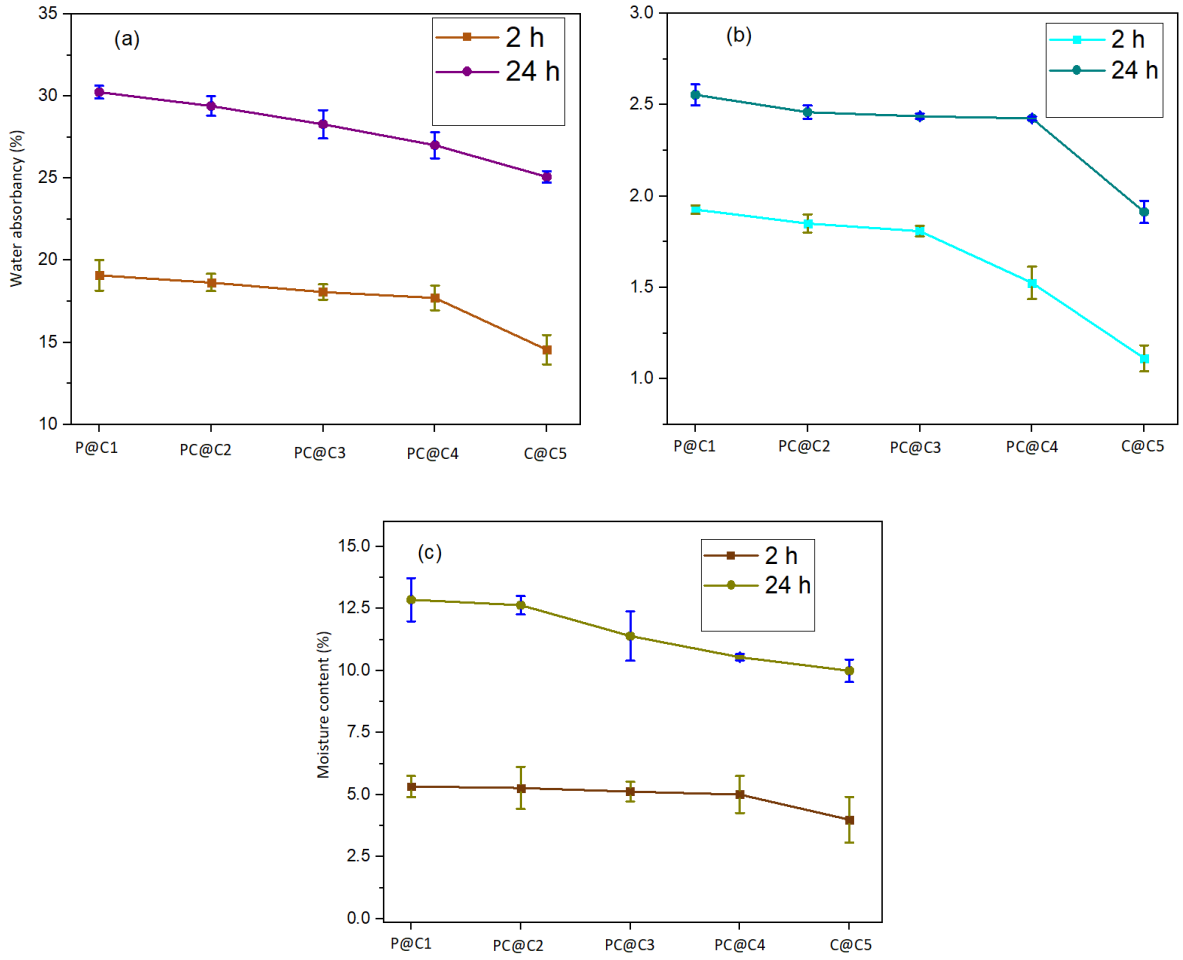

Figure 5.14: Physical properties of produced composite panels from coir fiber and scots pines reinforced with OPC: (a) water absorbency, (b) thickness swelling, and (c) moisture content.

5.3. Work package 3

5.3.1. Mechanical properties of composites

The tensile properties of composites are highly influential to assess the strength of produced materials. The tensile and flexural features of the manufactured composites (Figure 5.15) are given in Table 5.3. The tensile strengths of pure glass (G1), glass/flax (GF2 and GF3), and pure flax (F4) reinforced MDI composites take the values of 78.61 (8.2), 69.63 (2.77), 49.44 (2.05), and 21.19 (1.59) MPa, respectively. While GF2 (hybrid composite) exhibited the highest tensile modulus (7.59 (0.58) GPa), pure flax reinforced composite exhibited the lowest modulus and tensile strength too. It is found from Table 5.3 that, glass fiber reinforced composites are stronger than naturally originated flax reinforced composites. However, the laminated composites of glass/flax composites provided more strength than flax itself. Besides, it is also observed that, the more loading of glass with flax enhances the composites' strength. The

similar phenomenon was also described by other researchers for different design of fabric stackings (glass/flax) [241] with vinyl ester used as polymeric resin.

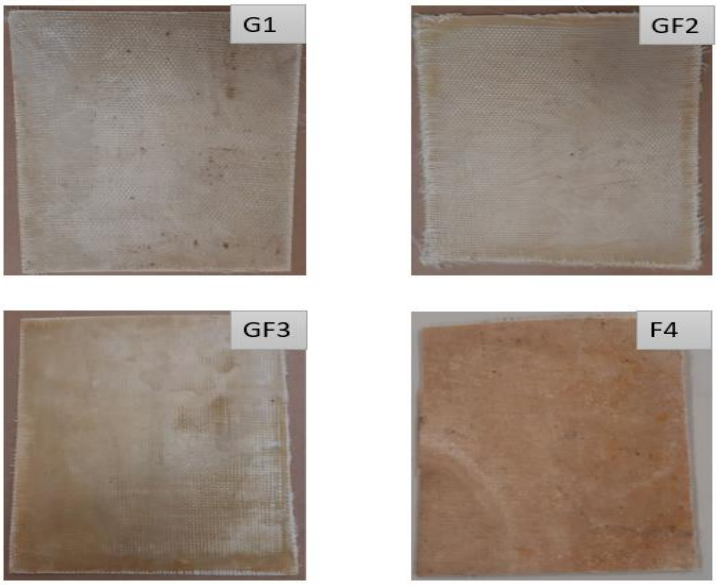

Figure 5.15: Representation of hybrid biocomposites: G1 (pure glass composite), GF2 (hybrid composite from glass/flax), GF3 hybrid composite from glass/flax, and F4 (pure flax composite).

The flexural strengths followed the similar trend as the tensile characteristics. The perceived flexural strengths were 211.9 (17.9), 147.7 (18.5), 58.9 (9.5), and 43.9 (3.5) MPa (Table 5.3), respectively for G1, GF2, GF3, and F4 composites. Besides, Young's modulus followed the similar pattern of flexural strengths (54.4 (1.8), 40.4 (7.8), 39.9 (4.4), and 3.9 (0.8) MPa). As expected, naturally originated flax reinforced composites provided the lowest strengths, whilst those with pure glass reinforcement produced the highest values. However, the strength values started to increase with the incorporation of more glass fiber loading into the hybrid composites [241]. Likewise, glass reinforced MDI composites provided higher bending modulus, with higher tendency to bend without breaking in contrast to flax reinforced composites.

Table 5.3: Tensile and flexural properties of produced composites (G1, GF2, GF3, and F4). Pure glass and hybrid composites exhibited better mechanical performances in contrast to natural flax. (Means with standard deviations in parentheses).

Laminated composites	**Tensile strength (MPa)**	**Young's modulus, E (GPa)**	**Flexural strength (MPa)**	**Bending modulus, MOE (GPa)**
G1 (100% glass)	78.61 (8.2)	6.82 (0.15)	211.9 (17.9)	54.4 (1.8)
GF2 (75% glass/ 25% flax)	69.63 (2.77)	7.59 (0.58)	147.7 (18.5)	40.4 (7.8)
GF3 (50% glass/ 50% flax)	49.44 (2.05)	6.73 (0.52)	58.9 (9.5)	39.9 (4)
F4 (100% flax)	21.19 (1.59)	2.54 (0.15)	43.9 (3.5)	3.9 (0.8)
R^2	0.66	0.57	0.41	0.89

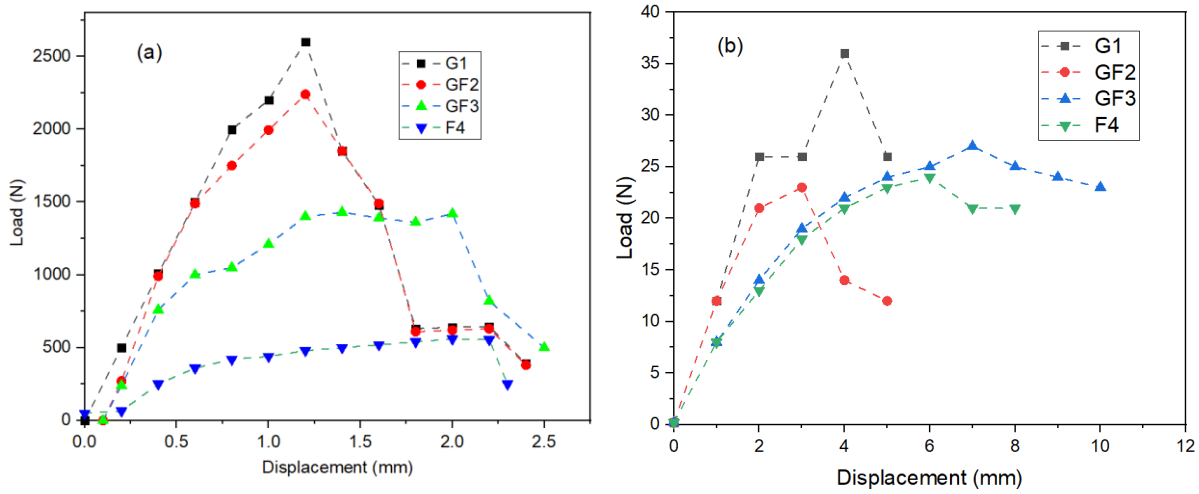

Figure 5.16: Load versus displacement graphs for G1, GF2, GF3, and F4 composites; (a) tensile test and (b) flexural test.

The load versus displacement behavior of the test pieces is illustrated in Figure 5.16 (a and b) both for tensile and flexural tests. In case of tensile displacements, all the curves showed a linear region initially; a non-linear region appeared whenever the cracking happened. Composite G1 attained a load of approximately 2000 N in the linear range in tension. After exhibiting a maximum load of around 2650 N at extended delamination, the load started to decline with the increase of displacement until failure. The decline of highest load depends on the onset of delamination and development of cracking in the laminates. In case of composites GF2 and GF3, the highest observed loads in the linear range were 1500 and 750 N, respectively. Linearity for F4 ended at 50 N, although load continued to increase with the increased delamination up to 500 N, then started to drop. In the course of flexural tests, the highest load attained in the linear range by the composites G1, GF2, GF3, and F4 was 26, 21, 14, and 7 N, respectively. Similar trends for load and displacement patterns were also discussed in some other studies.

5.3.2. Regression analysis for Mechanical performances

The regression analyses of all the composites mechanical performances were conducted in terms of glass fiber proportion in the composites. The R^2 values (Table 5.3) for all the composites are higher than 0.57, except for flexural strength with R^2=0.41. It seems that the presence of glass fiber results in higher mechanical performances of all the composites. The p values for tensile strength and tensile modulus (Table 5.4, Table 5.5, Table 5.6, Table 5.7) stand far less than 0.05 except for flexural strength and modulus, where the intercept parameter of the regression equation did not prove to be significant; see the corresponding p values shown in bold in the Table 5.6 and Table 5.7. These results support the existence of significant effects of glass fiber proportion on composite properties with slopes higher for strength than for modulus of elasticity.

Table 5.4: Regression analysis for tensile strength in terms of glass fiber compositions on different composites.

Effects	Tensile strength parameter	Tensile strength standard error	Tensile strength (t)	Tensile strength (p)
Intercept	27.96	6.97	4.01	0.002
Composition	0.44	0.10	4.36	0.001

Table 5.5: Regression analysis for tensile modulus in terms of glass fiber compositions on different composites.

Effects	Tensile modulus parameter	Tensile modulus standard error	Tensile modulus (t)	Tensile modulus (p)
Intercept	3.61	0.77	4.68	0.001
Composition	0.04	0.01	3.62	0.005

Table 5.6: Regression analysis for flexural strength in terms of glass fiber compositions on different composites.

Effects	Flexural strength parameter	Flexural strength standard error	Flexural strength (t)	Flexural strength (p)
Intercept	44.25	30.58	1.45	**0.18**
Composition	1.163	0.44	2.65	0.02

Table 5.7: Regression analysis for flexural modulus in terms of glass fiber compositions on different composites.

Effects	Flexural modulus parameter	Flexural modulus standard error	Flexural modulus (t)	Flexural modulus (p)
Intercept	7.65	3.64	2.10	**0.062**
Composition	0.47	0.05	9.01	0.00

The mechanical features of the produced composites were further analyzed conducting one-way ANOVA with the type of composites as categorical factor. Overall F-tests of significance for all the four mechanical properties provided evidence of effect of all the composite types. For pairwise comparisons of the four types Newman Keuls tests (Table 5.8, Table 5.9, Table 5.10, Table 5.11) were used since the statistical assumptions of ANOVA were not always met. These tests showed that strength properties of the different composites are significantly different as the p values are less than the assumed level of significance of 0.05. However, the modulus of elasticity values in two cases shown by bold in the (Table 5.9, Table 5.10, Table 5.11) do not exhibit significant difference; these are tensile modulus for composites G1 and GF2 as well as flexural modulus for GF2 and GF3.

Table 5.8: Newman Keuls test results for tensile strength in terms of different composites (G1, GF2, GF3, and GF3).

Composites	1	2	3	4
G1		0.00	0.003	0.00
GF2	0.00		0.00	0.00
GF3	0.00	0.00		0.00
F4	0.00	0.00	0.00	

Table 5.9: Newman Keuls test results for tensile modulus in terms of different composites (G1, GF2, GF3, and GF3).

Composites	1	2	3	4
G1		**0.50**	0.00	0.00
GF2	**0.50**		0.00	0.00
GF3	0.00	0.00		0.00
F4	0.00	0.00	0.00	

Table 5.10: Newman Keuls test results for flexural strength in terms of different composites (G1, GF2, GF3, and GF3).

Composites	1	2	3	4
G1		0.00	0.00	0.00
GF2	0.0001		0.001	**0.42**
GF3	0.00	0.001		0.001
F4	0.00	**0.42**	0.001	

Table 5.11: ANOVA test (Newman Keuls) for tensile modulus in terms of different composites (G1, GF2, GF3, and GF3).

Composites	1	2	3	4
G1		0.02	0.01	0.00
GF2	0.02		**0.45**	0.00
GF3	0.01	**0.45**		0.00
F4	0.0002	0.00	0.00	

5.3.3. SEM and EDX analysis of composites

The SEM micrographs clearly exhibit the uniform MDI polymer distributions on the respective glass and flax woven fabric reinforced composites. Although the stacked fibers cannot be observed in Figure 5.17 (a_2) (a_3), (c_2) (c_3), (e_2) (e_3), and (g_2) (g_3) for strong polymeric overlapping/coating on the surface but could be clearly seen on the fractured surfaces of the composites, see Figure 5.17 (b_2) (b_3), (d_2) (d_3), (f_2) (f_3), (h_2) (h_3). The surfaces of the composites

are flat, smooth, and uniform which indicates the perfect bonding of MDI resin with the glass and flax woven fabrics. However, few holes could also be observed which is indicating the weaker adhesion [242] between the fabric and resin into the matrix system. Such kind of holes were appeared only for Figure 5.17 (e_2) and (e_3) showing test pieces of 50% flax and 50% glass with MDI. The surfaces of 100% glass, 100% flax, or 83.33% glass/16.87% flax reinforced composites did not display any weak adhesion/interactions. However in case of Figure 5.17 (b_2) (b_3), (d_2) (d_3), (f_2) (f_3), (h_2) (h_3), there are explicit breakage and presence of fibers (flax and glass marked through red and yellow color, respectively). Besides, as the glass fabrics were treated with silane, it helped to form an interpenetrated network between the silane treated glass woven fabric and the MDI resin [243].

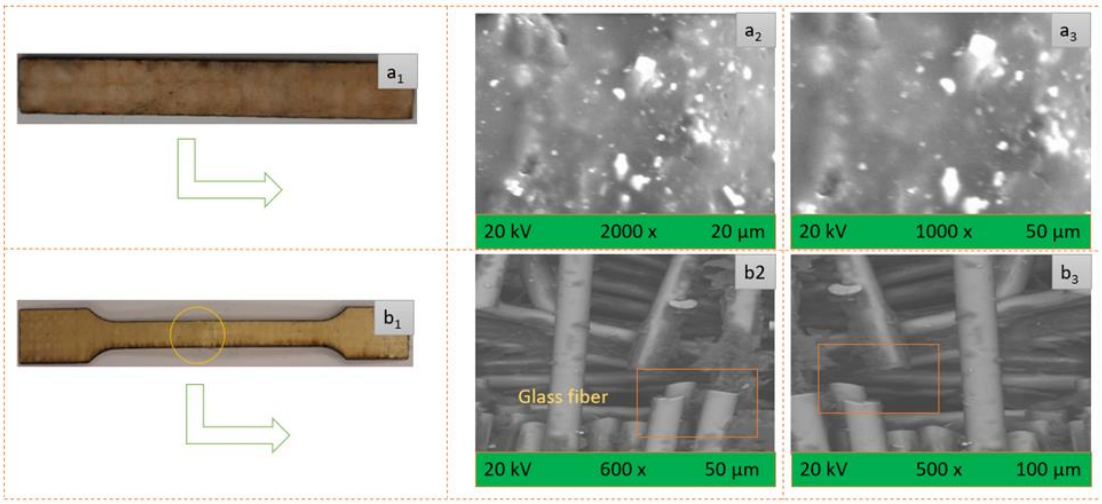

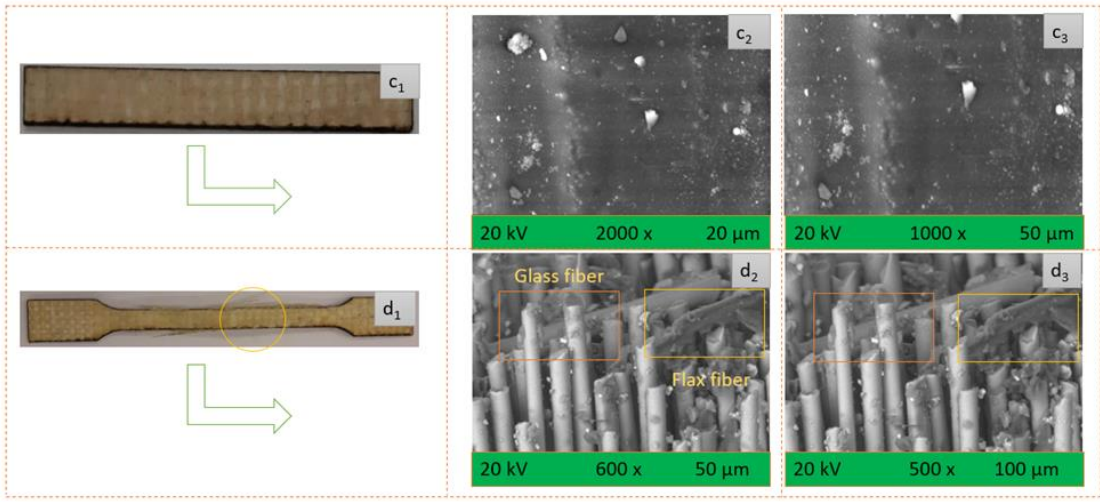

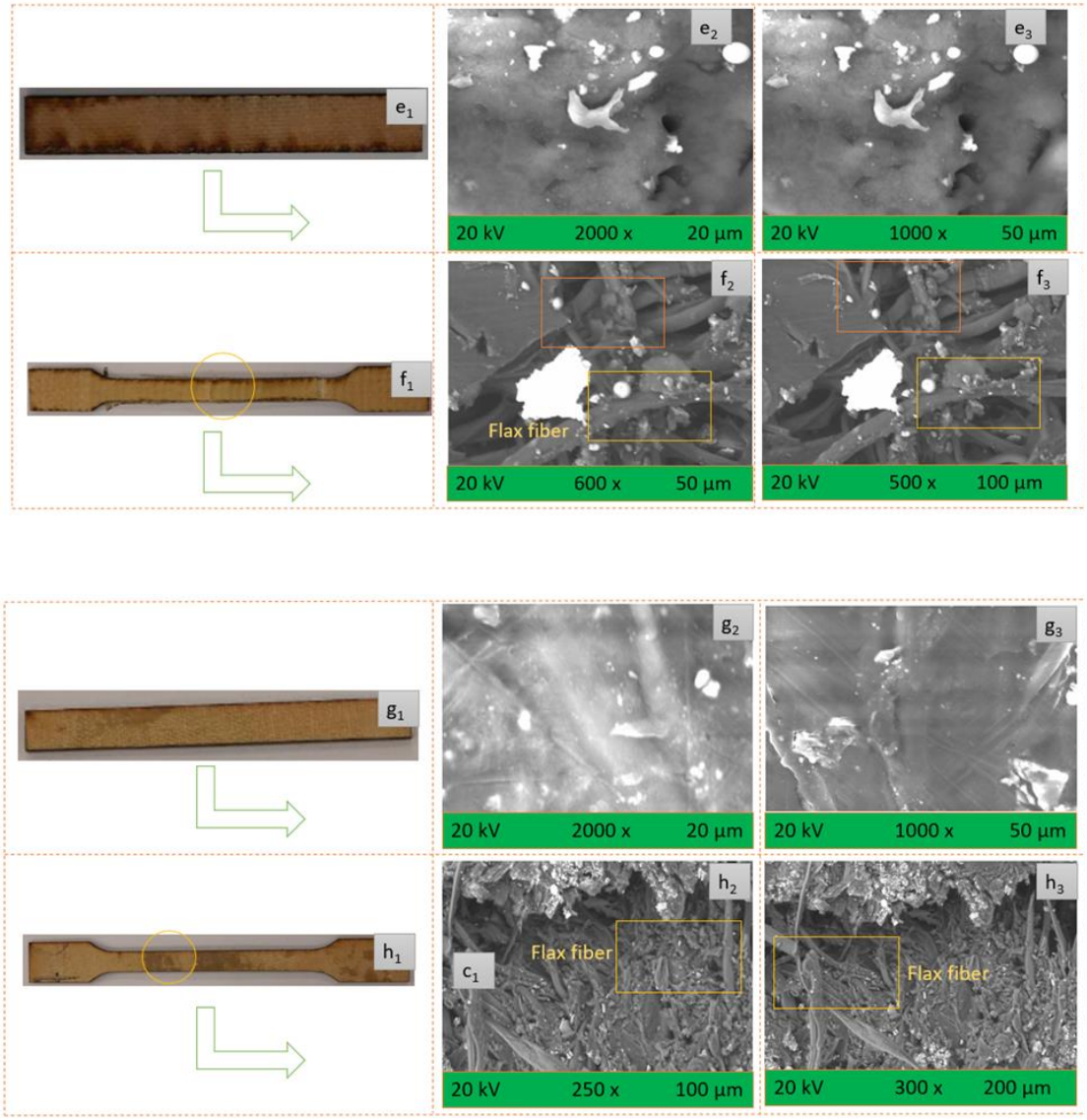

Figure 5.17: Morphological characterization of hybrid composites (a_1), (c_1), (e_1), and (g_1) for flexural test samples. Morphological characterization of fractured hybrid composites (b_1), (d_1), (f_1), and (h_1) for tensile test samples. Flat and uniform distribution of MDI resin on composites with reinforcement of pure glass (a_2) and (a_3), hybrid flax/glass (c_2), (c_3), (e_2), and (e_3), and pure flax (g_2) and (g_3) composites at different magnifications. Holes appeared for incompatibility between the MDI resin and woven fabrics (e_2) and (e_3). Fractured composites after applying tensile load on composites with reinforcement of pure glass (b_2) and (b_3), hybrid flax/glass (d_2), (d_3), (f_2), and (f_3), and pure flax (h_2) and (h_3) composites at different magnifications. Holes for incompatibility between the MDI resin and woven fabrics are presented through (e_2) and (e_3).

The EDX spectra provides the nature of glass, flax, and polymers embedded into the matrix. It is clearly observed from the Figure 5.18 that, silicon (Si) is one of the most significant chemical compound indicating the presence of glass into the composite system Figure 4(a). Besides, the detection of calcium (Ca), magnesium (Mg), and aluminum (Al) also confirm the presence of different oxides into the glass woven fabrics of the composites Figure 5.18 (a), (b), and (c). At the same time, the broad peak of C and oxygen (O) denotes the good bonding of MDI. In case of pure flax reinforced composite Figure 5.18 (d), there is no peak observed for silicon (Si) but there is for C and O (strong peaks for natural fibers) and chlorine (Cl). Contrary,

Cl did not show any peaks for G1 composites while they are present in the spectra of GF2, GF3, and F4 composites. Presumably this difference can be attributed to the presence of flax.

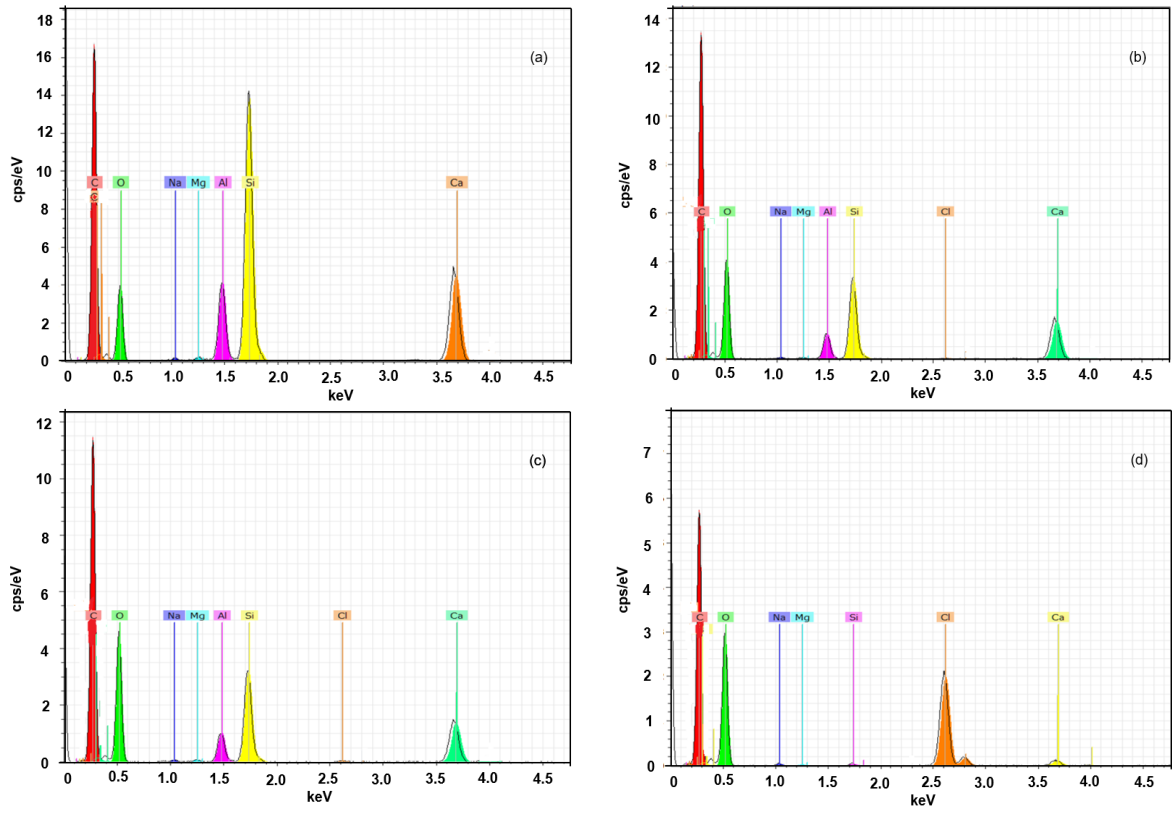

Figure 5.18: EDX spectrum of the composites (a) G1, (b) GF2, (c) GF3, and (d) F4. The glass fiber presence is observed through the presence of Si (a, b, and c), while the presence of flax is confirmed by the presence of C and O (b, c, and d).

5.3.4. FTIR analysis of composites

The chemical structures of MDI-based glass/flax reinforced composites were investigated by FTIR analysis. The broad absorption bands (Figure 5.19 (d)) at 3331 cm^{-1} indicates the presence of cellulosic structure (–OH unit) for flax fiber reinforced MDI composites. Besides, the peaks at 2851 cm^{-1} and 2920 cm^{-1} are related to the existence of CH_2 groups in the fiber. The presence of cellulosic structure in the composites could be further confirmed by the peaks at 1654 cm^{-1} and 1054 cm^{-1}. Similar phenomenon was described by other study [244]. The broad bands ranging from 1017 cm^{-1} to 3340 cm^{-1} (Figure 5.19 (a)) represent the glassy material-based composites [245]. Specifically, the peak at 1017 cm^{-1} is responsible for the Si–O–Si group and 1409 cm^{-1} for other types of oxides (boron oxide, aluminum oxide, calcium oxide, and so on), which are the specific chemical compositions of the glass fiber [246]. There are also a few weaker bonds found at 1654 cm^{-1} and 1409 cm^{-1}, which are related to water adsorptions occurring during the composites manufacturing process [245]. In Figure 5.19 (b) and (c), the peaks around 3340 cm^{-1} may be attributed to the bonding between the external hydrogen in glassy structures and cellulosic structures (flax) –OH groups [247, 248]. Besides, the peaks around 2850 cm^{-1} (Figure 5.19 (a), (b), and (c)) may be related to the treatment of glass surface with the silane. Further, the bonding of MDI with the cellulosic structure is also further confirmed by the peaks at 1508 cm^{-1} (CN–H, urethane holding secondary amide), 1698 cm^{-1} (carbonyl urethane, –C=O), and 1228 cm^{-1} (–C–O–C, ether

urethane) as can be seen in (Figure 5.19 (b), (c), and (d)) [249]. Finally, a successful reinforcement effect was found among the glass/flax and MDI matrix.

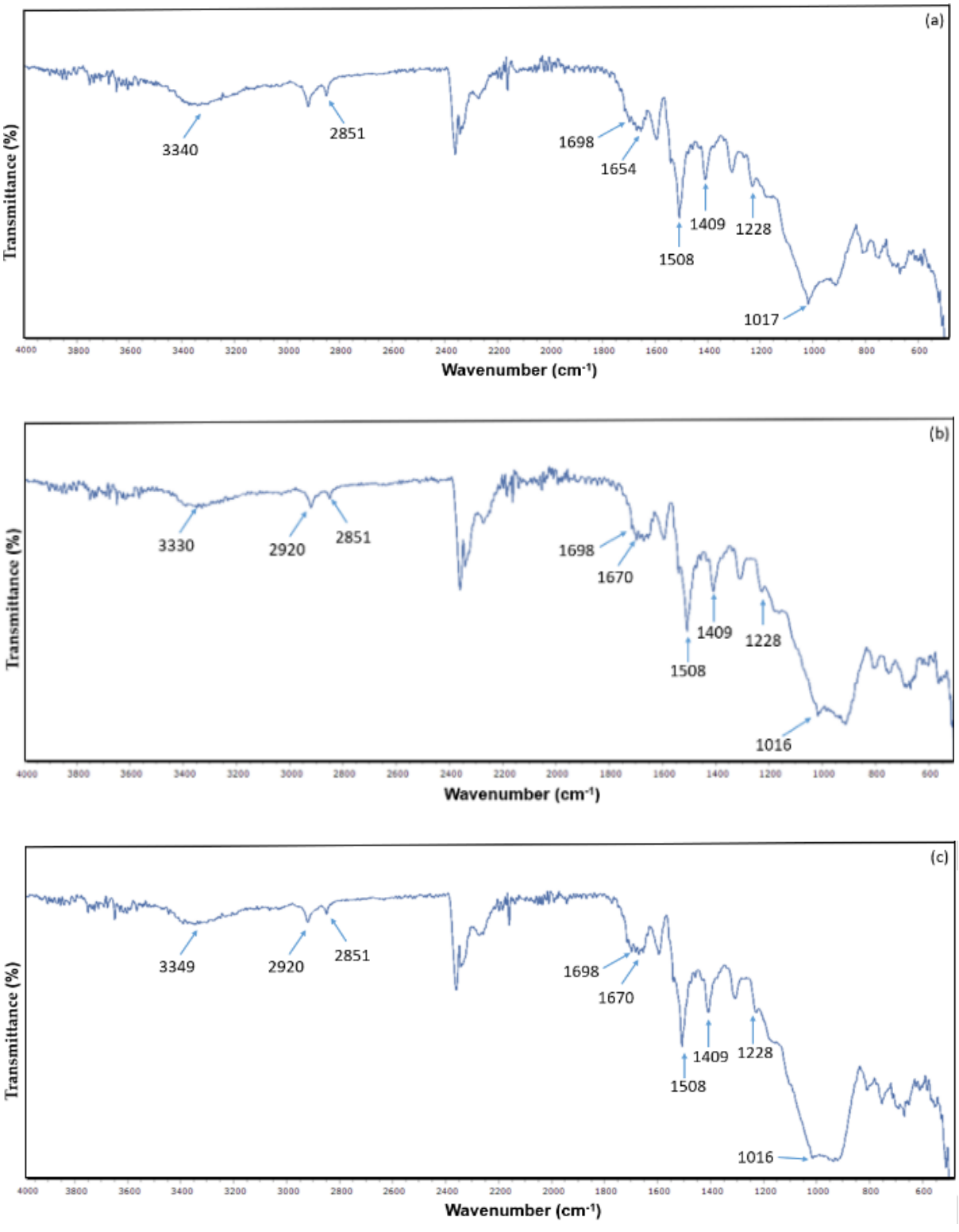

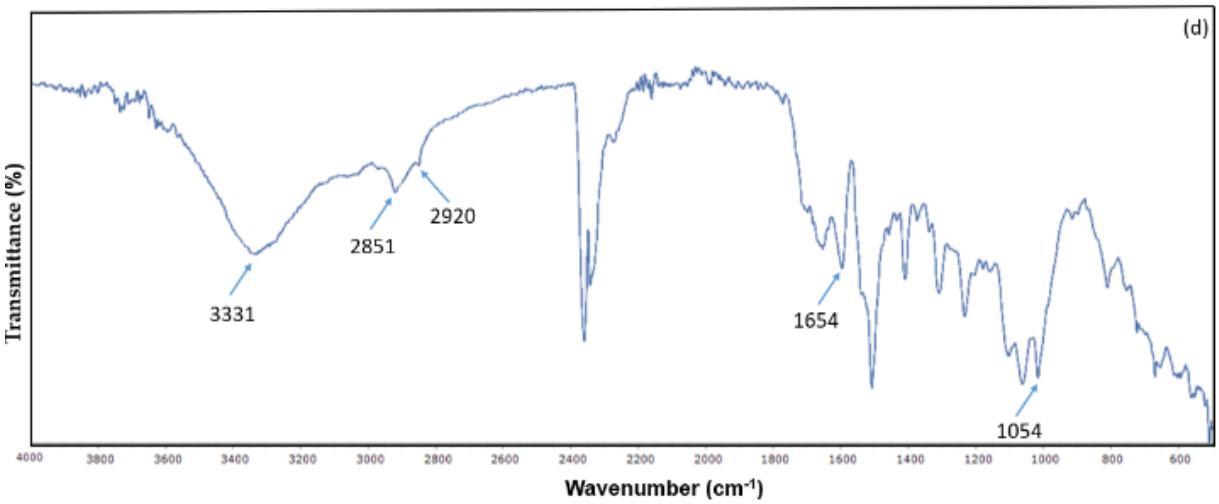

Figure 5.19: FTIR analysis of composites (G1, GF2, GF3, and F4). (a) pure glass composite, (b) and (c) hybrid composites, and (d) pure flax.

5.3.5. Thermogravimetric analysis

The thermal properties of glass/flax reinforced MDI composites are shown in Figure 5.20. Initially, all the composites except G1 displayed significant weight loss due to moisture evaporation probably because of the presence of MDI polymer or flax and glass fibrous material, as shown in Figure 5.20(a). Weight loss is gradually increasing with the increase of flax fiber content in the composites. Temperatures (around 100 °C) belonging to 5% weight loss of the composites are provided in Table 5.12. As illustrated in Figure 5.20, the maximum weight losses (10% to 60%) were occurred at temperatures ranging from 315 to 450 °C. Besides, residues of the composites G1, GF2, GF3, and F4 were amounted to 87.99, 36.01, 58.78, and 30.82%, respectively. In summary, it could be stated that, the combustion in the case of glass reinforcement is of lower level than in the case of reinforcements containing flax; Also, more residues are found for glass as compared to flax. The similar phenomenon was also described by other studies on glass with natural fiber-based laminated hybrid composites [241, 250, 251].

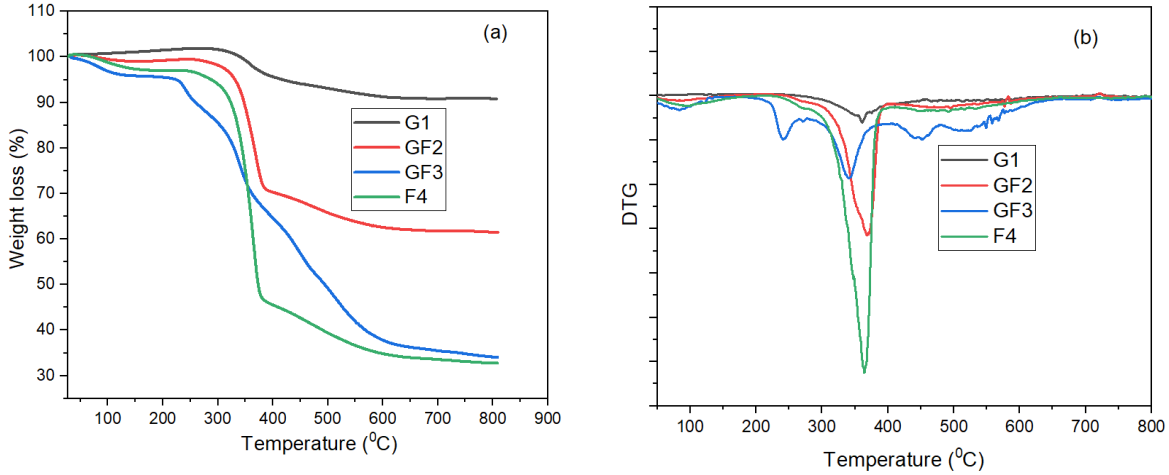

Figure 5.20: Thermal behaviour of composites (G1, GF2, GF3, and F4); (a) TGA and (b) DTG. Pure glass and hybrid glass composites are more stable than natural flax reinforced composite (b), (c), and (d).

DTG curves in Figure 5.20 (b), showing some small peaks ranging from 220 to 320 °C which are related to the decomposition of organic components of hybrid composites. The second stage degradation (330 to 380 °C) are associated with the hemicellulose decompositions from flax constituents. Cellulose degradation is indicated by the peaks within the range of 400 to 490 °C. The variation in temperatures are caused by the different proportions of glass fiber present in the composite stackings (GF2 and GF3). Similar study was conducted by Atiqah et. al. [251] for thermoplastic polymer-based sugar palm/glass composites (where they found organic elements decomposition within 230 to 330 °C, hemicellulose constituents decomposition within 340 to 390 °C, cellulose constituents degradations 400 to 480 °C from the DTG curves of composited products). The DTG curves have clearly displayed the decomposition pattern of glass/flax reinforced MDI polymeric composites.

Table 5.12: Onset and maximum temperature of hybrid composites (G1, GF2, GF3, and F4). Glass reinforced composites exhibit more residues compared to flax and hybrid composites.

Laminated hybrid composites	T_{onset} (°C)	T_{max} (°C)	Residues at 650 °C (weight%)
G1	359	650	87.99
GF2	310	650	36.01
GF3	197	650	58.78
F4	162	650	30.82

5.3.6. Physical properties of composites

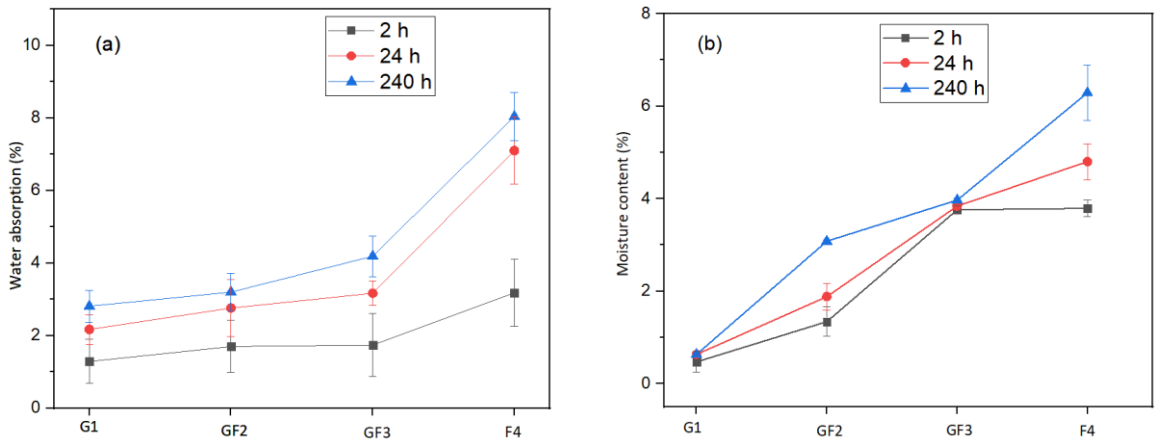

Figure 5.21: Water absorption (a) and moisture content (b) of composites (G1, GF2, GF3, and F4) within 2 h, 24 h, and 240 h time intervals. Natural flax reinforced composites absorb more water and exhibit higher moisture uptake compared to glass reinforced composites.

The water absorption by composition of pure flax, glass, and hybrid reinforcement is demonstrated in Figure 5.21 (a). As expected, the naturally originated flax reinforced composites exhibited higher water absorption than that reinforced with pure glass. This is because, the natural fibers contain hydrophillic groups (–OH, –COOH, –CO, and $–NH_2$) [252], whereas the synthetic glass fibers do not. As a natural fiber, flax contain enormous amounts of –OH groups (also found by FTIR analysis). Therefore, the saturation point is higher for flax-based composites than glass. The saturation point of flax decreases with the loading of more

glass woven fabrics into the hybrid composites. The sequence is G1<GF2<GF3<F4. The water absorption was observed from 2 h, 24 h, and 240 h as illustrated in Figure 5.21 (a). The moisture content of the pure glass, flax, and hybrid composites also exhibitted the same trend. The G1 (pure glass) sample absorbed the lowest moisture whereas F4 (pure flax) attained the highest moisture content. The hybrid composites (GF2) attained moisture content of 1.34 (0.32) %, 1.88 (0.29) %, and 2.15 (0.09) % moisture content after 2 h, 24 h, and 240 h; whereas GF3 showed 3.76 (0.08) %, 3.84 (0.33) %, and 3.97 (0.04) % moisture content within the same time period. Again, standard deviations are shown in parentheses. It is noticed that, the moisture content of flax reinforced composites starts to decline with the increased loading of glass woven fabrics.

5.4. Work package 4

The development of hybrid nanocomposites from green silver nanoparticle treated hemp/glass woven and epoxy resin is reported in this work package. Initially, the nanosilvers were in situ synthesized over the fabrics. The fabrics (both hemp and glass) were then laminated with epoxy resin to produce hybrid nanocomposites. The manufacturers may select any suitable combination from this study to produce nanocomposites.

5.4.1. Load-deformation behavior

Load versus displacement characteristics for flexural and tensile properties are of utmost importance in investigating the mechanical performances. The load versus displacement curves both for tensile and flexural properties are displayed in Figure 5.22. Initially, all the composites exhibited linear behavior for displacements, however a non-linear response is apparent from the point where cracking started to occur. Composite NC1 took a load of 1261 N at the limit of linearity in tension, however the maximum peak was observed with extended delaminations at 1338 N. Similarly, composite NC2 showed the initial quasi linear displacement up to 575 N and CC up to 266 N. At the same time, the maximum load 468 N for the test-piece of NC3 composite was found with largely extended displacements. The load versus deflection curves showed similar trends for flexural properties. Studies reported by other researchers for different types of fiber reinforced composites also traced the eye-catching differences in the load versus displacement behavior of nanosilver treated composites and those without treatment [253-255].

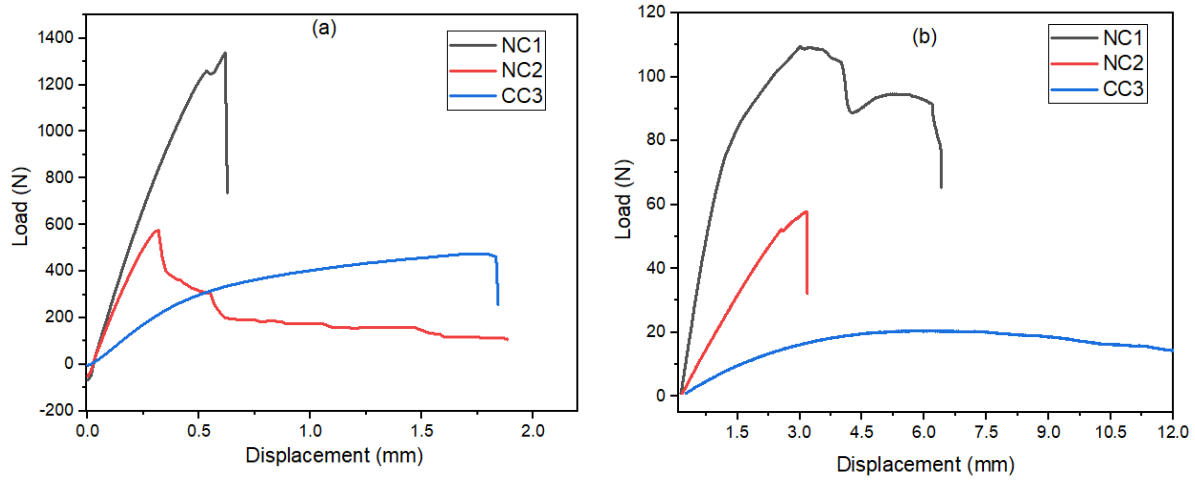

Figure 5.22: Load versus displacement curves for developed composites: (a) tensile properties and (b) flexural properties.

5.4.2. Strength and stiffness of composites

Strength and stiffness properties are the fundamental requirements for composite materials to ensure the suitability for potential application in products. The highest tensile strength of 40.9 (2.7) MPa was found for NC1, whereas CC3 exhibited the lowest value of 16.2 (0.6) MPa. NC2 provided moderate tensile strength by 18.9 (0.3) MPa between the two extremes. Similar trend of Youngs modulus was observed for the composite panels; 6.8 (0.3) GPa for NC1, 5.5 (0.6) GPa for NC2, and 2.2 (0.1) GPa for CC3. Bending strength and modulus of elasticity in bending of the produced composites showed a similar picture as seen in Table 5.13. NC1 displayed the highest performances compared to the NC2, and CC3. The higher bending strength for NC1 was found 109 (13.9) MPa, whereas NC2 displayed a modest 54.8 (9.1) MPa and CC3 showed the lowest values of 30.5 (1.0) MPa. Furthermore, bending modulus values proved to be 19.8 (0.3), 9.2 (0.6), and 3.5 (0.3) GPa. The associated elongation at break values displayed by the composite test-pieces were 0.8, 0.5, and 2.7%, respectively. Overall, it seems that the nanosilver treatment on the fabrics used for laminations positively influences the mechanical properties of the produced composite panels. The 1 mM loading of silver precursor has yielded the highest mechanical performances, although a 5 mM loading may have generated an agglomeration problem hence the mechanical properties declined, still remaining higher than those of the control composite panels.

Table 5.13: Mechanical properties of the developed hybrid composites (NC1, NC2, and CC3). Standard deviations are given in parentheses.

Laminated composites	**Density (Kg/m^3)**	**Tensile strength (MPa)**	**E (GPa)**	**MOR (MPa)**	**MOE (GPa)**	**Elongation at break (%)**
Control glass fabric	–	3.1 (0.4)	1.34 (0.067)	–	–	–
Control flax fabric	–	1.0 (0.1)	0.073 (0.002)	–	–	–
NC1	1298.4 (23.63)	40.9 (2.7)	6.8 (0.3)	109 (13.9)	19.8 (0.3)	0.8
NC2	1374 (32.03)	18.9 (0.3)	5.5 (0.6)	54.8 (9.1)	9.2 (0.6)	0.5
CC3	1052.5 (31.3)	16.2 (0.6)	2.2 (0.1)	30.5 (1.0)	3.5 (0.3)	2.7
R^2	0.98	0.98	0.99	0.92	0.99	0.9

* R^2 – Coefficient of determinations; E– Youngs modulus; MOR – Flexural modulus; MOE – Bending modulus

5.4.2.1. *Statistical analysis of mechanical properties*

Measurement data of the mechanical properties of the composites were statistically analyzed by using Analysis of Variances (ANOVA) tests in order to confirm the above statements on the effect of nanosilver treatment on the composites mechanical properties. All the properties were tested in terms of silver NPs loading on each composite panel. The R^2 values for all the composites was found above 0.93 for all the mechanical properties (see Table 5.13); accordingly, the overall tests of significance demonstrated in all cases that the presence of nanosilver results in significant change of the mechanical performances.

With respect to the different levels of nanosilver treatment, post-hoc pairwise comparisons were also performed for all the mechanical test results. Among the assumptions required for the validity of ANOVA test results, the homogeneity of variances was always found met. Normal distribution of the residuals however was found dubious in some cases, as evidenced by plotting the predicted vs. raw values. Therefore, in order to improve the reliability of the results of pairwise comparison, Fisher LSD, Tukey HSD, and Newman-Keuls options of these tests were conducted alike. The three options of these tests yielded identical results in terms of significance in all cases. Therefore, analysis results of the respective Tukey tests are given only in (Table 5.14, Table 5.15, Table 5.16, Table 5.17, Table 5.18). The probability values in these tables mean the smallest level of significance that would lead to rejection of the null hypothesis, i.e. no difference between the means. The figures are shown in bold when this probability is not higher than 0.05, indicating significant differences.

Table 5.14: Tukey HSD (ANOVA) test of nanosilver treatment% in case of tensile strengths of different composites (NC1, NC2, and CC3).

Hybrid Composites	1	2	3
NC1	**0.001**		**0.001**
NC2	0.542	**0.001**	
CC3		**0.001**	**0.542**

Table 5.15: Tukey HSD (ANOVA) test of nanosilver treatment% in case of tensile modulus of different composites (NC1, NC2, and CC3).

Hybrid composites	1	2	3
NC1	**0.00**		
NC2	**0.00**	**0.00**	**0.00**
CC3		**0.00**	**0.00**

Table 5.16: Tukey HSD (ANOVA) test of nanosilver treatment% in case of flexural strengths of different composites (NC1, NC2, and CC3).

Hybrid Composites	1	2	3
NC1	**0.01**		**0.03**
NC2	0.26	**0.03**	
CC3		**0.01**	**0.26**

Table 5.17: Tukey HSD (ANOVA) test of nanosilver treatment% in case of flexural modulus of different composites (NC1, NC2, and CC3).

Hybrid Composites	1	2	3
NC1	**0.00**		**0.00**
NC2	**0.00**	**0.00**	
CC3		**0.00**	**0.00**

Table 5.18: Tukey HSD (ANOVA) test of nanosilver treatment% in case of elongation at break% of different composites (NC1, NC2, and CC3).

Hybrid Composites	1	2	3
NC1	**0.00**		**0.00**
NC2	**0.00**	**0.00**	
CC3		**0.00**	**0.00**

It can be seen in Table 5.14, Table 5.15, Table 5.16, Table 5.17, Table 5.18 that higher $AgNO_3$ load (composite type NC2) did not result in the significant increase of tensile and flexural strength as compared to those obtained for the control type CC3. For all the rest of the mechanical properties investigated, there were significant differences found between the performances of the nanosilver treated and control composites, as well as between the performances of the composites treated at different levels. Similar results were also discussed in case of composite panels based on fiber loading (glass and flax) types in our previous study [195].

5.4.3. XRF and iCP OES analysis

The concentration of nanosilver on colloid was investigated in terms of ICP OES study, where the presence of silver was found at rates of 0, 820 and 1830 mg/L (Figure 5.23). The silver deposited on the composite surface was also measured using of XRF test. The nanosilver content values measured by XRF tests were 0, 655±23, and 1829±30 PPM for the composite types CC3, NC1, and NC2, respectively (Figure 5.23). The variation in nanosilver content may have been caused by the different loading of metallic silver precursor (1 and 5 mM, respectively). The similar phenomenon found by XRF measurements were also reported for nylon fabric coloration by using biosynthesized silver where chitosan was used as stabilizing and reducing agent [256].

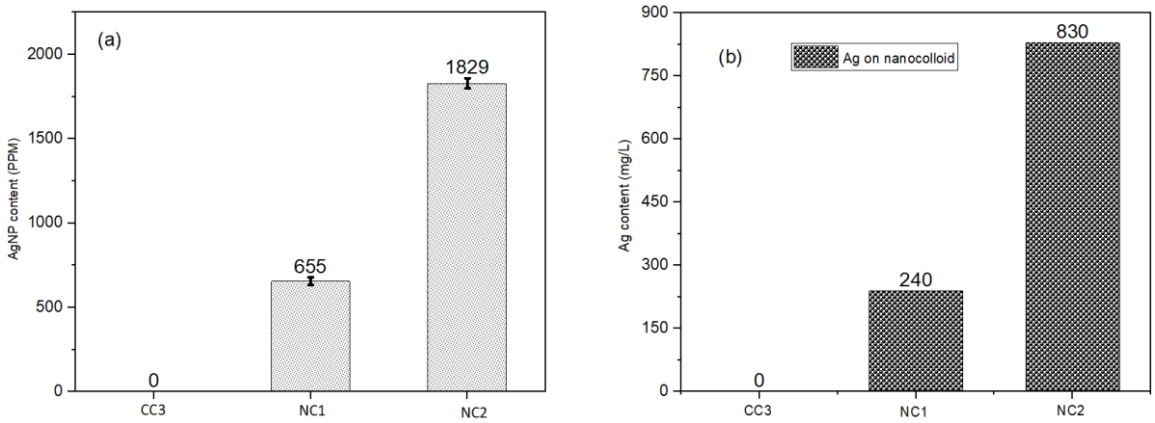

Figure 5.23: Quantification of nanosilver on composites: (a) XRF analysis and (b) iCP OES test.

5.4.4. SEM studies of composite panels

Morphological micrographs of glass and hemp woven fabrics are shown in Figure 5.24. The micrographs of the produced composites (NC1, NC2, and CC3) are shown in different magnifications. Generally, the composites exhibited a flat surface, probably due to the strong coating of epoxy adhesive. It seems that the epoxy resin was successfully cured with the glass

and hemp woven fabrics lamination. The existence of fiber in the laminated composites could be observed in fractured surfaces (Figure 5.24) after applying the tensile load. Split-up of fibers and associated cracking occurred. The degree of fracture also indicate how strong the bonding is between the fiber and matrix structure [257]. The fracture in fiber surfaces could happen for different reasons such as growing features of the hemp plants, fiber extraction methods, nodes in fibers, and the associated lengths of fiber as well [258]. Furthermore, comparatively smaller crack propagation in NC1 indicates the strong adhesion between the fiber and epoxy polymer, which may be due to the AgNP treatment on fabric surface. The higher cracking in CC3 indicates weaker adhesion, may be due to the control hemp/glass fibers present in the composite system. On the other hand, a moderate cracking is observed in the NC2 sample; the reason behind it may be that the higher loading of nanosilver led to agglomeration, resulting higher cracking than in NC1 samples, but still lower than in the untreated control samples [257, 259]. In summary, the treatment of glass and hemp woven fabrics using green AgNPs ensured a better adhesion within the matrix system.

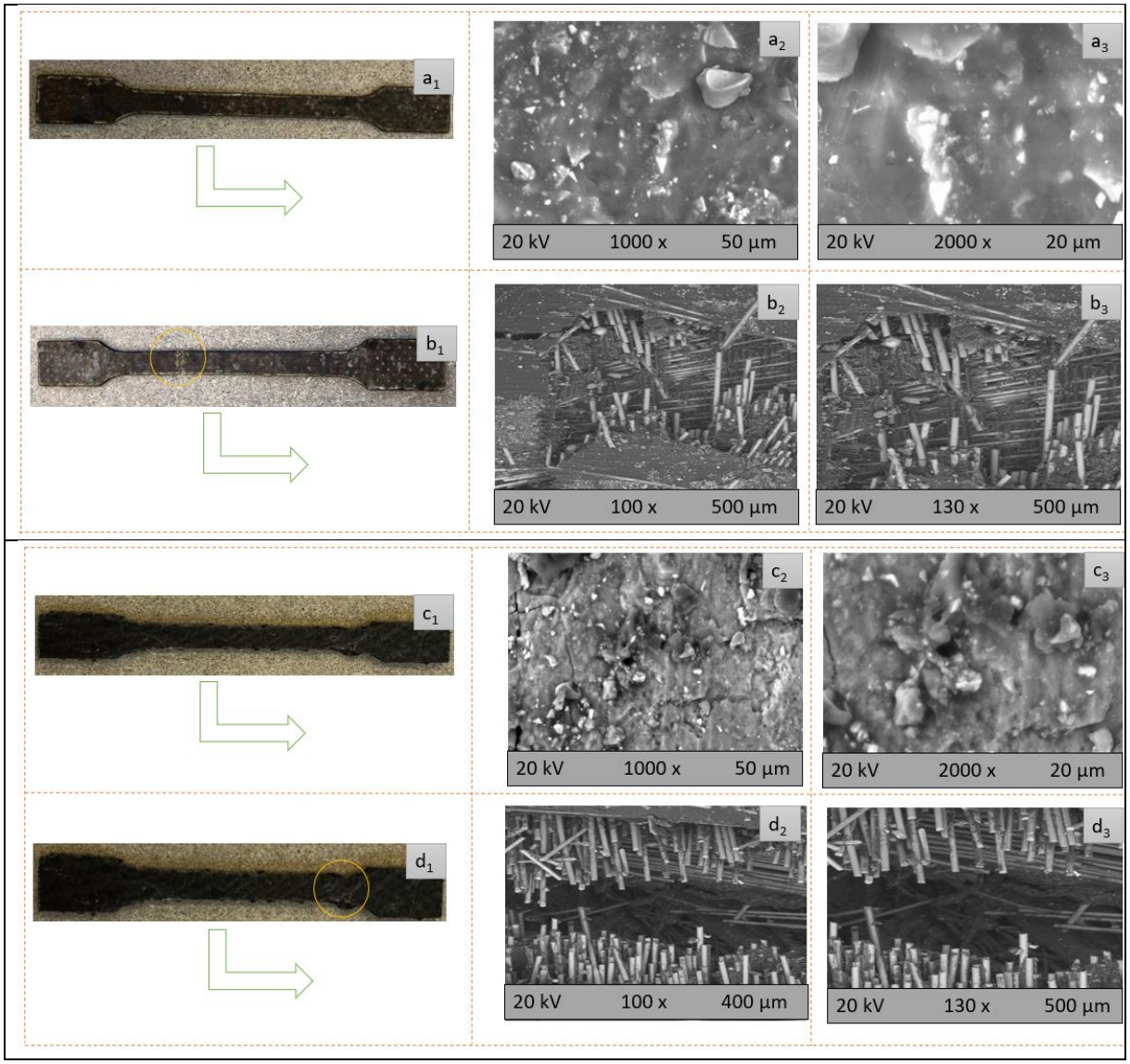

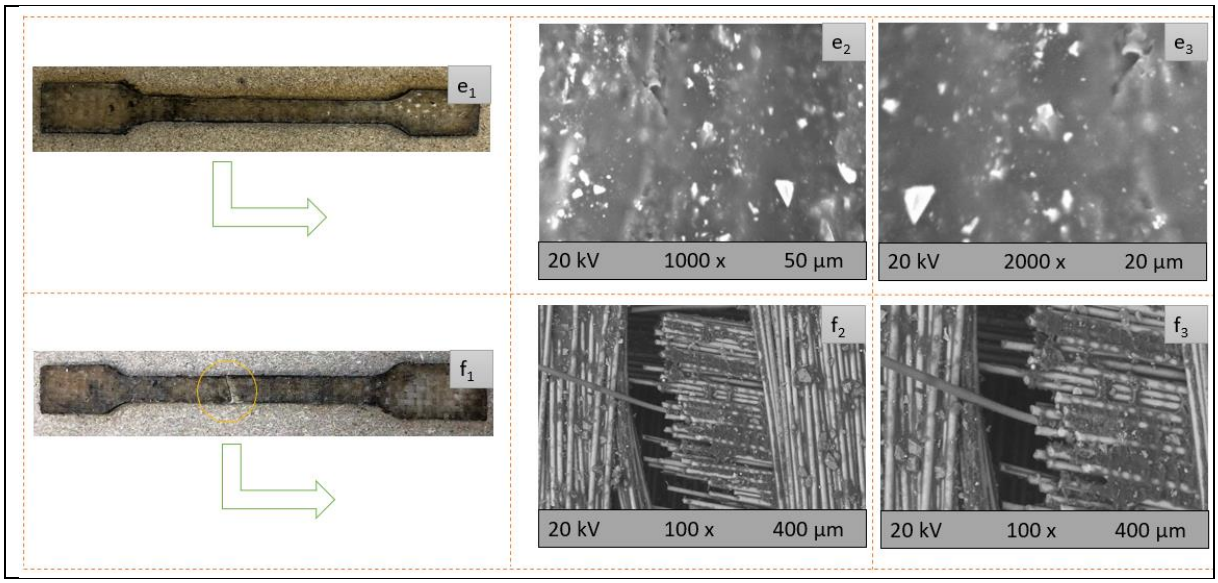

Figure 5.24: Morphological and SEM images and micrographs of developed hybrid composites: photographs of NC1, NC2, and CC3 composites before fracture (a_1, c_1, e_1), photographs of NC1, NC2, and CC3 composites after fracture (b_1, d_1, f_1), morphological micrographs of NC1, NC2, and CC3 composites before fracture (a_2 and a_3, c_2 and c_3, e_2 and e_3) at different magnifications, morphological micrographs of NC1, NC2, and CC3 composites after fracture (b_2 and b_3, e_2 and e_3, f_2 and f_3) at different magnifications.

5.4.5. TGA and DTG analysis of composites

The TGA analysis results of the control and nanocomposites are shown in Figure 5.25. There is an initial weight loss observed for all the composites, maybe due to the moisture evaporation from glass and hemp fibers and epoxy resin [260]. Nanocomposite (NC1) showed the highest thermal stability compared to the other two composites, NC2 and CC3. The control sample displayed the lowest stability against the temperature as shown in Table 5.19**.** However, a significant loss of weight (5–60%) is seen within the range of 310 to 470 °C. The residual was also found highest for NC1 and lowest in the case of NC2. The lower values of residue may have been caused by the agglomeration of the NP, which in some way decreased the stability at 5 mM dosage of the $AgNO_3$ precursor. Just like in the case of the mechanical properties, the use of 1 mM of $AgNO_3$ provided the maximum of thermal stability as well. These findings agree well with those in some other reports by different researchers and in our previous studies [195, 260].

The decomposition of various organic components from the developed composites is also seen through some smaller peaks within the range of 250 to 330 °C in the DTG analysis. At higher temperatures the degradation continued, which in the range of 367 to 445 °C is related to the hemicellulose degradation. Cellulose degradation could be detected within 479 to 605 °C. The weight loss witnessed within 300 to 450 °C can also be attributed to the decomposition of pectin, lignin, and various chemical crosslinkers present in hemp and epoxy resin/hardeners [261]. In summary, DTG investigation of the composites also exhibited the explicit decomposition trends in the different ranges of temperature which is also supported by previous researches [195]. On the other hand, the treatment of glass/hemp woven fabrics contributed to a strong chemical bonding between the epoxy matrix and fibers [261], which further improved the thermomechanical performances especially for NC1, where 1 mM silver precursor was used.

Table 5.19: Different temperature (T_{onset} and T_{max}) of hybrid composites (NC1, NC2, and CC3).

Laminated composites	T_{onset} (°C)	T_{max} (°C)	Residues @ 800 °C
NC1	320	808	79
NC2	313	808	33
CC3	305	808	36

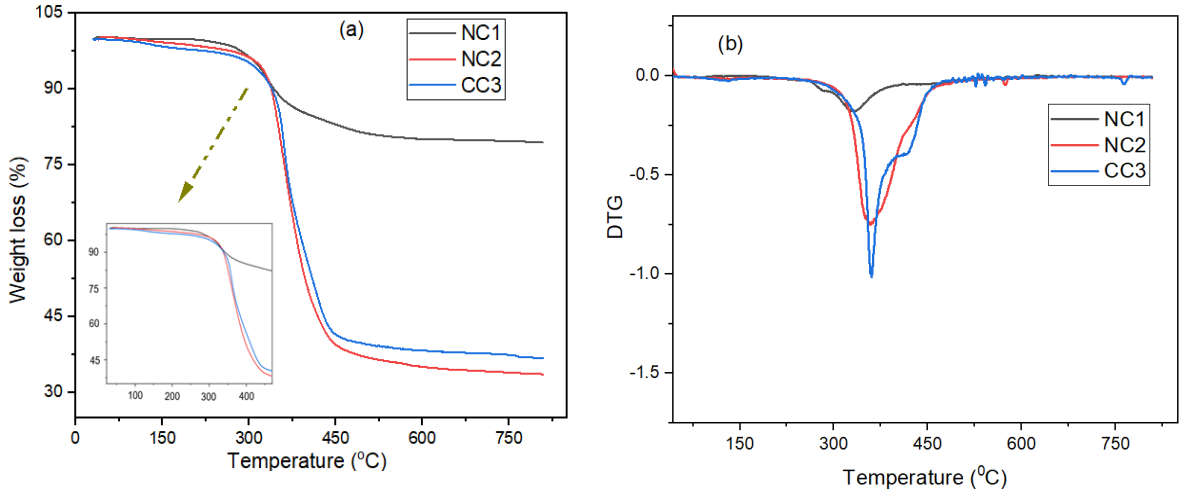

Figure 5.25: Thermal property analysis of developed hybrid composites: (a) TGA and (b) DTG.

5.4.6. Physical properties study of the composites

The cellulosic fibers like hemp contain –OH, –COOH, –NH_2, and –CO hydrophilic groups [241] which are responsible for the moisture absorption from the surrounding environment. On the other hand, glass fibers do not contain such kind of hydrophilic groups in their polymeric structure, hence their moisture content is extremely lower that we reported in one of our recent study [195]. Composites subjected to nanotreatment exhibited less water absorption, thickness swelling, and gained lower moisture contents than that without nanotreatment, which is also supported by another research where the AgNP was synthesized from eggshell reducing agent [261]. It was also found, that the composite made with higher AgNP loading demonstrates lower values of the physical properties investigated. These findings are illustrated in Figure 5.26. The sequence of the hybrid composites with respect to moisture content was NC1< NC2< CC3 (Figure 5.26). The same sequence was found for thickness swelling and water absorbency. It could be summarized from the above discussions that AgNP loading exerts a positive effect on the hygroscopic properties which can facilitate the applications as exterior parts of automotive or transportations vehicles.

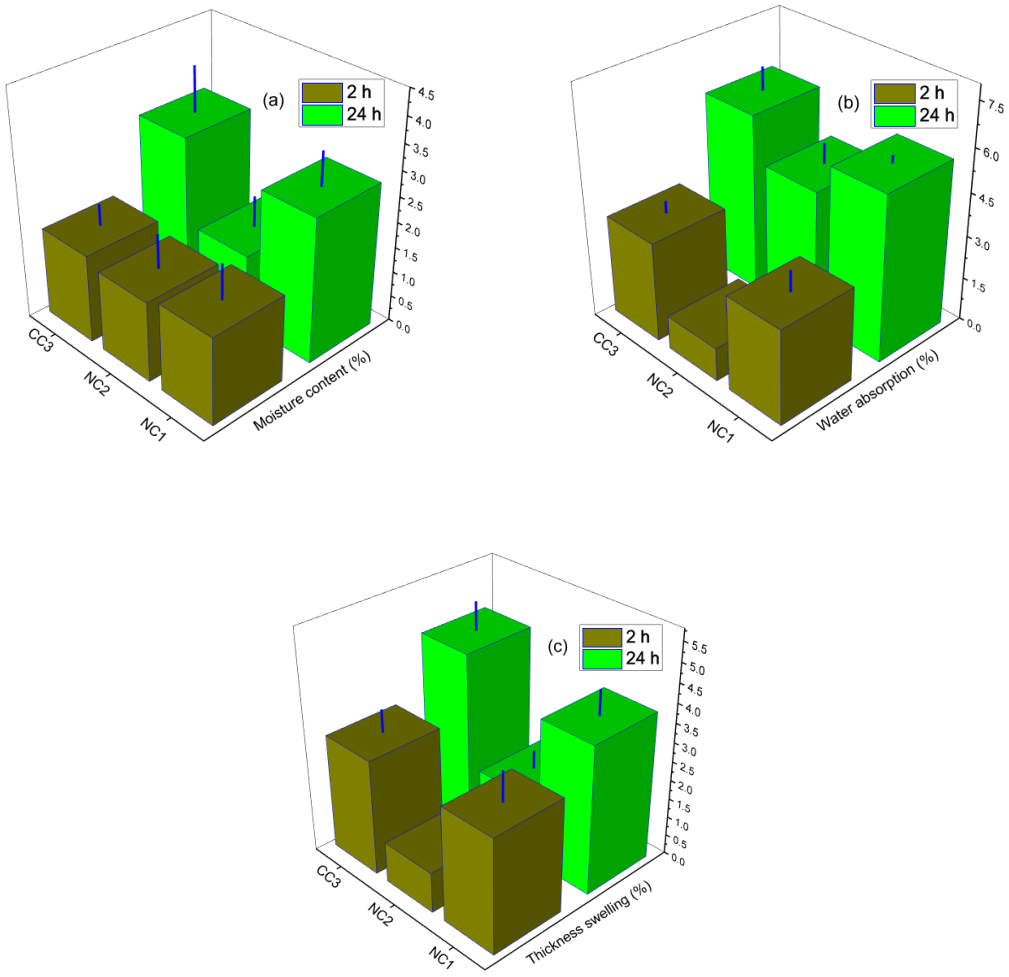

Figure 5.26: Physical properties of the developed composites: (a) moisture content; (b) water absorbency, and (c) thickness swelling.

5.4.7. Color properties assessment of composites

The treatment of laminated fabrics with green AgNPs provided bright color appearances (Figure 5.27) of the composite panels. In this study, it was also investigated to find out the color properties from developed nanocomposites compared to the untreated composites. The color properties were studied using CIE Lab values, where, CIE a* indicates the reddish to greenish tone, b* yellowish to bluish tone. CIE L* stands for the darkness/lightness of the colors and K/S is the color strength. In our experiments, all these values were found positive, demonstrating the dominance of reddish to yellowish tone of the developed composites. Visually, the composites seem darker reddish to brown color. The K/S value was found to be lower for NC1 which is showing lower values than for NC2, demonstrating that higher loading of NP increases the color strength. This increase is quite significant as shown by the data in Table 5.20. It can be concluded that the incorporation of green AgNPs has not only improved the mechanical and physical properties but also provided brilliant color appearances of the composites. Similar discussions have been provided in our previous communications but for differing applications [6, 262].

Figure 5.27: Images of developed composites: (a) control composite without any nanosilver treatment, (b) nanocomposite without 1 mM nanosilver treatment, (c) nanocomposite with 5 mM nanosilver treatment.

Table 5.20: Color properties of the developed composites (NC1, NC2, and CC3).

Samples	**Colorimetric values with associated color strength**			
	L*	a*	b*	K/S
CC3	45.8	3.3	18.3	2.3
NC1	31.7	8.8	22.6	6.5
NC2	23.7	4.2	13.1	11.8

* TC – *Tilia cordata*; K/S – Color strength, M_W – Molar weight

Chapter VI: Concluding Remarks

In case of work package 1, the reinforcement of rice straw and energy reed fibers for hybrid biocomposites production through using hot-pressing technology is a feasible and convenient manufacturing approach. The mechanical properties (IBS and flexural properties), thermal conductivity, and physical properties in terms of moisture content, water absorbency, and thickness swelling stability are found satisfactory with an increasing trend whilst the energy reeds incorporation was increased in the composite system. The EDX analysis provided the peaks for different chemical elements which are demonstrating a strong binding between the cellulosic rice straw and energy reed fibers with PF resin. The morphological characteristics also further shown a strong coating of PF resin with rice straw and energy reed reinforcement materials. The thermal conductivity tests provided significant potentiality of the biocomposite panels as prominent insulation materials. In this regard, the developed composites exhibited a superior potentiality for particle boards production, structural applications, light weight vehicles, and so on. Furthermore, energy reed fibers are also found to have a prominent potential as the reinforcement materials in the near futures. Moreover, this research work shown a new potentiality for future researchers and industrial production houses with novel hybrid biocomposite materials from renewable sources.

In case of work package 2, interest in green, environmentally friendly building products is increasing around the world. In this regard, naturally originated lignocellulosic materials are revealing new sustainable building material routes for the construction and building sector. The developed composites with variable densities were 1176.1 (35.76), 1021.03 (38.95), 1337.47 (65.64), 1118.4 (6.94), and 1150.17 (18.81) kg/m^3 for composite s 1, 2, 3, 4, and 5, respectively. These composites were made from lignocellulosic materials (coir fiber and Scots pine particle) bonded with OPC, and they provided satisfactory performances (mechanical, thermal, and physical). The thermo-mechanical properties of Scots pine improved with the loading of coir fibers in the composite systems. All the composite materials provided internal bonding strengths higher than 0.5 MPa, indicating strong materials for structural applications. The SEM analysis showed the explicit presence of coir fiber and Scots pine in the fractured composite panels, whereas the presence of lignocellulosic materials were further justified in terms of FTIR analysis. The EDX spectra of the composites also provides successful bonding of coir fiber and Scots pine with OPC in terms of chemical elements presence. The thermal conductivity values of the composites were 0.17045 (0.00352) W/(m.K) for P@C1, 0.16651 (0.00265) for CP@C2, 0.11646 (0.00263) for CP@C3, 0.11265 (0.00409) for CP@C4, and 0.10547 (0.00657) W/m.K) for C@C5, which provides explicit proof of the developed panels as potential insulation materials. Overall, the current research is going to explore and open new routes toward producing green and sustainable products in building and construction sector.

In case of work package 3, the fabrication of composites reinforced by laminated flax and glass woven fabric with the use of MDI polymeric resin was performed successfully. The glass woven fabric reinforcement with MDI resin provided highest flexural and tensile strengths, whereas the flax reinforced composites showed the lowest performance. However, when the loading of glass was increased into flax/glass reinforced hybrid composites, the strengths started to increase. The GF2 sample as a hybrid composites developed through reinforcing by natural and synthetic fibers together (83.33% glass and 16.87% flax) provided satisfactory mechanical performance (tensile strength 69.63 (2.77) MPa and flexural strength 147.7 (18.5) MPa). The SEM micrographs also showed flat and uniform surfaces of the produced composites with homogeneous distribution of MDI resin into the woven fabric reinforced matrix. The EDX characterization of the composites confirmed the successful reinforcement of glass and flax woven fabrics with MDI resin through testifying their footprint

of elemental compositions. The thermogram studies of the produced composites have proved the satisfactory thermal stability. The addition of glass on flax/glass hybrid composites also enhanced the thermal stability. The FTIR analysis provides the fingerprint of glass and flax fibers presence on the hybrid composites. The water absorption and moisture content investigation has showed that, natural flax reinforced composite contain higher moisture than that of pure glass. However, with the increased incorporation of synthetic glass, both the water absorption and moisture content started to decline. But, the incorporation of glass into the composites have significant influence on tensile strength, tensile modulus, and flexural modulus (regression analysis). The ANOVA test has further confirmed about the significance of mechanical properties with the produced composites. The incorporation of glass into the composites have significant influence on tensile strength, tensile modulus, flexural strength, and flexural modulus quantified by regression analysis. The ANOVA test has further confirmed about the significance of the improvement of mechanical properties with the produced composites. As MDI is popularly used by particle board manufacturing companies, so this report could be a benchmark for hybrid composites manufacturing to the industries.

In case of work package 4, his study was conducted for fabricating laminated hybrid composites using hemp and high performance glass woven fabric reinforcement treated by bio-based AgNP (1% and 5%) and applying epoxy resin as matrix material. The content of AgNP was quantified by using XRF (0, 655±23, and 1829±30 PPM for CC3, NC1 and NC2 composites respectively) and ICP OES analysis, confirming the successful synthesis of NPs in aqueous solutions. The laminated hybrid composites were characterized in terms of morphological, thermal, mechanical, and physical properties to investigate their performances and suitability for industrial applications. The mechanical properties of the developed composites are strongly influenced by the incorporation of nanosilver. The nanosilver loaded composites provided improved values of mechanical properties compared to the control samples without any nanotreatment. The morphological analysis has shown a strong compatibility between the AgNP treated glass and flax woven fabrics with epoxy resin. This study further justified the stronger bonding between the laminated fabrics and epoxy polymer in the composite systems. Thermal properties of the nanotreated composites showed improved thermal stability against thermal degradation. DTG analysis has further confirmed the signals of cellulose, hemicellulose, lignin, protein, and pectin decomposition from the composite materials at different temperatures. The study of hygroscopic properties has proved that an optimum level of nanosilver incorporation (1%) minimizes water absorption, moisture content and thickness swelling.

Moreover, there is still a long way to with the explorations of new cellulosic fiber sources abundantly available in the nature. Interestingly, semi-dry tecjnology mediated insulation panels needed more researches to make them industrially feasible as it will minimize the water and energy consumption from production processes. Additionally, the development on nanocomposite is still in early stages which needs more investigations to find most feasible route to apply industrially. Furthermore, the physical and biological methods of pretreatment is also needed more attention to minimize the dependency on traditional chemical-based petreatments. Besides, as still now most of the polymers are not biodegradable, hence needed more research to explore more biodegadable polymeric materials to make the 100% biodegradable products. Overall, lignocellulosic fiber materials reinforced composites are still not fit for so many advanced applications due to their inherent incompatibilities, low mechanical and physical properties compared to the synthetic fiber reinforced composites. Therefore the composite community and researchers needed more attempts to resolve the difficulties to produce sustainable composite materials.

Chapter VII: Novel Findings of the Research

Thesis 1:

Novel hybrid composites were developed from rice straw and energy reeds. According to our knowledge, no research were conducted before regarding the fabrication of rice straw and energy reed materials with PF resin through applying hot-pressing technology. Novel findings are, that 100% energy reed panels are suitable for structural purposes because of high strength and good moisture resistance, and 100% rice straw panels are rather suitable for thermal insulation purposes. There was an increased pattern of mechanical properties found with the increase in energy reed materials in the composite. The highest performances against internal bonding failure are displayed by the 100% energy reed fiber reinforced composite panels (0.52 (0.04) MPa) compared to all other types of panel (0.25 (0.02), 0.31 (0.09), and 0.34 (0.04) MPa) for composite 1, 2, and 3). The maximum value for MOR was seen for 100% energy reeds reinforced composites by 21.47 (2.12) MPa, whereas the lowest value was observed for 100% rice straw reinforced panels just only 11.18 (1.91) MPa with a 47.9 % decline from the highest one. Obtained better fiber to matrix interaction in the composite systems as seen in morphological studies. The SEM micrographs shown the strongly interacted lignocellulosic materials. 100% rice straw reinforced composite displayed lowest values of thermal conductivity (0.061 (0.00083)) W/(m.K), whereas the highest values found for 100% energy reed fibers reinforced composites (0.104790 (0.000571)) demonstrating rice straw materials exist better thermal insulation properties than that of energy reeds. The water absorption, thickness swelling, and moisture content studies of the developed hybrid biocomposite panels shown that 100% rice straw reinforced composites provided the maximum values (54.284 (2.6580)% for water absorbency, 38.572 (0.1744)% for thickness swelling, and 5.92 (0.6464)% for moisture content) whereas the energy reed fiber (100%) reinforced composites provided the lowest values (7.746 (0.3391)% for water absorbency, 9.383 (0.5115)% for thickness swelling, and 5.11 (0.2423)% for moisture content) after 2 h. the similar trend is also noticed after 24 h although the absorption rates started to decline gradually after 2 h. The sequence of the physical properties in terms of higher values is for the composites are clearly noticed in the figure which demonstrates that the values starts to increase with the increase in rice straw content in composite system.

Thesis 2:

Thesis 2.1: A novel semi-dry fabrication technology was implemented for the production of cementitious composite panels from scots pine and coir fibers. Novel insulation panels were developed from scots pine and coir fibers reinforcing with the cement. The obtained thermal conductivity values are 0.17045 (0.00352) W/(m.K) for 100% pine reinforcements, whereas 60% pine and 40% coir reinforcement was 0.16651 (0.00265), 50% pine and 50% coir reinforcement was 0.11646 (0.00263), 40% pine and 60% coir reinforcement was 0.11265 (0.00409), and 100% coir reinforcement was 0.10547 (0.00657) W/(m.K). Interestingly, when the coir fiber was induced in composite systems, the thermal conductivity values started to decline. That is why our study reveals the 100% coir fiber-reinforced cementitious composite to be the best insulation material (according to our tested result), whereas 100% scots pine displayed the lowest thermal conductivity according to the performance perspectives.

Thesis 2.2: The developed panels providing superior mechanical performances needed for construction and building materials. The flexural properties obtained for five composite panels were 6.22 (0.78), 6.77 (0.12), 6.78 (0.73), 7.97 (0.8), and 8.02 (0.87) MPa, respectively for 100% pine reinforcements, 60% pine and 40% coir reinforcement 50% pine and 50% coir

reinforcement, 40% pine and 60% coir reinforcement, and 100% coir reinforcement after 28 days of air curing in the laboratory. The flexural strengths of 100% scots pine reinforced cementitious matrix was the lowest, whereas the patterns increase with the increase of coir fiber contents. Additionally, the internal bonding strengths of P@C1 displayed 0.63 (0.08) MPa, whereas PC@C2 was 0.64 (0.03), PC@C3 was 0.66 (0.02), PC@C4 was 0.68 (0.03) MPa, and C@C5 was 0.72 (0.06) MPa. The properties shown improved performances when coir fiber was induced in the composite systems. Obtained significant dimensional stability (water absorbency, thickness swelling, and moisture content) of the developed sustainable products. The incorporation of coir fiber leads to decreased moisture content as well as decreased water uptake. 100% coir fiber-reinforced cementitious materials also exhibited better stability against water compared to 100% scots pine reinforced cementitious composite panels. The moisture content for composite 1 (100% scots pine reinforced cementitious composite) was 5.3 (0.4)% and 3.9 (0.9)% for composite 5 (100% coir reinforced cementitious composite).

Thesis 3:

Novel composite panels were developed from pretreated flax and glass through reinforcing with MDI resin. Composite panels were developed with four different ratios of glass and flax woven fabric reinforcement (100/0, 83.33/16.67, 50/50, and 0/100) to investigate their performances with MDI resin.

Thesis III.1: Pretreatment of the fibers provided better fiber to matrix interactions and better thermomechanical performances. The tensile strengths of pure glass (G1), glass/flax (GF2 and GF3), and pure flax (F4) reinforced MDI composites take the values of 78.61 (8.2), 69.63 (2.77), 49.44 (2.05), and 21.19 (1.59) MPa, respectively. The flexural strengths followed the similar trend as the tensile characteristics. The perceived flexural strengths were 211.9 (17.9), 147.7 (18.5), 58.9 (9.5), and 43.9 (3.5) MPa, respectively for G1, GF2, GF3, and F4 composites. The regression analyses of all the composites mechanical performances were conducted in terms of glass fiber proportion in the composites. The R^2 values for all the composites are higher than 0.57, except for flexural strength with R^2=0.41. The presence of glass fiber results in better mechanical performances of all the hybrid composites. The mechanical features of the produced composites were further analyzed conducting one-way ANOVA with the type of composites as categorical factor. These tests showed that strength of the different composites are significantly different as the p values are less than the assumed level of significance of 0.05. Better dimensional stability. The G1 (pure glass) sample absorbed the lowest moisture whereas F4 (pure flax) attained the highest moisture content. The hybrid composites (GF2) attained moisture content of 1.34 (0.32) %, 1.88 (0.29) %, and 2.15 (0.09) % moisture content after 2 h, 24 h, and 240 h; whereas GF3 showed 3.76 (0.08) %, 3.84 (0.33) %, and 3.97 (0.04) % moisture content within the same time period.

Thesis III.2. Better thermal stability of developed hybrid composites was also found. The maximum weight losses (10% to 60%) were occurred at temperatures ranging from 315 to 450 °C. Besides, residues of the composites G1, GF2, GF3, and F4 were amounted to 87.99, 36.01, 58.78, and 30.82%, respectively.

Thesis 4:

Green silver nanoparticles were synthesized from *Tilia cordata* leaf extracts over hemp and glass woven materials. Novel nanocomposites were developed from nanosilver treated glass and hemp woven fabrics laminated with epoxy resin. The nanosilver content values measured by XRF tests (0, 655±23, and 1829±30 PPM) for the composite types CC3, NC1, and NC2,

respectively. The developed products also provided better thermomechanical performances with the increase in silver precursor in the colloid system. The highest tensile strength of 40.9 MPa was found for NC1, whereas CC3 exhibited the lowest value of 16.2 MPa. NC2 provided moderate tensile strength (18.9 MPa) between the two extremes. In case of bending strength, NC1 displayed the highest performances compared to the NC2, and CC3. The 1 mM loading of silver precursor has yielded the highest mechanical performances, although a 5 mM loading may have generated an agglomeration problem hence the mechanical properties declined, still remaining higher than those of the control composite plates. It seems that the nanosilver treatment on the fabrics used for laminations positively influences the mechanical properties of the produced composite panels. All the properties were tested in terms of silver NPs loading on each composite panel. The R^2 values for all the composites was found the values above 0.93 for all the mechanical properties demonstrating that the presence of nanosilver results in significant changes of the mechanical performances. The homogeneity of variances was always found met through ANOVA test as well. The developed composites also shown brownish coloration effects, whereas color strengths increased with the increase in nanosilver loading (control sample shown the K/S values by 2.3, 1.0 mM and 5.0 mM $AgNO_3$ loaded composites provided 3.5 and 11.8 values, respectively).

List of publications

Journal publication (published):

1**. Hasan, K.M.F.**, P.G. Horváth, M. Bak, Z.M. Mucsi, L. Duong Hung Anh, and T. Alpár. Rice straw and energy reeds fiber reinforced phenol formaldehyde resin hybrid polymeric composite panels. Cellulose. **28** (2021) P. 7859–7875

2.**Hasan, K.M.F.**, P.G. Horváth, and T. Alpár. Development of lignocellulosic fiber reinforced cement composite panels using semi-dry technology. Cellulose. 28(6) (2021) P. 3631–3645.

3. **Hasan, K.M.F.**, P.G. Horváth, Z. Kóczán, and T. Alpár. Thermo-mechanical properties of pretreated coir fiber and fibrous chips reinforced multilayered composites. Scientific Reports. 11(1) (2021) P. 1-13.

4. **Hasan, K.M.F**, P.G. Horváth, and T. Alpár. Potential Natural Fiber Polymeric Nanobiocomposites: A Review. Polymers. 12(5) (2020) P. 1072.

5. **Hasan, K.F.**, et al., P.G. Horváth, A. Horváth, and T. Alpár. Coloration of woven glass fabric using biosynthesized silver nanoparticles from Fraxinus excelsior tree flower. Inorganic Chemistry Communications. 126 (2021) P. 108477.

6. **Hasan, K.M.F.**, P.G. Horváth, M. Bak, and T. Alpár. A state-of-the-art review on coir fiber-reinforced biocomposites. RSC Advance. 11(18) (2021) P. 10548-10571.

7. **Hasan, K.F.**, P.G. Horváth, T. Alpár. Thermomechanical Behavior of Methylene Diphenyl Diisocyanate-Bonded Flax/Glass Woven Fabric Reinforced Laminated Composites. ACS Omega. 6(9) (2021) P. 6124–6133.

8. **Hasan, K.M.F.**, P.G. Horváth, G. Markó, and T. Alpár. Thermomechanical characteristics of flax-woven-fabric-reinforced poly (lactic acid) and polypropylene biocomposites. Green Materials. 40(XXXX) (2021) P. 1-10.

10.Mahmud, S., **Hasan, K.M.F.** M.A. Jahid, K. Mohiuddin, R. Zhang, and J. Zhu. Comprehensive review on plant fiber-reinforced polymeric biocomposites. Journal of Materials Science. 56 (2021) P. 7231–7264.

11**. Hasan, K.M.F.**, P.G. Horváth, Z. Kóczán, M. Bak, A. Horváth, and T. Alpár. Coloration of flax woven fabric using *Taxus baccata* heartwood extract mediated nanosilver. Colour Technol. **00** (2021) P. 1-11.

12. **Hasan, K.M.F.**, P.G. Horváth, K. Zsolt, Z. Kóczán, M. Bak, A. Horváth, et al. Hemp/glass woven fabric reinforced laminated nanocomposites via in-situ synthesized silver nanoparticles from Tilia cordata leaf extract. Composite Interfaces. (2021) P. 1-19.

13. **Hasan, K.M.F.**, P.G. Horváth, Z. Kóczán, D.H.A. Le, M. Bak, L. Bejó, et al. Novel insulation panels development from multilayered coir short and long fiber reinforced phenol formaldehyde polymeric biocomposites. Journal of Polymer Research. 28(12) (2021) P. 1-16.

14. **Hasan, K.M.F.**, P.G. Horváth, Z. Kóczán, M. Bak, and T. Alpár. Colorful and facile in situ nanosilver coating on sisal/cotton interwoven fabrics mediated from European larch heartwood. Scientific Reports. 11(1) (2021) P. 1-13.

15. **Hasan, K.M.F.**, P.G. Horváth, Z. Kóczán, M. Bak, and T. Alpár. Semi-dry technology-mediated coir fiber and Scots pine particle-reinforced sustainable cementitious composite panels. Construction and Building Materials. 305 (2021) P. 124816.

16. **Hasan, K.M.F.**, X. Liu, Z. Kóczán, P.G. Horváth, M. Bak, L. Bejó, et al. Nanosilver coating on hemp/cotton blended woven fabrics mediated from mammoth pine bark with improved coloration and mechanical properties. The Journal of The Textile Institute (2021) P. 1-10.

Journal publication (under consideration/review/ under preparations):

17. **Hasan, K.F.**, Hasan, K.M.F., P.G. Horváth, Z. Kóczán, M. Bak, and T. Alpár. Effects of Sisal/Cotton Interwoven Fabric and Jute Fibers Loading on Polylactide Reinforced Biocomposites. Fibers and Polymers. Accepted.
18. **Hasan, K.F.**, et al. Sustainable coloration of aramid fabrics with Fomes fomentarius mushroom extracted nanosilver. Textile Research Journal. Under review.
19. **Hasan, K.F.**, et al. Green silver nanoparticle synthesis from sustainable coloration, biocidal, UV-protection, and thermal point of view: 2000 to 2020, A comprehensive review on game changing material, Progress in Polymer Coating. Under consideration.
20. **Hasan, K.F.**, et al. Flame retardant hybrid composites manufacturing through reinforcing lignocellulosic and carbon fibers with epoxy resin (F@LC). Industrial Crops and Products. Under consideration.
21. **Hasan, K.F.**, et al. Potential flame retardant hybrid composite panels development from fibers defibrated from cones and poplar. Composites Part A: Applied Science and Manufacturing. Under consideration.

Book chapter publication (Published/ under processing):

1. Topic: Nanotechnology for waste wood recycling, Publisher: Elsevier.
2. Topic: Introduction to biomass and biocomposites, Publisher: CRC Press (Taylor and Francis).
3. Topic: Design and fabrication technology in biocomposite manufacturing, Publisher: CRC Press (Taylor and Francis).
4. Topic: Silk protein and its nanocomposites, Publisher: Elsevier.
5. Topic: Industrial Flame-Retardants for Polyurethanes, Publisher: American Chemical Society (ACS).
6. Topic: Coir Fibre: Geographic distribution, and cultivation, Publisher: Elsevier.
7. Topic: Physicochemical and Morphological Properties of Microcrystalline cellulose and Nanocellulose Extracted from Coir Fibres and its composites, Publisher: Elsevier.
8. Topic: Nanomaterials-based smart and sustainable protective textiles, Publisher: Elsevier.
9. Topic: Community Entrepreneurship and Environmental Sustainability of Handloom Sector, Publisher: Springer.
10. Topic: Natural fibre reinforced vinyl ester composites: Influence of hybridization on the mechanical and thermal properties, Publisher: CRC Press.

Conference paper:

1. **Hasan, K.M.F.**, F.Z. Brahmia, M. Bak, P.G. Horváth, G. Markó, L. Dénes, et al. Effects of cement on lignocellulosic fibres. in 9TH HARDWOOD PROCEEDINGS PT. I. 2020. Sopron, Hungary.
2. **Hasan, K.M.F.**, P.G. Horváth, and T. Alpár. Effects of alkaline treatments on coconut fiber reinforced biocomposites in 9th Interdisciplinary Doctoral Conference. 2020. Pecs, Hungary: Doctoral Student Association of the University of Pécs.
3. **Hasan, K.M.F.**, P.G. Horváth, M. Bak, and T. Alpár, *Morphological study on composite materials developed through reinforcing natural and synthetic woven fabrics from glass and hemp*, in *ITMC Conference*. 2021: Montreal, canada.
4. **Hasan, K.M.F.**, P.G. Horváth, M. Bak, and T. Alpár, Energy reed fiber reinforced thermosetting polymeric biocomposite, in Springwind Conference. 2021: Sopron, Hungary.
5. Hasan, K.M.F., P.G. Horváth, M. Bak, and T. Alpár, Thermal and Mechanical Characterization of NaOH Treated Coir materials reinforced composites. Proceedings of the

2021 Society of Wood Science and Technology. International Convention, Flagstaff, Arizona. August 1-6, 2021.
6. **Hasan, K.M.F.**, P.G. Horváth, M. Bak, and T. Alpár, Green insulation panels development from industrial lignocellulosic materials reinforced cementitious composites. 5th International Conference on Building Energy and Environment. July 2022, Montreal, Canada.
7. **Hasan, K.M.F.**, P.G. Horváth, M. Bak, and T. Alpár, et al. Morphological analysis of carbon woven and nonwoven fabric reinforced composite products. Interdisciplinary Doctoral Conference. 2021. Pecs, Hungary: Doctoral Student Association of the University of Pécs.

References:

1. Gholampour, A. and T. Ozbakkaloglu. A review of natural fiber composites: properties, modification and processing techniques, characterization, applications. Journal of Materials Science. 55 (2020) P. 829–892.
2. Karade, S. Cement-bonded composites from lignocellulosic wastes. Construction and Building Materials. 24(8) (2010) P. 1323-1330.
3. Hasan, K.F., P.G. Horváth, and T. Alpár. Development of lignocellulosic fiber reinforced cement composite panels using semi-dry technology. Cellulose. 28 (2021) P. 3631–3645.
4. Hasan, K., B. Fatima Zohra, M. Bak, P.G. Horváth, L. Dénes, and T.L. Alpár. Effects of cement on lignocellulosic fibres. in 9th Hardwood Proceedings. 2020. Sopron, Hungary: University of Sopron Press.
5. Hasan, K.F., P.G. Horváth, K. Zsolt, Z. Kóczán, M. Bak, A. Horváth, et al. Hemp/glass woven fabric reinforced laminated nanocomposites via in-situ synthesized silver nanoparticles from Tilia cordata leaf extract. Composite Interfaces. (2021) P.
6. Hasan, K.F., P.G. Horváth, A. Horváth, and T. Alpár. Coloration of woven glass fabric using biosynthesized silver nanoparticles from *Fraxinus excelsior* tree flower. Inorganic Chemistry Communications. 126 (2021) P. 108477.
7. Mahmud, S., K.F. Hasan, M.A. Jahid, K. Mohiuddin, R. Zhang, and J. Zhu. Comprehensive review on plant fiber-reinforced polymeric biocomposites. Journal of Materials Science. 56 (2021) P. 7231–7264.
8. Gurunathan, T., S. Mohanty, and S.K. Nayak. A review of the recent developments in biocomposites based on natural fibres and their application perspectives. Composites Part A: Applied Science and Manufacturing. 77 (2015) P. 1-25.
9. Amiandamhen, S., M. Meincken, and L. Tyhoda. Natural Fibre Modification and Its Influence on Fibre-matrix Interfacial Properties in Biocomposite Materials. Fibers and Polymers. 21 (2020) P. 677-689.
10. BAJPAI, P., BIERMANN'S HANDBOOK OF PULP AND PAPER: Paper and Board Making. Vol. 3. 2018, Amsterdam, Netherlands: Elsevier.
11. Li, X., L.G. Tabil, and S. Panigrahi. Chemical treatments of natural fiber for use in natural fiber-reinforced composites: a review. Journal of Polymers and the Environment. 15(1) (2007) P. 25-33.
12. Azeez, M.A. and J.I. Orege. Bamboo, Its Chemical Modification and Products. Bamboo: Current and Future Prospects. (2018) P. 25.
13. Prasad, G.E., B.K. Gowda, and R. Velmurugan. Prediction of flexural properties of coir polyester composites by ANN. in Mechanics of Composite and Multi-functional Materials, Volume 7 Cham, Switzerland Springer; 2016. p. 173-180.
14. Hasan, K., P.G. Horváth, and T. Alpár. Potential Natural Fiber Polymeric Nanobiocomposites: A Review. Polymers. 12(5) (2020) P. 1072.
15. Alpár Tibor, M.G., Koroknai, László. Natural Fiber Reinforced PLA Composites: Effect of Shape of Fiber Elements on Properties of Composites. in Handbook of Composites from Renewable Materials, Design and Manufacturing New Jersey, United States Willey and Sons 2017. p. 287-309.
16. Islam, M.S., M.B. Ahmad, M. Hasan, S.A. Aziz, M. Jawaid, M.M. Haafiz, et al. Natural fiber-reinforced hybrid polymer nanocomposites: effect of fiber mixing and nanoclay on physical, mechanical, and biodegradable properties. BioResources. 10(1) (2015) P. 1394-1407.
17. Shahzad, A. Hemp fiber and its composites–a review. Journal of Composite Materials. 46(8) (2012) P. 973-986.
18. Basu, A., M. Nazarkovsky, R. Ghadi, W. Khan, and A.J. Domb. Poly (lactic acid)-based nanocomposites. Polymers for Advanced Technologies. 28(8) (2017) P. 919-930.

19. Ayrilmis, N., S. Jarusombuti, V. Fueangvivat, P. Bauchongkol, and R.H. White. Coir fiber reinforced polypropylene composite panel for automotive interior applications. Fibers and Polymers. 12(7) (2011) P. 919-926.
20. Muzyczek, M. The use of flax and hemp for textile applications. in Handbook of natural fibres Duxford, United Kingdom Elsevier BV: Woodhead Publishing; 2020. p. 147-167.
21. Zhang, Y., Y. Li, H. Ma, and T. Yu. Tensile and interfacial properties of unidirectional flax/glass fiber reinforced hybrid composites. Composites Science and Technology. 88 (2013) P. 172-177.
22. Battegazzore, D., A. Frache, T. Abt, and M.L. Maspoch. Epoxy coupling agent for PLA and PHB copolymer-based cotton fabric bio-composites. Composites Part B: Engineering. 148 (2018) P. 188-197.
23. Holt, G., P. Chow, J. Wanjura, M. Pelletier, and T. Wedegaertner. Evaluation of thermal treatments to improve physical and mechanical properties of bio-composites made from cotton byproducts and other agricultural fibers. Industrial Crops and Products. 52 (2014) P. 627-632.
24. Shibata, M., N. Teramoto, T. Nakamura, and Y. Saitoh. All-cellulose and all-wood composites by partial dissolution of cotton fabric and wood in ionic liquid. Carbohydrate Polymers. 98(2) (2013) P. 1532-1539.
25. Shen, M., L. Wang, and J.-J. Long. Biodegumming of ramie fiber with pectinases enhanced by oxygen plasma. Journal of Cleaner Production. 101 (2015) P. 395-403.
26. Yu, T., J. Ren, S. Li, H. Yuan, and Y. Li. Effect of fiber surface-treatments on the properties of poly (lactic acid)/ramie composites. Composites Part A: Applied Science and Manufacturing. 41(4) (2010) P. 499-505.
27. Rajak, D.K., D.D. Pagar, P.L. Menezes, and E. Linul. Fiber-reinforced polymer composites: Manufacturing, properties, and applications. Polymers. 11(10) (2019) P. 1667.
28. Verma, D. and P. Gope. The use of coir/coconut fibers as reinforcements in composites. in Biofiber Reinforcements in Composite Materials Duxford, United Kingdom Woodhead Publishing; 2015. p. 285-319.
29. Menezes, P.L., P.K. Rohatgi, and M.R. Lovell. Studies on the tribological behavior of natural fiber reinforced polymer composite. in Green Tribology Springer; 2012. p. 329-345.
30. Razali, N., M.S. Salit, M. Jawaid, M.R. Ishak, and Y. Lazim. A study on chemical composition, physical, tensile, morphological, and thermal properties of roselle fibre: Effect of fibre maturity. BioResources. 10(1) (2015) P. 1803-1824.
31. Pereira, J.F., D.P. Ferreira, J. Bessa, J. Matos, F. Cunha, I. Araújo, et al. Mechanical performance of thermoplastic olefin composites reinforced with coir and sisal natural fibers: Influence of surface pretreatment. Polymer Composites. 40(9) (2019) P. 3472-3481.
32. Essabir, H., M. Bensalah, D. Rodrigue, R. Bouhfid, and A. Qaiss. Structural, mechanical and thermal properties of bio-based hybrid composites from waste coir residues: Fibers and shell particles. Mechanics of Materials. 93 (2016) P. 134-144.
33. Zhu, Z., M. Hao, and N. Zhang. Influence of contents of chemical compositions on the mechanical property of sisal fibers and sisal fibers reinforced PLA composites. Journal of Natural Fibers. (2018) P.
34. Annandarajah, C., P. Li, M. Michel, Y. Chen, R. Jamshidi, A. Kiziltas, et al. Study of agave fiber-reinforced biocomposite films. Materials. 12(1) (2019) P. 99.
35. Hasan, K.F., P.G. Horváth, and T. Alpár. Potential fabric-reinforced composites: a comprehensive review. Journal of Materials Science. (2021) P. 1-35.

36. Jamshaid, H. and R. Mishra. Thermomechanical characteristics of basalt hybrid and nonhybrid woven fabric–reinforced epoxy composites. Polymer Composites. 37(10) (2016) P. 2982-2994.
37. Zhou, G., Q. Sun, D. Li, Z. Meng, Y. Peng, D. Zeng, et al. Effects of fabric architectures on mechanical and damage behaviors in carbon/epoxy woven composites under multiaxial stress states. Polymer Testing. 90 (2020) P. 106657.
38. Aghaei, M., M.M. Shokrieh, and R. Mosalmani. Effect of warp and fill-fiber volume fractions on mechanical properties of glass/epoxy woven fabric composites. Journal of Composite Materials. 54(24) (2020) P. 3501-3513.
39. Chen, J.-C. and Y.-F. Zhuang. Tension and compression of sandwich composites with weft-knit fabric cores. Modern Physics Letters B. 34(07n09) (2020) P. 2040004.
40. Ramakrishna, S. Characterization and modeling of the tensile properties of plain weft-knit fabric-reinforced composites. Composites Science and Technology. 57(1) (1997) P. 1-22.
41. Hearle, J.W., P. Grosberg, and S. Backer. Structural mechanics of fibers, yarns, and fabrics. New York, United States Wiley-Interscience; 1969.
42. Liang, Y., H. Wang, and X. Gu. In-plane shear response of unidirectional fiber reinforced and fabric reinforced carbon/epoxy composites. Polymer Testing. 32(3) (2013) P. 594-601.
43. Feraboli, P., T. Cleveland, M. Ciccu, P. Stickler, L. DeOto, and Manufacturing. Defect and damage analysis of advanced discontinuous carbon/epoxy composite materials. Composites Part A: Applied Science. 41(7) (2010) P. 888-901.
44. Nassar, A. and E. Nassar. Effect of fiber orientation on the mechanical properties of multi layers laminate nanocomposites. Heliyon. 6(1) (2020) P. e03167.
45. Mohammed, L., M.N. Ansari, G. Pua, M. Jawaid, and M.S. Islam. A review on natural fiber reinforced polymer composite and its applications. International Journal of Polymer Science. 2015 (2015) P.
46. Tibor, L.A., G.H. Péter, and K.M.F. Hasan. Introduction to biomass and biocomposites. in Toward the value-added biocomposites: technology, innovation and opportunity Boca Raton, USA CRC Press; 2021.
47. Ku, H., H. Wang, N. Pattarachaiyakoop, and M. Trada. A review on the tensile properties of natural fiber reinforced polymer composites. Composites Part B: Engineering. 42(4) (2011) P. 856-873.
48. Zhang, L., S. Lv, C. Sun, L. Wan, H. Tan, and Y. Zhang. Effect of MAH-g-PLA on the properties of wood fiber/polylactic acid composites. Polymers. 9(11) (2017) P. 591.
49. Jawaid, M., M.S. Salit, and O.Y. Alothman, Green biocomposites: design and applications. 2017: Springer.
50. Polymerdatabase.com. Crystallization Behaviour of polymers. 2015-2022 [cited 2022 10th February]; Available from: https://polymerdatabase.com/polymer%20physics/Crystalline%20Polymers.html.
51. Sun, G., R. Liang, Z. Lu, T. Shi, P. Geng, and L. Zongjin. Remarkable mechanical enhancement achieved by interfacial strengthening of organic/inorganic/fiber composites. Construction and Building Materials. 142 (2017) P. 7-10.
52. Khan, B.A., V.S. Chevali, H. Na, J. Zhu, P. Warner, and H. Wang. Processing and properties of antibacterial silver nanoparticle-loaded hemp hurd/poly (lactic acid) biocomposites. Composites Part B: Engineering. 100 (2016) P. 10-18.
53. Aydin, L., H.S. Artem, E. Oterkus, O. Gundogdu, and H. Akbulut. Mechanics of fiber composites. in Fiber Technology for Fiber-Reinforced Composites United Kingdom Woodhead Publishing; 2017. p. 5-50.

54. Tavares, R.P., A.R. Melro, M.A. Bessa, A. Turon, W.K. Liu, and P.P. Camanho. Mechanics of hybrid polymer composites: analytical and computational study. Computational Mechanics. 57(3) (2016) P. 405-421.
55. Shokrieh, M.M. and S.M. Kamali. Theoretical and experimental studies on residual stresses in laminated polymer composites. Journal of composite materials. 39(24) (2005) P. 2213-2225.
56. Shokrieh, M.M. and S.M.K. Shahri. Modeling residual stresses in composite materials. in Residual stresses in composite materials Elsevier; 2021. p. 193-213.
57. Knops, M. and C. Bögle. Gradual failure in fibre/polymer laminates. Composites Science and Technology. 66(5) (2006) P. 616-625.
58. Kalia, S., B. Kaith, and I. Kaur. Pretreatments of natural fibers and their application as reinforcing material in polymer composites—a review. Polymer Engineering & Science. 49(7) (2009) P. 1253-1272.
59. Mukhopadhyay, S. and R. Fangueiro. Physical modification of natural fibers and thermoplastic films for composites—a review. Journal of Thermoplastic Composite Materials. 22(2) (2009) P. 135-162.
60. Zille, A., F.R. Oliveira, and A.P. Souto. Plasma treatment in textile industry. Plasma processes and Polymers. 12(2) (2015) P. 98-131.
61. Sparavigna, A. Plasma treatment advantages for textiles. arXiv preprint arXiv:0801.3727. (2008) P.
62. Khoathane, M.C., E.R. Sadiku, and C.S. Agwuncha. Surface modification of natural fiber composites and their potential applications. Surface Modification of Biopolymers. Hoboken, NJ, USA: John Wiley & Sons, Inc. (2015) P. 370-400.
63. Ferreira, D.P., J. Cruz, and R. Fangueiro. Surface modification of natural fibers in polymer composites. in Green composites for automotive applications Elsevier; 2019. p. 3-41.
64. Kalia, S., K. Thakur, A. Celli, M.A. Kiechel, and C.L. Schauer. Surface modification of plant fibers using environment friendly methods for their application in polymer composites, textile industry and antimicrobial activities: A review. Journal of Environmental Chemical Engineering. 1(3) (2013) P. 97-112.
65. George, M., P.G. Mussone, and D.C. Bressler. Surface and thermal characterization of natural fibres treated with enzymes. Industrial Crops and Products. 53 (2014) P. 365-373.
66. Araujo, R., M. Casal, and A. Cavaco-Paulo. Application of enzymes for textile fibres processing. Biocatalysis and Biotransformation. 26(5) (2008) P. 332-349.
67. Nair, A.B., P. Sivasubramanian, P. Balakrishnan, K.A.N. Ajith Kumar, and M.S. Sreekala. Environmental effects, biodegradation, and life cycle analysis of fully biodegradable “green” composites. in Polymer Composites Weinhiem, Germany Willey-VCH; 2013. p. 515-568.
68. Nakamura, R. and A.N. Netravali. Fully biodegradable “green” composites. in Polymer Composites Weinhiem, Germany Willey-VCH; 2013. p. 431-463.
69. Komal, U.K., V. Verma, T. Ashwani, N. Verma, and I. Singh. Effect of chemical treatment on thermal, mechanical and degradation behavior of banana fiber reinforced polymer composites. Journal of Natural Fibers. 17(7) (2018) P. 1026-1038
70. Youssef, A., M. Hasanin, M. Abd El-Aziz, and O. Darwesh. Green, economic, and partially biodegradable wood plastic composites via enzymatic surface modification of lignocellulosic fibers. Heliyon. 5(3) (2019) P. e01332.
71. Narayan, R. Biodegradability.. Bioplastics Magazine. 4 (2009) P. 28-31.
72. Peltola, H., E. Pääkkönen, P. Jetsu, and S. Heinemann. Wood based PLA and PP composites: Effect of fibre type and matrix polymer on fibre morphology, dispersion

and composite properties. Composites Part A: Applied Science and Manufacturing. 61 (2014) P. 13-22.
73. Hasan, K.M.F., P.G. Horváth, and T. Alpár. Potential natural fiber polymeric nanobiocomposites: A review. Polymers. 12(5) (2020) P. 1-25.
74. Rodriguez, L.J., P. Peças, H. Carvalho, and C.E. Orrego. A literature review on life cycle tools fostering holistic sustainability assessment: An application in biocomposite materials. Journal of Environmental Management. 262 (2020) P. 110308.
75. Ketola, A.E., A. Strand, A. Sundberg, J. Kouko, A. Oksanen, K. Salminen, et al. Effect of micro-and nanofibrillated cellulose on the drying shrinkage, extensibility, and strength of fibre networks. BioResources. 13(3) (2018) P. 5319-5342.
76. Thakur, V., A. Singha, and M. Thakur. In-air graft copolymerization of ethyl acrylate onto natural cellulosic polymers. International Journal of Polymer Analysis and Characterization. 17(1) (2012) P. 48-60.
77. Agarwal, J., S. Sahoo, S. Mohanty, and S.K. Nayak. Progress of novel techniques for lightweight automobile applications through innovative eco-friendly composite materials: a review. Journal of Thermoplastic Composite Materials. 33(7) (2020) P. 978-1013.
78. Badia, J., E. Strömberg, T. Kittikorn, M. Ek, S. Karlsson, and A. Ribes-Greus. Relevant factors for the eco-design of polylactide/sisal biocomposites to control biodegradation in soil in an end-of-life scenario. Polymer Degradation and Stability. 143 (2017) P. 9-19.
79. Mazlan, M., K. Ahmad, F. Hashim, M. Razab, M. Omar, A. Shaiful, et al. Experimental and Numerical Approach to Study the Effect of Biocomposite Material to Enhance Durability of Wood based Composite Material. International Journal of Engineering & Technology. 7(3.28) (2018) P. 157-162.
80. Rosdi, N., M. Mohamed, M. Mohamad, M.H.M. Amini, M. Aziz, and Z.I. Rizman. Effect of biocomposite materials to enhance durability of selected wood species (intsia palembanica miq, neobalanocarpus heimii, shorea plagata) in Malaysia. ARPN Journal of Engineering and Applied Sciences. 10(1) (2015) P. 313-320.
81. Salehnejad, M.A., A. Mohammadi, M. Rezaei, and H. Ahangari. Cracking failure analysis of an engine exhaust manifold at high temperatures based on critical fracture toughness and FE simulation approach. Engineering Fracture Mechanics. 211 (2019) P. 125-136.
82. Suman, S. and P. Biswas. Thermo-mechanical study of single and multi-pass welding of CSEF steel for residual stresses and deformations considering solid state phase transformation. Materials Today: Proceedings. (2020) P.
83. Potluri, R. Mechanical properties evaluation of T800 carbon fiber reinforced hybrid composite embedded with silicon carbide microparticles. Multidiscipline Modeling in Materials and Structures. (2018) P.
84. Hasan, K.F., P.G. Horváth, K. Zsolt, and T. Alpár. Design and fabrication technology in biocomposites manufacturing. in Value-added biocomposites: technology, innovation, and opportunity Boca Raton CRC Press; 2021. p. 158-183.
85. Barbu, M.I.a.M.C. Wood-based panel technology. in Wood-based panels, An introduction for specialists. H. Thoemen, M. Irle, and M. Sernek. Editors UB8 3PH, London, England Brunel University Press; 2010. p. 1-90.
86. Naresh, K., K. Shankar, B. Rao, and R. Velmurugan. Effect of high strain rate on glass/carbon/hybrid fiber reinforced epoxy laminated composites. Composites Part B: Engineering. 100 (2016) P. 125-135.
87. Jawaid, M., M. Thariq, and N. Saba, Mechanical and physical testing of biocomposites, fibre-reinforced composites and hybrid composites. 2018, Duxford, United Kingdom: Woodhead Publishing.

88. Latif, R., S. Wakeel, N. Zaman Khan, A. Noor Siddiquee, S. Lal Verma, and Z. Akhtar Khan. Surface treatments of plant fibers and their effects on mechanical properties of fiber-reinforced composites: A review. Journal of Reinforced Plastics and Composites. 38(1) (2019) P. 15-30.
89. Ramraji, K., K. Rajkumar, and P. Sabarinathan. Tailoring of tensile and dynamic thermomechanical properties of interleaved chemical-treated fine almond shell particulate flax fiber stacked vinyl ester polymeric composites. Proceedings of the Institution of Mechanical Engineers, Part L: Journal of Materials: Design and Applications. 233(11) (2019) P. 2311-2322.
90. Hasan, K.M.F., G.H. Péter, and L.A. Tibor. Design and fabrication technology in biocomposite manufacturing. in Toward the value-added biocomposites: technology, innovation and opportunity Boca Raton, USA CRC Press; 2021.
91. Rouison, D., M. Sain, and M. Couturier. Resin transfer molding of hemp fiber composites: optimization of the process and mechanical properties of the materials. Composites Science and Technology. 66(7-8) (2006) P. 895-906.
92. Chandekar, H., V. Chaudhari, and S. Waigaonkar. A review of jute fiber reinforced polymer composites. Materials Today: Proceedings. 26(2) (2020) P. 2079-2082.
93. Djafar, Z., I. Renreng, and M. Jannah. Tensile and Bending Strength Analysis of Ramie Fiber and Woven Ramie Reinforced Epoxy Composite. Journal of Natural Fibers. 18(12) (2020) P. 2315-2326.
94. Akhtar, M.N., A.B. Sulong, M.F. Radzi, N. Ismail, M. Raza, N. Muhamad, et al. Influence of alkaline treatment and fiber loading on the physical and mechanical properties of kenaf/polypropylene composites for variety of applications. Progress in Natural Science: Materials International. 26(6) (2016) P. 657-664.
95. Gupta, M. and R. Srivastava. Properties of sisal fibre reinforced epoxy composite. Indian Journal of Fibre & Textile Research. 41(3) (2016) P. 235-41.
96. Fiorelli, J., D.d.L. Sartori, J.C.M. Cravo, H. Savastano Junior, J.A. Rossignolo, M.F.d. Nascimento, et al. Sugarcane bagasse and castor oil polyurethane adhesive-based particulate composite. Materials Research. 16(2) (2013) P. 439-446.
97. Cabral, M.R., E.Y. Nakanishi, V. Dos Santos, J.H. Palacios, S. Godbout, H. Savastano, et al. Evaluation of pre-treatment efficiency on sugarcane bagasse fibers for the production of cement composites. Archives of Civil and Mechanical Engineering volume 18 (2018) P. 1092-1102.
98. Xia, T., H. Huang, G. Wu, E. Sun, X. Jin, and W. Tang. The characteristic changes of rice straw fibers in anaerobic digestion and its effect on rice straw-reinforced composites. Industrial Crops and Products. 121 (2018) P. 73-79.
99. Takagi, H. and Y. Ichihara. Effect of fiber length on mechanical properties of “green” composites using a starch-based resin and short bamboo fibers. JSME International Journal Series A Solid Mechanics and Material Engineering. 47(4) (2004) P. 551-555.
100. Jayabal, S. and U. Natarajan. Influence of fiber parameters on tensile, flexural, and impact properties of nonwoven coir–polyester composites. The International Journal of Advanced Manufacturing Technology volume. 54(5) (2011) P. 639-648.
101. Ramnath, B.V., S.J. Kokan, R.N. Raja, R. Sathyanarayanan, C. Elanchezhian, A.R. Prasad, et al. Evaluation of mechanical properties of abaca–jute–glass fibre reinforced epoxy composite. Materials & Design. 51 (2013) P. 357-366.
102. Odusote, J. and A. Oyewo. Mechanical properties of pineapple leaf fiber reinforced polymer composites for application as a prosthetic socket. Journal of Engineering and Technology. 7(1) (2016) P. 125-139.
103. Dong, Y., A. Ghataura, H. Takagi, H.J. Haroosh, A.N. Nakagaito, and K.-T. Lau. Polylactic acid (PLA) biocomposites reinforced with coir fibres: Evaluation of

mechanical performance and multifunctional properties. Composites Part A: Applied Science and Manufacturing. 63 (2014) P. 76-84.
104. Hidalgo-Salazar, M.A. and E. Salinas. Mechanical, thermal, viscoelastic performance and product application of PP-rice husk Colombian biocomposites. Composites Part B: Engineering. 176 (2019) P. 107135.
105. Ferrandez-Garcia, M.T., C.E. Ferrandez-Garcia, T. Garcia-Ortuño, A. Ferrandez-Garcia, and M. Ferrandez-Villena. Experimental evaluation of a new giant reed (Arundo Donax L.) composite using citric acid as a natural binder. Agronomy. 9(12) (2019) P. 882.
106. Khan, M.Z., S.K. Srivastava, and M. Gupta. Tensile and flexural properties of natural fiber reinforced polymer composites: A review. Journal of Reinforced Plastics and Composites. 37(24) (2018) P. 1435-1455.
107. Sathish, S., K. Kumaresan, L. Prabhu, and N. Vigneshkumar. Experimental investigation on volume fraction of mechanical and physical properties of flax and bamboo fibers reinforced hybrid epoxy composites. Polymers and Polymer Composites. 25(3) (2017) P. 229-236.
108. Durante, M., A. Formisano, L. Boccarusso, A. Langella, and L. Carrino. Creep behaviour of polylactic acid reinforced by woven hemp fabric. Composites Part B: Engineering. 124 (2017) P. 16-22.
109. Saba, N., F. Mohammad, M. Pervaiz, M. Jawaid, O. Alothman, and M. Sain. Mechanical, morphological and structural properties of cellulose nanofibers reinforced epoxy composites. International Journal of Biological Macromolecules. 97 (2017) P. 190-200.
110. Tserki, V., P. Matzinos, N. Zafeiropoulos, and C. Panayiotou. Development of biodegradable composites with treated and compatibilized lignocellulosic fibers. Journal of Applied Polymer Science. 100(6) (2006) P. 4703-4710.
111. Yan, L., N. Chouw, and K. Jayaraman. Flax fibre and its composites–A review. Composites Part B: Engineering. 56 (2014) P. 296-317.
112. Sanjay, M., P. Madhu, M. Jawaid, P. Senthamaraikannan, S. Senthil, and S. Pradeep. Characterization and properties of natural fiber polymer composites: A comprehensive review. Journal of Cleaner Production. 172 (2018) P. 566-581.
113. Suhaily, S., M. Jawaid, H.A. Khalil, A.R. Mohamed, and F. Ibrahim. A review of oil palm biocomposites for furniture design and applications: potential and challenges. BioResources. 7(3) (2012) P. 4400-4423.
114. Abrate, S. Impact on laminated composites: recent advances. Applied Mechanics Reviews. 47(11) (1994) P. 517-544.
115. Johnson, A.F., A.K. Pickett, and P. Rozycki. Computational methods for predicting impact damage in composite structures. Composites Science and Technology. 61(15) (2001) P. 2183-2192.
116. Lin, H. and Y. Lee. On the inelastic impact of composite laminated plate and shell structures. Composite Structures. 14(2) (1990) P. 89-111.
117. Hassoon, O.H., M. Tarfaoui, and A. El Moumen. Progressive damage modeling in laminate composites under slamming impact water for naval applications. Composite Structures. 167 (2017) P. 178-190.
118. Adam, H. Carbon fibre in automotive applications. Materials & Design. 18(4-6) (1997) P. 349-355.
119. Barile, C., C. Casavola, and F. De Cillis. Mechanical comparison of new composite materials for aerospace applications. Composites Part B: Engineering. 162 (2019) P. 122-128.
120. Chillara, V. and M. Dapino. Review of morphing laminated composites. Applied Mechanics Reveiws. 72(1) (2020) P. 1-16.

121. Liu, D., Y. Tang, and W. Cong. A review of mechanical drilling for composite laminates. Composite Structures. 94(4) (2012) P. 1265-1279.
122. Guo, Y., Q. Dong, J. Chen, X. Yao, X. Yi, and Y. Jia. Comparison between temperature and pyrolysis dependent models to evaluate the lightning strike damage of carbon fiber composite laminates. Composites Part A: Applied Science and Manufacturing. 97 (2017) P. 10-18.
123. Sinmazçelik, T., E. Avcu, M.Ö. Bora, and O. Çoban. A review: Fibre metal laminates, background, bonding types and applied test methods. Materials & Design. 32(7) (2011) P. 3671-3685.
124. Hasan, K.M.F., P.G. Horváth, and T. Alpár. Silk protein and its nanocomposites. in Biopolymeric Nanomaterials: Fundamentals and Applications Elsevier; 2021. p. 309-323.
125. Balaji, A., B. Karthikeyan, and C.S. Raj. Bagasse fiber–the future biocomposite material: a review. International Journal of Cemtech Research. 7(1) (2014) P. 223-233.
126. Mallick, P.K., Fiber-reinforced composites: materials, manufacturing, and design. 2007: CRC press.
127. Biocomposites Market 2020 29th October, 2020]; Available from: https://www.marketsandmarkets.com/Market-Reports/biocomposite-market-258097936.html.
128. Mahdi, E. and A. Dean. The effect of filler content on the tensile behavior of polypropylene/cotton fiber and poly (vinyl chloride)/cotton fiber composites. Materials. 13(3) (2020) P. 753.
129. Ng, W., M. Johar, H. Israr, and K. Wong. A review on the interfacial characteristics of natural fibre reinforced polymer composites. Interfaces in Particle and Fibre Reinforced Composites. (2020) P. 163-198.
130. Farahbakhsh, N., P. Shahbeigi-Roodposhti, H. Sadeghifar, R.A. Venditti, and J.S. Jur. Effect of isolation method on reinforcing capability of recycled cotton nanomaterials in thermoplastic polymers. Journal of Materials Science. 52(9) (2017) P. 4997-5013.
131. Battegazzore, D., T. Abt, M.L. Maspoch, and A. Frache. Multilayer cotton fabric bio-composites based on PLA and PHB copolymer for industrial load carrying applications. Composites Part B: Engineering. 163 (2019) P. 761-768.
132. Ashraf, M.A., M. Zwawi, M. Taqi Mehran, R. Kanthasamy, and A. Bahadar. Jute based bio and hybrid composites and their applications. Fibers. 7(9) (2019) P. 77.
133. Dinesh, S., P. Kumaran, S. Mohanamurugan, R. Vijay, D.L. Singaravelu, A. Vinod, et al. Influence of wood dust fillers on the mechanical, thermal, water absorption and biodegradation characteristics of jute fiber epoxy composites. Journal of Polymer Research. 27(1) (2020) P. 1-13.
134. Tanasă, F., M. Zănoagă, C.A. Teacă, M. Nechifor, and A. Shahzad. Modified hemp fibers intended for fiber-reinforced polymer composites used in structural applications—A review. I. Methods of modification. Polymer Composites. 41(1) (2020) P. 5-31.
135. del Borrello, M., M. Mele, G. Campana, and M. Secchi. Manufacturing and characterization of hemp-reinforced epoxy composites. Polymer Composites. 41(6) (2020) P. 2316-2329.
136. Aliotta, L., V. Gigante, M.-B. Coltelli, P. Cinelli, A. Lazzeri, and M. Seggiani. Thermo-mechanical properties of PLA/short flax fiber biocomposites. Applied Sciences. 9(18) (2019) P. 3797.
137. Zhang, H., D. Liu, T. Huang, Q. Hu, and H. Lammer. Three-dimensional printing of continuous flax fiber-reinforced thermoplastic composites by five-axis machine. Materials. 13(7) (2020) P. 1678.

138. Munde, Y.S., R.B. Ingle, and I. Siva. Investigation to appraise the vibration and damping characteristics of coir fibre reinforced polypropylene composites. Advances in Materials and Processing Technologies. 4(4) (2018) P. 639-650.
139. Mishra, S., C. Nayak, M.K. Sharma, and U.K. Dwivedi. Influence of coir fiber geometry on mechanical properties of SiC filled epoxy composites. Silicon. 13(2) (2021) P. 301-307.
140. Saxena, M., A. Pappu, R. Haque, and A. Sharma. Sisal fiber based polymer composites and their applications. in Cellulose fibers: Bio-and nano-polymer composites Berlin, Germany Springer; 2011. p. 589-659.
141. Chaitanya, S., I. Singh, and J.I. Song. Recyclability analysis of PLA/Sisal fiber biocomposites. Composites Part B: Engineering. 173 (2019) P. 106895.
142. Manral, A. and P.K. Bajpai. Static and dynamic mechanical analysis of geometrically different kenaf/PLA green composite laminates. Polymer Composites. 41(2) (2020) P. 691-706.
143. Asumani, O. and R. Paskaramoorthy. Fatigue and impact strengths of kenaf fibre reinforced polypropylene composites: effects of fibre treatments. Advanced Composite Materials. 30(2) (2021) P. 103-115.
144. Sitticharoen, W., A. Chainawakul, T. Sangkas, and Y. Kuntham. Rheological and mechanical properties of silica-based bagasse-fiber-ash-reinforced recycled HDPE composites. Mechanics of Composite Materials. 52(3) (2016) P. 421-432.
145. Wirawan, R. and S. Sapuan. Sugarcane bagasse-filled poly (vinyl chloride) composites: A review. in Natural fibre reinforced vinyl ester and vinyl polymer composites Duxford, United Kingdom Elsevier BV: Woodhead Publishing; 2018. p. 157-168.
146. Das, M. Bamboo fiber-based polymer composites. in Composite Materials Cham, Switzerland Springer Science and Business Media LLC; 2017. p. 627-645.
147. Lokesh, P., T.S. Kumari, R. Gopi, and G.B. Loganathan. A study on mechanical properties of bamboo fiber reinforced polymer composite. Materials Today: Proceedings. 22 (2020) P. 897-903.
148. Choi, H.Y. and J.S. Lee. Effects of surface treatment of ramie fibers in a ramie/poly (lactic acid) composite. Fibers and Polymers. 13(2) (2012) P. 217-223.
149. Djafar, Z., I. Renreng, and M. Jannah. Tensile and bending strength analysis of ramie fiber and woven ramie reinforced epoxy composite. Journal of Natural Fibers. (2020) P. 1-12.
150. Hasan, K., P.G. Horváth, and T. Alpár. Potential fabric-reinforced composites: a comprehensive review. J. Mater. Sci. 56 (2021) P. 14381–14415.
151. Alpár, T., K.F. Hasan, and P.G. Horváth. Introduction to biomass and biocomposites. in Value-added biocomposites: technology, innovation, and opportunity Boca Raton CRC Press; 2021. p. 1-33.
152. Alpár, T., K.F. Hasan, and P.G. Horváth. Natural fibre reinforced vinyl ester composites: Influence of hybridization on the mechanical and thermal properties in Vinyl ester-based Biocomposites Boca Raton, USA CRC Press; 2022.
153. Hasan, K.F., P.G. Horváth, M. Bak, D.H.A. Le, Z.M. Mucsi, and T. Alpár. Rice straw and energy reed fibers reinforced phenol formaldehyde resin polymeric biocomposites. Cellulose. 28 (2021) P. 7859–7875.
154. Hasan, K.F., P.G. Horváth, Z. Kóczán, M. Bak, and T. Alpár. Semi-dry technology-mediated coir fiber and Scots pine particle-reinforced sustainable cementitious composite panels. Construction and Building Materials. 305 (2021) P. 124816.
155. Hasan, K.F., P.t.G.r. Horváth, and T. Alpár. Thermomechanical behavior of methylene diphenyl diisocyanate-bonded flax/glass woven fabric reinforced laminated composites. ACS Omega. 6(9) (2021) P. 6124–6133.

156. Hasan, K.F., P.G. Horváth, K. Zsolt, Z. Kóczán, M. Bak, A. Horváth, et al. Hemp/glass woven fabric reinforced laminated nanocomposites via in-situ synthesized silver nanoparticles from Tilia cordata leaf extract. Compos Interfaces. (2021) P. 1-19.
157. Energianövény. Resources for the future. 2021 [cited 2021 14th March]; Available from: http://www.energianoveny.hu/.
158. 67, T.U.o.A.S. Reed energy. 2008 [cited 2021 6th March]; Available from: http://julkaisut.turkuamk.fi/isbn9789522160355.pdf.
159. Wahid, R., S.F. Nielsen, V.M. Hernandez, A.J. Ward, R. Gislum, U. Jørgensen, et al. Methane production potential from Miscanthus sp.: Effect of harvesting time, genotypes and plant fractions. Biosystems Engineering. 133 (2015) P. 71-80.
160. Xie, X., Z. Zhou, M. Jiang, X. Xu, Z. Wang, and D. Hui. Cellulosic fibers from rice straw and bamboo used as reinforcement of cement-based composites for remarkably improving mechanical properties. Composite Part B Engineering. 78 (2015) P. 153-161.
161. Pham, T.D., C.M. Vu, and H.J.J.P.S. Choi, Series A. Enhanced fracture toughness and mechanical properties of epoxy resin with rice husk-based nano-silica. Polymer Science. 59(3) (2017) P. 437-444.
162. Basta, A.H., H. El-Saied, and V.F. Lotfy. Performance of rice straw-based composites using environmentally friendly polyalcoholic polymers-based adhesive system. Pigment & Resin Technology. (2013) P.
163. Rout, A. and A.J.P.E. Satapathy. Analysis of dry sliding wear behaviour of rice husk filled epoxy composites using design of experiment and ANN. Procedia Engineering. 38 (2012) P. 1218-1232.
164. El-Kassas, A. and A.I. Mourad. Novel fibers preparation technique for manufacturing of rice straw based fiberboards and their characterization. Materials & Design. 50 (2013) P. 757-765.
165. Zhang, L. and Y. Hu. Novel lignocellulosic hybrid particleboard composites made from rice straws and coir fibers. Materials & Design. 55 (2014) P. 19-26.
166. El-Sabbagh, A. Effect of coupling agent on natural fibre in natural fibre/polypropylene composites on mechanical and thermal behaviour. Composites Part B: Engineering. 57 (2014) P. 126-135.
167. Njoku, C., J. Omotoyinbo, K. Alaneme, and M. Daramola. Chemical modification of Urena lobata (Caeser weed) fibers for reinforcement applications. Journal of Physics: Conference Series. 1378(2) (2019) P. 1-6.
168. Hasan, K.M.F., P.G. Horváth, and T. Alpár. Development of lignocellulosic fiber reinforced cement composite panels using semi-dry technology. Cellulose. 28(6) (2021) P. 3631–3645.
169. Alpar, T.L., É. SELMECZI, and L. CSOKA. Advanced wood cement compatibility with nano mineral. in International Scientific Conference 2012. Sopron, Hungary: Citeseer.
170. Akinyemi, B.A. and C. Dai. Development of banana fibers and wood bottom ash modified cement mortars. Construction and Building Materials. 241 (2020) P. 118041.
171. Alpár, T. and I. Rácz. Production of cement-bonded particleboards from poplar (Populus euramericana cv.„I 214 “). Drvna industrija: Znanstveni časopis za pitanja drvne tehnologije. 60(3) (2009) P. 155-160.
172. Lee, A.W., Z. Hong, D.R. Phillips, and C.Y. Hse. Effect of cement/wood ratios and wood storage conditions on hydration temperature, hydration time, and compressive strength of wood-cement mixtures. Wood and Fiber Science. 19(3) (1987) P. 262-268.
173. Semple, K. and P.D. Evans. Adverse effects of heartwood on the mechanical properties of wood-wool cement boards manufactured from radiata pine wood. Wood and Fiber Science. 32(1) (2007) P. 37-43.

174. Misi, D., R. Puchałka, C. Pearson, I. Robertson, and M. Koprowski. Differences in the climate-growth relationship of scots pine: A case study from Poland and Hungary. Forests. 10(3) (2019) P. 243.
175. Gaspar, F., A. Bakatovich, N. Davydenko, and A. Joshi. Building insulation materials based on agricultural wastes. in Bio-Based Materials and Biotechnologies for Eco-Efficient Construction Duxford, United Kingdom Woodhead Publishing; 2020. p. 149-170.
176. Zhang, H. Cement. in Building materials in civil engineering. H. Zhang. Editor Duxford, United Kingdom Woodhead Publishing; 2011. p. 47-80.
177. Wang, L., M.L. Chen, and D.C. Tsang. Green remediation by using low-carbon cement-based stabilization/solidification approaches. in Sustainable Remediation of Contaminated Soil and Groundwater: Materials, Processes, and Assessment. H. Deyi. Editor Oxford, United Kingdom Butterworth-Heinemann; 2019. p. 93-118.
178. Savastano Jr, H., S. Santos, J. Fiorelli, and V. Agopyan. Sustainable use of vegetable fibres and particles in civil construction. in Sustainability of Construction Materials Duxford, United Kingdom Woodhead Publishing; 2016. p. 477-520.
179. Evans, T., A. Majumdar, and J. Ryder. A semi-dry method for the production of lightweight glass-fibre-reinforced gypsum. International Journal of Cement Composites and Lightweight Concrete. 3(1) (1981) P. 41-44.
180. Malkapuram, R., V. Kumar, and Y.S. Negi. Recent development in natural fiber reinforced polypropylene composites. Journal of Reinforced Plastics and Composites. 28(10) (2009) P. 1169-1189.
181. Khan, M.Z.R., S.K. Srivastava, and M. Gupta. A state-of-the-art review on particulate wood polymer composites: Processing, properties and applications. Polymer Testing. (2020) P. 106721.
182. Ferreiro, S., D. Herfort, and J. Damtoft. Effect of raw clay type, fineness, water-to-cement ratio and fly ash addition on workability and strength performance of calcined clay–limestone Portland cements. Cement and Concrete Research. 101 (2017) P. 1-12.
183. Khodabakhshi, K. and S.M. Mirabedini. Composites and Nanocomposites of PU Polymers Filled with Natural Fibers and Their Nanofibers. in Polyurethane Polymers Elsevier; 2017. p. 253-276.
184. Ahmadi, B., M. Kassiriha, K. Khodabakhshi, and E.R. Mafi. Effect of nano layered silicates on automotive polyurethane refinish clear coat. Progress in Organic Coatings. 60(2) (2007) P. 99-104.
185. Kau, C., A. Hiltner, E. Baer, and L. Huber. Damage processes in reinforced reaction injection molded polyurethanes. Journal of Reinforced Plastics and Composites. 8(1) (1989) P. 18-39.
186. Barahona, F., B. Albero, J.L. Tadeo, and A. Martín-Esteban. Molecularly imprinted polymer-hollow fiber microextraction of hydrophilic fluoroquinolone antibiotics in environmental waters and urine samples. Journal of Chromatography A. 1587 (2019) P. 42-49.
187. Bajracharya, R.M., A.C. Manalo, W. Karunasena, and K.-t. Lau. An overview of mechanical properties and durability of glass-fibre reinforced recycled mixed plastic waste composites. Materials & Design. 62 (2014) P. 98-112.
188. Bajpai, P.K., K. Ram, L.K. Gahlot, and V.K. Jha. Fabrication of glass/jute/epoxy composite based industrial safety helmet. Materialstoday: proceedings. 5(2) (2018) P. 8699-8706.
189. Sudhakar, R. and G. Renjini. Evaluation and prediction of fused fabric composites properties–A review. Journal of Industrial Textiles. (2020) P. 1-39.

190. Li, M., P. Wang, F. Boussu, and D. Soulat. A review on the mechanical performance of three-dimensional warp interlock woven fabrics as reinforcement in composites. Journal of Industrial Textiles. (2020) P. 1528083719894389.
191. Swaminathan, G., C. Palanisamy, G. Chidambaram, G. Henri, and C. Udayagiri. Enhancing the interfacial strength of glass/epoxy composites using ZnO nanowires. Composite Interfaces. 25(2) (2018) P. 151-168.
192. Thomas, S., R.K. Mishra, and A.M. Asiri, Sustainable polymer composites and nanocomposites. 2019, Cham, Switzerland: Springer.
193. Hasan, K.F., H. Wang, S. Mahmud, and C. Genyang. Coloration of aramid fabric via in-situ biosynthesis of silver nanoparticles with enhanced antibacterial effect. Inorganic Chemistry Communications. 119 (2020) P. 1-8.
194. Hasan, K., M. Pervez, M. Talukder, M. Sultana, S. Mahmud, M. Meraz, et al. A novel coloration of polyester fabric through green silver nanoparticles (G-AgNPs@ PET). Nanomaterials. 9(4) (2019) P. 569.
195. Hasan, K.M.F., H. Péter György, and A. Tibor. Thermomechanical Behavior of Methylene Diphenyl Diisocyanate-Bonded Flax/Glass Woven Fabric Reinforced Laminated Composites. ACS Omega. 6(9) (2020) P. 6124–6133.
196. Szabó, B., E. Vincze, and B. Czúcz. Flowering phenological changes in relation to climate change in Hungary. International Journal of Biometeorology 60(9) (2016) P. 1347-1356.
197. Selig, M. and H. Bohne. Drought stress reactions of different populations of *Quercus robur L.* and *Tilia cordata Mill*. Journal of Environmental Horticulture. 35(1) (2017) P. 6-12.
198. Vanlalveni, C., S. Lallianrawna, A. Biswas, M. Selvaraj, B. Changmai, and S.L. Rokhum. Green synthesis of silver nanoparticles using plant extracts and their antimicrobial activities: a review of recent literature. RSC Advance. 11(5) (2021) P. 2804-2837.
199. Lee, H.Y., H.K. Park, Y.M. Lee, K. Kim, and S.B. Park. A practical procedure for producing silver nanocoated fabric and its antibacterial evaluation for biomedical applications. Chemical Communications. (28) (2007) P. 2959-2961.
200. Hasan, K.F., P.G. Horváth, Z. Kóczán, M. Bak, A. Horváth, and T. Alpár. Coloration of flax woven fabric using *Taxus baccata* heartwood extract mediated nanosilver. Colouration Technology. 00 (2021) P. 1-11.
201. Shao, Y., C. Wu, T. Wu, C. Yuan, S. Chen, T. Ding, et al. Green synthesis of sodium alginate-silver nanoparticles and their antibacterial activity. International Journal of Biological Macromolecules. 111 (2018) P. 1281-1292.
202. Hasan, K.F., P.G. Horváth, Z. Kóczán, and T. Alpár. Thermo-mechanical properties of pretreated coir fiber and fibrous chips reinforced multilayered composites. Scientific Reports. 11(1) (2021) P. 1-13.
203. Rokbi, M., H. Osmani, A. Imad, and N. Benseddiq. Effect of chemical treatment on flexure properties of natural fiber-reinforced polyester composite. Procedia Engineering. 10 (2011) P. 2092-2097.
204. Mishra, S., A. Mohanty, L. Drzal, M. Misra, S. Parija, S. Nayak, et al. Studies on mechanical performance of biofibre/glass reinforced polyester hybrid composites. Composites Science and Technology. 63(10) (2003) P. 1377-1385.
205. Li, X., Z. Cai, J.E. Winandy, and A.H. Basta. Selected properties of particleboard panels manufactured from rice straws of different geometries. Bioresource Technology. 101(12) (2010) P. 4662-4666.
206. Hasan, K.F., P.G. Horváth, M. Bak, Z.M. Mucsi, L. Duong Hung Anh, and T. Alpár. Rice straw and energy reeds fiber reinforced phenol formaldehyde resin hybrid polymeric composite panels. Cellulose. (2021) P.

207. Vietnam, R. Hmong Hand Woven Vintage Hemp Fabric Soft Cool Hill Tribe Natural Organic. 2021 [cited 2021 29th Jnuary]; Available from: https://www.etsy.com/listing/256976466/hmong-hand-woven-vintage-hemp-fabric?transaction_id=1944602222&campaign_label=shipping_notification_boe_convourl_treatment&utm_source=transactional&utm_campaign=shipping_notification_boe_convourl_treatment_010170_433263510924_0_0&utm_medium=email&utm_content=&email_sent=1592981368&euid=PIKJXkRlHYjQ_aokRIaI-9rFnnRM&eaid=865034306946&x_eaid=ff43b5d870.
208. Ahmed, S., Saifullah, M. Ahmad, B.L. Swami, and S. Ikram. Green synthesis of silver nanoparticles using Azadirachta indica aqueous leaf extract. Journal of Radiation Research and Applied Sciences. 9(1) (2016) P. 1-7.
209. Tran, L.Q.N., T.N. Minh, C. Fuentes, T.T. Chi, A.W. Van Vuure, and I. Verpoest. Investigation of microstructure and tensile properties of porous natural coir fibre for use in composite materials. Industrial Crops and Products. 65 (2015) P. 437-445.
210. Wong, K., S. Zahi, K. Low, and C. Lim. Fracture characterisation of short bamboo fibre reinforced polyester composites. Materials & Design. 31(9) (2010) P. 4147-4154.
211. De Olveira, L.Á., J.C.d. Santos, T.H. Panzera, R.T.S. Freire, L.M.G. Vieira, and J.C.C. Rubio. Investigations on short coir fibre–reinforced composites via full factorial design. Polymers and Polymer Composites. 26(7) (2018) P. 391-399.
212. Kalagar, M., H. Khademieslam, B. Bazyar, and S. Hejazi. Morphology and mechanical properties of alkali-treated rice straw flour-polypropylene composites. BioResources. 6(4) (2011) P. 4238-4246.
213. Wang, Z., X. Qiao, and K. Sun. Rice straw cellulose nanofibrils reinforced poly (vinyl alcohol) composite films. Carbohydrate Polymers. 197 (2018) P. 442-450.
214. Manimaran, P., P. Senthamaraikannan, M. Sanjay, M. Marichelvam, and M. Jawaid. Study on characterization of Furcraea foetida new natural fiber as composite reinforcement for lightweight applications. Carbohydrate Polymers. 181 (2018) P. 650-658.
215. Mounika, M., K. Ramaniah, A.R. Prasad, K.M. Rao, and K.H.C. Reddy. Thermal conductivity characterization of bamboo fiber reinforced polyester composite. International Communications in Heat and Mass Transfer. 3(6) (2012) P. 1109-1116.
216. Hasan, K.F., P.G. Horváth, Z. Kóczán, and T. Alpár. Thermo-mechanical properties of pretreated coir fiber and fibrous chips reinforced multilayered composites. Sci Rep. 11(1) (2021) P. 1-13.
217. Ramanaiah, K., A. Ratna Prasad, and K.H. Chandra Reddy. Mechanical properties and thermal conductivity of Typha angustifolia natural fiber–reinforced polyester composites. International Journal of Polymer Analysis and Characterization. 16(7) (2011) P. 496-503.
218. Qin, L., J. Qiu, M. Liu, S. Ding, L. Shao, S. Lü, et al. Mechanical and thermal properties of poly (lactic acid) composites with rice straw fiber modified by poly (butyl acrylate). Chemical Engineering Journal. 166(2) (2011) P. 772-778.
219. Ismail, M., A.A. Yassen, and M. Afify. Mechanical properties of rice straw fiber-reinforced polymer composites. Fibers and Polymers. 12(5) (2011) P. 648-656.
220. Arshad, M.N., H. Mohit, M. Sanjay, S. Siengchin, A. Khan, M.M. Alotaibi, et al. Effect of coir fiber and TiC nanoparticles on basalt fiber reinforced epoxy hybrid composites: physico–mechanical characteristics. Cellulose. 28(6) (2021) P. 3451-3471.
221. El Mansouri, N.E., Q. Yuan, and F. Huang. Preparation and characterization of phenol-formaldehyde resins modified with alkaline rice straw lignin. BioResources. 13(4) (2018) P. 8061-8075.
222. Hasan, K.F., P.G. Horváth, B. Miklos, and T. Alpár. A state-of-the-art review on coir fiber-reinforced biocomposites. RSC Advance. 11 (2021) P. 10548-10571.

223. Vinod, A., T.Y. Gowda, R. Vijay, M. Sanjay, M.K. Gupta, M. Jamil, et al. Novel Muntingia Calabura bark fiber reinforced green-epoxy composite: A sustainable and green material for cleaner production. Journal of Cleaner Production. 294 (2021) P. 126337.
224. Hasan, K.F., P.G. Horváth, G. Markó, and T. Alpár. Thermomechanical characteristics of flax-woven-fabric-reinforced poly (lactic acid) and polypropylene biocomposites. Green Materials. 40(XXXX) (2021) P. 1-10.
225. Zhang, W., X. Xu, H. Wang, F. Wei, and Y. Zhang. Experimental and numerical analysis of interfacial bonding strength of polyoxymethylene reinforced cement composites. Construction and Building Materials. 207 (2019) P. 1-9.
226. He, P., M.U. Hossain, C.S. Poon, and D.C. Tsang. Mechanical, durability and environmental aspects of magnesium oxychloride cement boards incorporating waste wood. Journal of Cleaner Production. 207 (2019) P. 391-399.
227. Furtos, G., L. Silaghi-Dumitrescu, P. Pascuta, C. Sarosi, and K. Korniejenko. Mechanical properties of wood fiber reinforced geopolymer composites with sand addition. Journal of Natural Fibers. 18(2) (2021) P. 285-296.
228. Ghofrani, M., K.N. Mokaram, A. Ashori, and J. Torkaman. Fiber-cement composite using rice stalk fiber and rice husk ash: Mechanical and physical properties. Journal of Composite Materials. 49(26) (2015) P. 3317-3322.
229. Antwi-Boasiako, C., L. Ofosuhene, and K.B. Boadu. Suitability of sawdust from three tropical timbers for wood-cement composites. Journal of Sustainable Forestry. 37(4) (2018) P. 414-428.
230. Cheah, C.B. and M. Ramli. The implementation of wood waste ash as a partial cement replacement material in the production of structural grade concrete and mortar: An overview. Resources, Conservation and Recycling. 55(7) (2011) P. 669-685.
231. Ashori, A., T. Tabarsa, and S. Sepahvand. Cement-bonded composite boards made from poplar strands. Construction and Building Materials. 26(1) (2012) P. 131-134.
232. Wei, Y.M., T. Fujii, Y. Hiramatsu, A. Miyatake, S. Yoshinaga, T. Fujii, et al. A preliminary investigation on microstructural characteristics of interfacial zone between cement and exploded wood fiber strand by using SEM-EDS. Journal of Wood Science 50(4) (2004) P. 327-336.
233. Ramos, T., A.M. Matos, and J. Sousa-Coutinho. Mortar with wood waste ash: Mechanical strength carbonation resistance and ASR expansion. Construction and Building Materials. 49 (2013) P. 343-351.
234. Udoeyo, F.F., H. Inyang, D.T. Young, and E.E. Oparadu. Potential of wood waste ash as an additive in concrete. Journal of Materials in Civil Engineering. 18(4) (2006) P. 605-611.
235. Mňahončáková, E., M. Jiřičková, Z. Pavlík, L. Fiala, P. Rovnaníková, P. Bayer, et al. Effect of moisture on the thermal conductivity of a cementitious composite. International Journal of Thermophysics. 27(4) (2006) P. 1228-1240.
236. Mwaikambo, L.Y. and M.P. Ansell. Chemical modification of hemp, sisal, jute, and kapok fibers by alkalization. Journal of Applied Polymer Science. 84(12) (2002) P. 2222-2234.
237. Mohammadkazemi, F., R. Aguiar, and N. Cordeiro. Improvement of bagasse fiber–cement composites by addition of bacterial nanocellulose: an inverse gas chromatography study. Cellulose. 24(4) (2017) P. 1803-1814.
238. Djouani, F., C. Connan, M. Delamar, M.M. Chehimi, and K. Benzarti. Cement paste–epoxy adhesive interactions. Construction and Building Materials. 25(2) (2011) P. 411-423.
239. Akinyemi, A.B., E.T. Omoniyi, and G. Onuzulike. Effect of microwave assisted alkali pretreatment and other pretreatment methods on some properties of bamboo fibre

reinforced cement composites. Construction and Building Materials. 245 (2020) P. 118405.
240. Aggarwal, L., S. Agrawal, P. Thapliyal, and S. Karade. Cement-bonded composite boards with arhar stalks. Cement and Concrete Composites. 30(1) (2008) P. 44-51.
241. Kumar, C.N., M. Prabhakar, and J.-i. Song. Effect of interface in hybrid reinforcement of flax/glass on mechanical properties of vinyl ester composites. Polymer Testing. 73 (2019) P. 404-411.
242. Cui, Y., J. Chang, and W. Wang. Fabrication of glass fiber reinforced composites based on bio-oil phenol formaldehyde resin. Materials. 9(11) (2016) P. 886.
243. Sánchez-Soto, M., P. Pagés, T. Lacorte, K. Briceño, and F. Carrasco. Curing FTIR study and mechanical characterization of glass bead filled trifunctional epoxy composites. Composites Science and Technology. 67(9) (2007) P. 1974-1985.
244. Karahan, M., F. Ozkan, K. Yildirim, and N. Karahan. Investigation of the properties of natural fibre woven fabrics as a reinforcement materials for green composites. Fibres and Textiles in Eastern Europe. 118 (2016) P. 98-104.
245. Upadhyay, A., R. Tiwari, and K. Singh. Optical and electrical properties of carbon nanotube-containing Se85Te10Ag5 glassy composites. Philosophical Magazine. 96(6) (2016) P. 576-583.
246. Xu, B., J. Long, G. Xu, J. Yang, Y. Liang, and J. Hu. Facile fabrication of superhydrophobic and superoleophilic glass-fiber fabric for water-in-oil emulsion separation. Textile Research Journal. 89(13) (2019) P. 2674-2681.
247. Pamukchieva, V., K. Todorova, O. Mocioiu, M. Zaharescu, A. Szekeres, and M. Gartner. IR studies of impurities in chalcogenide glasses and thin films of the Ge-Sb-S-Te system. Journal of Physics: Conference Series. 356(1) (2012) P. 1-6.
248. Sharma, G., A.R. Sharma, R. Bhavesh, J. Park, B. Ganbold, J.-S. Nam, et al. Biomolecule-mediated synthesis of selenium nanoparticles using dried Vitis vinifera (raisin) extract. Molecules. 19(3) (2014) P. 2761-2770.
249. Teo, S.C., D.N.U. Lan, P.L. Teh, and L.Q.N. Tran. Mechanical behavior of palm oil–based composite foam and its sandwich structure with a flax–epoxy composite. Journal of Applied Polymer Science. 133(45) (2016) P.
250. Garay, A.C., V. Heck, A.J. Zattera, J.A. Souza, and S.C. Amico. Influence of calcium carbonate on RTM and RTM light processing and properties of molded composites. Journal of Reinforced Plastics and Composites. 30(14) (2011) P. 1213-1221.
251. Atiqah, A., M. Jawaid, S. Sapuan, M. Ishak, and O.Y. Alothman. Thermal properties of sugar palm/glass fiber reinforced thermoplastic polyurethane hybrid composites. Composite Structures. 202 (2018) P. 954-958.
252. Kumar, C.N., M. Prabhakar, and J.-i. Song. Effect of interface in hybrid reinforcement of flax/glass on mechanical properties of vinyl ester composites. Polym. Test. 73 (2019) P. 404-411.
253. Ramesh, M., K. Palanikumar, and K.H. Reddy. Mechanical property evaluation of sisal–jute–glass fiber reinforced polyester composites. Composites Part B: Engineering. 48 (2013) P. 1-9.
254. Silva, R., D. Spinelli, W. Bose Filho, S.C. Neto, G. Chierice, and J. Tarpani. Fracture toughness of natural fibers/castor oil polyurethane composites. Composites Science and Technology. 66(10) (2006) P. 1328-1335.
255. Fiore, V., L. Calabrese, T. Scalici, P. Bruzzaniti, and A. Valenza. Experimental design of the bearing performances of flax fiber reinforced epoxy composites by a failure map. Composites Part B: Engineering. 148 (2018) P. 40-48.
256. Hasan, K.M.F., H. Wang, S. Mahmud, M.A. Jahid, M. Islam, W. Jin, et al. Colorful and antibacterial nylon fabric via in-situ biosynthesis of chitosan mediated nanosilver. Journal of Materials Research & Technology. 9(6) (2020) P. 16135-16145.

257. Sapiai, N., A. Jumahat, M. Jawaid, M. Midani, and A. Khan. Tensile and flexural properties of silica nanoparticles modified unidirectional kenaf and hybrid glass/kenaf epoxy composites. Polymers. 12(11) (2020) P. 2733.
258. Hasan, K.M.F., G.H. Péter, M. Gábor, and A. Tibor. Thermo-mechanical characteristics of flax woven fabric reinforced PLA and PP biocomposites. Green Materials. (2021) P. 1-9.
259. Hidayah, I.N., D.N. Syuhada, H.A. Khalil, Z. Ishak, and M. Mariatti. Enhanced performance of lightweight kenaf-based hierarchical composite laminates with embedded carbon nanotubes. Materials & Design. 171 (2019) P. 107710.
260. Branda, F., G. Malucelli, M. Durante, A. Piccolo, P. Mazzei, A. Costantini, et al. Silica treatments: A fire retardant strategy for hemp fabric/epoxy composites. Polymers. 8(8) (2016) P. 313.
261. Bhoopathi, R. and M. Ramesh. Influence of eggshell nanoparticles and effect of alkalization on characterization of industrial hemp fibre reinforced epoxy composites. Journal of Polymers and the Environment. 28 (2020) P. 2178-2190.
262. Mahmud, S., M.N. Pervez, K.F. Hasan, M. Abu Taher, and H.-H. Liu. In situ synthesis of green AgNPs on ramie fabric with functional and catalytic properties. Emerging Materials Research. (2019) P. 1-11.